



NTNU – Trondheim
Norwegian University of
Science and Technology

Kinetics study of CO₂ absorption in AMP and Piperazine solutions

Muhammad Usman

Chemical Engineering

Submission date: June 2012

Supervisor: Hallvard Fjøsne Svendsen, IKP

Co-supervisor: Ardi Hartono, IKP

Norwegian University of Science and Technology
Department of Chemical Engineering

Acknowledgement

This research thesis would not have been possible without the support of many people. The author wishes to express his gratitude to his supervisor, Prof. Halvard F.Svendsen who was abundantly helpful and offered invaluable assistance, support and guidance. Deepest gratitude are also to Dr. Ardi Hartono. This study would not have been successful without his assistance and help at each stage. I would like to thank Juliana Monteiro for her help in the modelling work. I would pay my special thanks also to all my friends for sharing the literature and invaluable assistance.

The author wishes to express his love and gratitude to my beloved parents for their endless love and help throughout the duration of my studies.

I want to dedicate my thesis work to my beloved father who passed away last year.

I declare that this is an independent work according to the exam regulations of Norwegian University of Science and Technology.

NTNU, Trondheim

27.06.2012

Author

Abstract

Kinetics of CO₂ in AMP (2-amino 2-methyl 1-propanol) with concentration of 0.1/0.5/1.0/2.0/3.0/4.0 M, 3M AMP with CO₂ loadings of 0.15/0.22/0.29 and 0.1/0.5/1.0/1.5M piperazine solutions were measured at a temperature range of 25-70°C. The AMP system was measured at 1KPa pressure of CO₂ while CO₂- loaded AMP and piperazine were measured at different partial pressures that range from 1-9KPa. The experiments for AMP system were performed in string of disc contactor while PZ system was measured in wetted wall column. The results for rate constants were interpreted in terms of termolecular mechanism for the reaction of CO₂ with amine.

The physiochemical properties like density, solubility and viscosity of AMP, CO₂-loaded 3M AMP and PZ solutions were also measured to study the kinetics of CO₂ in AMP and PZ solutions. Density was measured in Anton Paar DMA 4500M density meter at all above mentioned concentrations and within a temperature range of 20-80°C. Viscosity was measured in Physica MCR 100 rheometer at a temperature range of 20-80°C while solubility was calculated from the experiments in stirred jacketed glass vessel for CO₂-loaded AMP and PZ (0.5 and 1.5M).

Different nitrogen flow rates, gas circulation rates and liquid flow rates were also measured in string of discs contactor to determine the exact value of these to be used for the whole experiments.

Simple models based on temperature and concentration was applied on Excel sheet in order to calculate the density, solubility and viscosity. Soft model was applied to calculate the back pressure of CO₂ in the 3M AMP loaded systems. The absorption flux of CO₂ in AMP (unloaded and CO₂-loaded) and PZ solutions, Henry's constants, mass transfer coefficients and second order rate constants were determined for each case and compared these with the reported data for AMP and PZ.

Table of Contents

Chapter 1 Introduction

1.1	CO₂ capture technologies	1
1.1.1	Pre combustion CO ₂ capture.....	2
1.1.2	Post combustion CO ₂ capture	2
1.1.3	Oxy-Fuel Combustion CO ₂ capture	2
1.2	CO₂ capture processes	3
1.2.1	Chemical absorption	3
1.2.2	Physical absorption	3
1.2.3	Physical adsorption	4
1.2.4	Membrane separation processes	4
1.2.5	Phase separation.....	4
1.3	CO₂ transport and storage	4
1.4	Research and future	4
1.5	Scope of present work	5

Chapter 2 Theoretical Background

2.1	Physiochemical properties	7
2.1.1	Density	7
2.1.2	Diffusivity	8
2.1.3	Solubility.....	8
2.1.4	Viscosity	9
2.2	Kinetics of alkanolamines	9
2.2.1	Zwitterion mechanism	9
2.2.2	Termolecular mechanism.....	11
2.2.3	Base-catalyzed hydration mechanism	12
2.3	Mass transfer with a chemical reaction	13
2.3.1	Two-Film Model	13
2.3.2	Penetration theory.....	15
2.3.3	Surface renewal model	15
2.4	Reaction mechanism	16
2.5	Reaction regime	17
2.6	Liquid film mass transfer coefficient	18
2.7	Gas film mass transfer coefficient	19
2.8	Gas side resistance	20

2.9	Soft Model	20
2.10	Kinetic rate constant	21
2.11	Activity based rate constant	22
Chapter 3 Materials and Experimental Methods		
3.1	Chemicals	24
3.2	Amine and CO₂ analyses of liquid samples	25
3.2.1	Amine analysis	25
3.2.2	CO ₂ analysis	26
3.3	Density measurements	27
3.4	Viscosity measurements	27
3.5	Solubility measurements	28
3.6	Kinetics measurements	31
3.6.1	String of discs apparatus (SDC)	31
3.6.2	Wetted Wall Column (WWC)	34
Chapter 4 Results and Discussion		
4.1	Density measurements	36
4.2	Viscosity measurements	38
4.3	Solubility measurements	41
4.4	Liquid flow rate	45
4.5	Nitrogen flow rate	45
4.6	Gas circulation rate	46
Kinetics of CO₂ absorption in AMP aqueous solutions		
4.7	Absorption flux dependency over temperature and concentration	47
4.8	Reproducibility of the data	48
4.9	Overall mass transfer coefficient	49
4.10	Second order rate constant	49
Kinetics of CO₂ absorption in loaded AMP solutions		
4.11	Flux dependency over loading and temperature	53
Kinetics of CO₂ absorption in Piperazine		
4.12	Absorption flux dependency over concentration	55
4.13	Comparison of physiochemical properties data with literature	57
4.13.1	Density	58
4.13.2	Viscosity	59
4.13.3	Solubility	61

4.14	Comparison of second order rate constant with literature.....	63
4.15	Comparison of AMP with MEA.....	64
Appendices		
Appendix A.....		
Physiochemical Properties		
Appendix B		
	Kinetics data of AMP	75
Appendix C		
	Kinetics of Loaded 3M AMP	78
Appendix D.....		
	Kinetics data of Piperazine.....	83
Appendix E		
	Results of CO₂ Analyses for PZ	90

Nomenclature

$E_{A\infty}$	Infinite enhancement factor
μ	Viscosity
A	Arrhenius constant
AmH	Amine
AMP	2-amino 2-methyl 1-propanol
B	Base
CO ₂	carbon dioxide
E	Activation energy
E_A	Enhancement factor
$E_{A,pen}$	Enhancement factor for penetration theory
GHG	Green House Gas Emissions
H ₂	Hydrogen
Ha	Hatta number
K_{app}	Apparent rate constant
K_B	Rate constant of base
KG	Mass transfer coefficient
K_l	Liquid mass transfer coefficient
K_{obs}	Observed rate constant
KPa	Kilo pascal

L	Liter
M	Molarity
MEA	Monoethanolamine
MFC	Mass flow controllers
Mol	Mole
N _{CO₂}	Flux of CO ₂
n _d	Number of discs
NO _x	Nirtogen oxides
°C	Celsius scale
P [*] _{CO₂}	Partial pressure of CO ₂ at interface
PZ	Piperazine
Re	Reynold number
Sc	Schmidt number
Sh	Sherwood number
So _x	Sulfur oxides
T _c	Critical temperature
ρ	Density

List of Figures

Figure 1.1. Graphical representation of CO ₂ captures techniques (IPCC, 2005)	2
Figure 3.1(a) Mettler Toledo G-20 setup for amine analysis.....	25
Figure 3.1(b) Metrohm 809 titrando setup for CO ₂ analysis	26
Figure 3.2 Density meter (Anton Paar DMA 4500M)	27
Figure 3.3 Pysica MCR 100 rheometer setup for viscosity measurements.....	28
Figure 3.4 Experimental setup for solubility measurements	29
Figure 3.5 Experimental set-up of string of discs contactor apparatus	32
Figure 3.6 Experimental set-up of wetted wall column	35
Figure 4.1(a) Experimental measured densities of AMP solutions at different temperatures (20-80°C)	37
Figure 4.1(b) Experimental measured densities of piperazine solutions at different temperatures (20-80°C)	37
Figure 4.2 Densities of 3M AMP solution with different CO ₂ loadings (L=loading)	38
Figure 4.3 Experimental viscosity data of 4/3/2/1/0.5/0.1M AMP at different temperatures (20-80°C)	39
Figure 4.4 Experimental data for viscosities of piperazine solutions at different temperatures (20-70°C)	39
Figure 4.5 Experimental viscosities of 3M AMP Loaded solutions at temperatures (20-80°C); L=loading	40
Figure 4.6 Comparison of experimental and model data points for AMP (left) and PZ (right)	40
Figure 4.7 Henry's constant for different concentrations of AMP at temperature range of 25-80°C; 0.358 xw/4M, 0.268xw/3M, 0.179xw/2M, 0.089xw/1M, 0.044xw/0.5M, 0.0089xw/0.1M	42
Figure 4.8 Henry's constant for different concentrations of PZ at temperature range of 25-80°C; 0.11 xw/1.5M, 0.0419xw/0.5M	42
Figure 4.9 Henry's constant for 3M AMP with 0.15 and 0.35 CO ₂ loadings (α) at temperature 25-100°C	43
Figure 4.10 Temperature dependencies of Henry's constants for different concentrations of AMP	43
Figure 4.11 Temperature dependency of Henry's constants for different concentrations of PZ	44
Figure 4.12 CO ₂ -Absorption fluxes for different liquid flow rates.....	45
Figure 4.13 Mass transfer resistances for different nitrogen flow rates	46
Figure 4.14 Experimental data of gas circulation rates.....	46
Figure 4.15 Experimental data for absorption flux of CO ₂ for all AMP solutions at temperatures (25-70°C).....	47
Figure 4.16 Reproducibility of the data for (4,3 and 2M) AMP solutions on string of discs.....	48
Figure 4.17 Gas side mass transfer coefficient at different temperatures and concentrations of AMP	49
Figure 4.18 Arrhenius type temperature dependency of second order rate constant for AMP solutions	50
Figure 4.18(a) Arrhenius type second order rate constant for 0.1M AMP(left) and 0.5M AMP (right)	50
Figure 4.18(b) Arrhenius type second order rate constant for 1M AMP(left) and 2M AMP (right)	51
Figure 4.18(c) Arrhenius type second order rate constant for 3M AMP(left) and 4M AMP (right).....	51
Figure 4.18(d) Comparison of experimental and calculated second order rate constant for AMP	52
Figure 4.19 Experimental measured data of 3M AMP solutions with CO ₂ loadings of 0.15/0.22/0.29.....	54
Figure 4.20 Experimental measurements of 1.5M PZ at temperature range of 25-70°C	55
Figure 4.21 Experimental measurements of 1.0M PZ at temperature range of 25-70°C	55
Figure 4.22 Experimental measurements of 0.5M PZ at temperature range of 25-70°C	56
Figure 4.23 Experimental measurements of 0.1M PZ at temperature range of 25-70°C	57
Figure 4.24 Comparison of density data of AMP with literature	58
Figure 4.25 Comparison of density data of PZ with literature	59
Figure 4.26 Comparison of experimental viscosity data of AMP with literature.....	60

Figure 4.27 Comparison of experimental viscosity data of PZ with literature.....	61
Figure 4.28 Comparison of experimental data of AMP with reported literature	62
Figure 4.29 Comparison of experimental data of PZ with reported literature	63
Figure 4.30 Comparison of K ₂ values of AMP with the literature	64
Figure 4.31 Comparison of second order rate constants of AMP with MEA	64

List of Tables

Table 1.1. Details of the present work	6
Table 1.2. Measured physiochemical properties of AMP and PZ.....	6
Table 3.1 Amine solvents used in the present work.....	24
Table 4.1 Literature data reported for AMP and PZ	59
Table 4.2 Comparison of experimental solubility data of AMP and PZ with reported literature	61
Table 4.3 Literature data for second order rate constants of AMP	63
Table A1 Experimental density data of AMP solutions at temperatures 20-80°C	70
Table A2 Experimental density data of PZ solutions at temperatures 20-80°C.....	71
Table A3 Experimental density data of AMP solutions loaded with CO ₂ at temperatures 20-80°C.....	72
Table A4 Parameters used in equations 4.1 and 4.2.....	72
Table A5 Experimental viscosity data of AMP solutions at temperatures 20-80°C	73
Table A6 Experimental viscosity data of PZ solutions at temperatures 20-70°C.....	73
Table A7 Experimental viscosity data of AMP solutions loaded with CO ₂ at temperatures 20-80°C.....	73
Table A8 Parameters for viscosity model of AMP and PZ	73
Table A9 Henry's constants for AMP solutions at temperatures (25-80°C).....	74
Table A10 Henry's constants for Piperazine solutions at temperatures (25-100°C)	74
Table A11 Henry's Constants of 3M AMP with different CO ₂ loadings (0.15/0.35/0.93).....	74
Table A12 Parameters for solubility model fitting of AMP and PZ.....	74

Chapter 1

Introduction

Global climate change, energy efficiency and switching from fossil fuels are the most important issues related to environment, energy and economy. Global climate is changing due to greenhouse gas emissions. These GHG emissions include carbon dioxide, water vapors, methane, NO_x, SO_x etc. Carbon dioxide (CO₂) is one of the important greenhouse gases (GHG) responsible for about 70% of the enhanced greenhouse effect and global warming (Wu et al., 2010). The sources for CO₂ emissions arise from human activities like burning of fossil fuel used in power generation, transportation, industrial processes (cement manufacturing, hydrogen production), and residential and commercial buildings (Abanades et al., 2005).

The major contribution of CO₂ emissions is from burning of fossil fuels. Fossil fuel comprises 80% of total world energy demand (Torpet et al., 2006). The strategy for reduction of CO₂ emissions is to improve energy efficiency and fuel switching from coal to natural gas. Analysts and policy makers have realized to develop end of pipe technologies for mitigation of CO₂ emissions. These end-of-pipe technologies are known as carbon capture and storage. Carbon capture and storage involves capturing, compression, transport and storage.

1.1 CO₂ capture technologies

CO₂ is captured from large point sources like fossil fuel power plants, fuel processing plants, during manufacturing of cement and chemicals. There are three basic systems for capturing CO₂ on the basis of fossil fuels in power plants and industrial plants.

- Pre-combustion capture
- Post-combustion capture
- Oxy-fuel combustion capture

1.1.1 Pre combustion CO₂ capture

Pre-combustion capture involves the separation of CO₂ before combustion process. Fuel and air is reacted to produce synthesis gas consisting of carbon monoxide and hydrogen. This synthesis gas is further reacted with water to give mainly carbon dioxide and hydrogen. CO₂ is then separated by absorption process and hydrogen is used as a fuel.

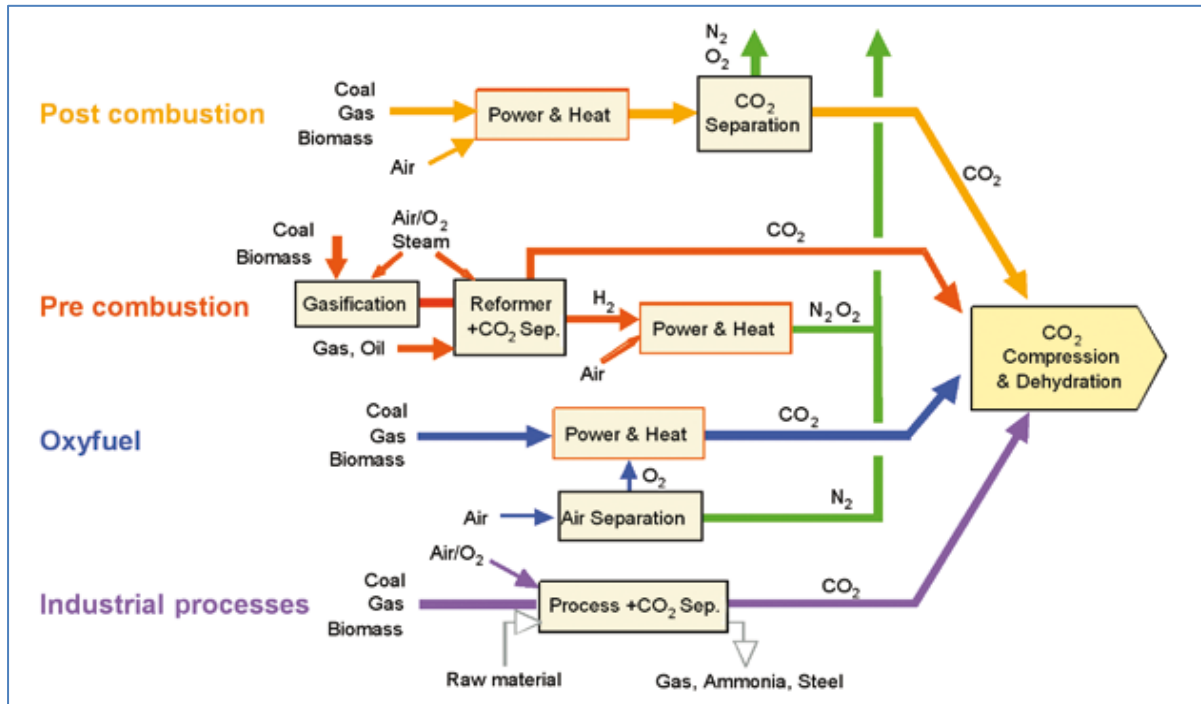


Figure 1.1. Graphical representation of CO₂ captures techniques (IPCC, 2005)

1.1.2 Post combustion CO₂ capture

Post combustion carbon capture involves the separation of CO₂ from flue/combustion gases emitted from combustion of fuel. Flue gases must be recovered from CO₂ before being emitted to atmosphere. A chemical solvent is used for the separation of CO₂ from flue gases. The solvent can be regenerated by stripping the rich mixture. CO₂ separated is compressed and injected into a storage site.

Post-combustion capture is the easiest method to implement on large industrial scale due to retrofitting of existing plants and CO₂ capture unit can be installed separately from power plant.

1.1.3 Oxy-Fuel Combustion CO₂ capture

Fuel is burnt with oxygen and recycled gas contains CO₂ and water mainly. This CO₂ can be separated out by cooling and water condensation. Oxy-fuel combustion technology

decreases the cost for gas separation due to fewer amounts being produced and increases the cost on the other hand due to separation of oxygen from air. Oxygen is separated out from air by cryogenic separation, ion transport membranes and pressure swing adsorption techniques. The advantage of oxy-fuel combustion technology over other two is of fewer emissions of NO_x and Sox (IEA, 2006).

1.2 CO₂ capture processes

There exist physical processes and other methods that can be implemented to accomplish separation of CO₂. Fundamental research is necessary to improve the efficiency and reduce the cost of all these processes (GCEP, 2005).

All the available processes/technologies used for carbon capture are described as under. (GCEP, 2005)

- Chemical Absorption
- Physical Absorption
- Physical Adsorption
- Membrane Separation Processes
- Phase Separation

1.2.1 Chemical absorption

This process involves the use of chemical solvent to absorb CO₂. This technology is mostly used for low concentrations of CO₂. Scale, efficiency and stability become a problem for the use of this technology when gas volume flow is high. This technique requires high investment cost and energy consumption. Amine solvents which include MEA, DEA and MDEA are the most common examples used for this technique.

1.2.2 Physical absorption

Gas is permeated through a solid or liquid under set conditions and desorb at other conditions of temperature and pressure. Less energy and more absorbent will be required for small differences in conditions. The advantage of physical solvent over chemical absorption is of higher absorption capacity and low energy requirements for regeneration of solvent as it is not limited by reaction stoichiometry.

Selexol, a liquid glycol-based solvent are the commonly used physical solvents.

1.2.3 Physical adsorption

Adsorbents are used for the removal of CO₂ during this technique. Adsorbents separate CO₂ by attracting the material stream to its surface at high pressures through weak van der Waals forces.

Activated carbon, zeolites (molecular sieve adsorption), and hydrotalcites are commonly used adsorbents.

1.2.4 Membrane separation processes

CO₂ is separated by passing the material stream through a selective permeable membrane. Membrane will allow one component to pass through it and other components will remain in permeate. Commonly used membrane types for CO₂ and H₂ separation include polymeric membranes, inorganic micro porous membranes, and palladium membranes (Davison, 2011).

1.2.5 Phase separation

Phase separation involves condensing the gas below a certain temperature on the basis of partial pressure of other gases in a mixture. Cryogenic separation technique is the basis of phase separation. Cryogenic processes are widely used to separate gases into very pure streams (Wong, 2002).

1.3 CO₂ transport and storage

Carbon sequestration (storage) is the isolation of carbon dioxide (CO₂) from the earth's atmosphere. One method is to store CO₂ underground in rock formations. CO₂ can be stored there for long period of time. The CO₂ would remain in small pore spaces inherent in rocks. These pore spaces contain traces of oil and natural gas. It would enhance oil recovery from reservoirs. CO₂ will be transported through pipeline or ships.

1.4 Research and future

The stability of the most chemical and physical absorbents at elevated temperature and pressure is the important research problem. Corrosion and fouling/foaming problems are associated with the degradation products and formation of heat stable salts. So, it is necessary to continuously remove these impurities. Processes to purify are lacking. Since CO₂ capture at low pressure is difficult and expensive than at higher pressure, it is essential to have more precise data on the physical properties of solvents, reaction rates and packing

characteristics (MEISEN AXEL). Conventional organic membranes have low CO₂ permeability, lack of selectivity and not suitable at high temperatures (flue gas temperature). High temperature polymeric membranes, supported by inorganic substrates, are another approach. Cryogenic processes are difficult to apply because these cause fouling and corrosion due to other gases present in the mixture stream.

Research is going on to find the best absorbent for CO₂ capture. A lot of data is required to measure the physical and fundamental properties of amine systems.

1.5 Scope of present work

The cost of absorption process using aqueous solutions of alkanolamines as conventional solvents is still relatively high. The major reasons for the high cost include high regeneration energy, absorbent loss due to evaporation, corrosion of process equipment and high degradation rate. The capital cost can be reduced by selecting the better solvents for CO₂ absorption processes.

Alkanolamines such as monoethanolamine are common absorbents in CO₂ capture process. Sterically hindered amines such as 2-amino-2-methyl-1-propanol (AMP) and piperazine belong to a special class of primary / secondary amines having bulky groups attached to the nitrogen atom of the amine molecule so as to partially shield the amine group from the reacting acid gas. In this way, carbamate stability is reduced without significantly compromising reactivity. Sterically hindered amines arguably appear poised to become the leading technology for CO₂ capture.

Detailed kinetic data are required for the optimal design and operation of an absorber. AMP (2-amion 2-methyl 1-propanol) and Piperazine (PZ) have been selected for the kinetics study of CO₂ absorption. The purpose of this study is to see the reaction rates of both the solvents at different temperatures and driving forces. The kinetics of AMP and piperazine at different temperatures and driving forces of partial pressure of CO₂ are measured. Aqueous solutions of AMP loaded with CO₂ are also being measured during the present study at different temperatures and driving forces of CO₂ partial pressure.

Table 1.1. Details of the present work

Solvent	Solution Concentration (mol/L)	Temperature (°C)	Driving Forces (KPa)	Loading (nCO ₂ /n Amine)
2-amino 2-methyl 1-propanol(AMP)	0.1/0.5/1.0/2.0/3.0/4.0	25,40,50,60,70	1	3M AMP with loading of 0.15/0.22/0.29
Piperazine	0.1/0.5/1.0/1.5	25,40,50,60,70	1,4,7,9	-----

Some physiochemical properties were also measured during the present study in order to measure the kinetics of CO₂ absorption into amine solutions of AMP and PZ. Density, viscosity and solubility were measured at different temperatures. The details of the present work have been shown in the table 1.2.

Table 1.2. Measured physiochemical properties of AMP and PZ

Solvent	Physiochemical Property	Solution Concentration (mol/L)	Loading (molCO ₂ /molAmH)	Temperature (°C)
2-amino 2-methyl 1-propanol(AMP)	Density (g/cm ³)	0.1/0.5/1.0/2.0/3.0/4.0	3M AMP 0.15/0.22/0.29/0.35	25,40,50,60,70
	Viscosity(m.Pa.s)	0.1/0.5/1.0/2.0/3.0/4.0	3M AMP 0.15/0.22/0.29/0.35	20,30,40,50,60,70
	Solubility(kPa.m ³ /mol)	0.1/0.5/1.0/2.0/3.0/4.0	3M AMP 0.15/0.29/0.93	25,40,50,60,70,80
Piperazine(PZ)	Density (g/cm ³)	0.1/0.5/1.0/1.5	-	25,40,50,60,70
	Viscosity(m.Pa.s)	0.1/0.5/1.0/1.5	-	20,30,40,50,60,70
	Solubility(kPa.m ³ /mol)	1.5 0.5	-	25,40,60,80,100 25,40,50,60,70,80

Chapter 2

Theoretical Background

Physiochemical properties like density, viscosity and solubility of acid gases in aqueous amine solutions are of highly importance for the development of new solvents for CO₂ capture and the design of gas absorption/ desorption systems. Binary and tertiary data of systems containing (amine+water+CO₂) are needed to develop the equilibrium and kinetic models. Density, viscosity and solubility of CO₂ in the aqueous solutions of AMP and piperazine, and loaded AMP solutions are measured at different temperatures and concentrations.

2.1 Physiochemical properties

2.1.1 Density

The pure liquid components data in the DIPPR (version 4.1.0, 2004) can be estimated by using the equation 2.1 below. Critical temperature was used for the regression of the parameters.

$$\rho \left(\frac{g}{cm^3} \right) = \frac{AM}{B \left[1 + \left[1 - \frac{T}{T_c} \right]^C \right]^{1000}} \quad (2.1)$$

A, B and C are adjusted parameters and M is the molar mass of the solvent. T is the temperature to be measured and T_c, the critical temperature. Redlich-Kister model is usually implemented to predict the densities of aqueous amine solutions. However many parameters are required. To reduce the parameter, the empirical correlations were suggested by Aronu et al., 2011 as given by equations 2.2 and 2.3 respectively.

$$\rho \left(\frac{g}{cm^3} \right) = \left(K_1 + \frac{K_2 C_S}{T} + \frac{K_3}{T^2} \right) \exp \left(\frac{K_4}{T} + K_5 \left(\frac{C_S}{T} \right)^2 \right) \quad (2.2)$$

$$\rho \left(\frac{g}{cm^3} \right) = \left(k_1 + \frac{k_2 x_2}{T} \right) \exp \left(\frac{k_3}{T^2} + \frac{k_4 x_1}{T} + k_5 \left(\frac{x_1}{T} \right)^2 \right) \quad (2.3)$$

2.1.2 Diffusivity

The diffusivity of the gases like CO₂ and N₂O in water or infinite dilute solution can be calculated by the correlation proposed by Little (Little et al., 1992) and Versteeg (Versteeg et al., 1988). The Stokes-Einstein correlation was proposed for the diffusivity of CO₂ and alkanolamine in aqueous solutions.

2.1.3 Solubility

The solubility of acid gas CO₂ is measured at different temperatures and concentrations of amine solutions for developing a kinetic model and thermodynamics of the system. CO₂ reacts with amines due to which, it is not possible to measure directly the solubility of CO₂ in the amine solution. This property can then be estimated by using N₂O which is a non-reacting gas with amine solutions. N₂O analogy is applied to calculate the solubility of CO₂ into amine solution. N₂O analogy was proposed by Clarke (Clarke, 1964) and verified by Laddha (Laddha et al., 1981). The N₂O analogy can be shown as under by equation:

$$H_{N_2O}^{Am} = C_1 H_{CO_2}^{Am}$$

And $C_1 = H_{N_2O}^{H_2O} / H_{CO_2}^{H_2O}$

According to Versteeg and van Swaaij (Versteeg et al., 1988), the value of C₁ can be calculated by:

$$C_1 = \frac{H_{N_2O}^{H_2O}}{H_{CO_2}^{H_2O}} = 3.04 \exp\left(\frac{-240}{T}\right)$$

The Redlich-Kister equation correlates the solubility at different temperatures and concentrations based on the excess properties. The excess Henry's constant can be calculated by equation (2.4): (Edwards et al., 1975) and (Tiepel et al., 1972)

$$\hat{A} = \ln(k_{HM}) - x_1 \ln(k_{H_1}) - x_1 \ln(k_{H_2}) \quad (2.4)$$

k_{HM} , k_{H_1} and k_{H_2} represent Henry's law constant of N₂O into the mixture of amine +water, pure AMP and pure water respectively. The excess Henry's constant was correlated to Redlich-Kister equation by: (Prausnitz et al., 1999)

$$\hat{A} = x_1 x_2 \sum_{n=1} A_n (1 - 2x_2)^{n-1} \quad (2.5)$$

Where x_1 and x_2 are the mole fractions of amine and water respectively and A_n is Redlich-Kister coefficient. A_n can be determined by regression for each temperature.

2.1.4 Viscosity

Viscosity gives the fluid resistance to flow. Fluids resist the motion of the layers and relative motion of the immersed object with differing velocities in them (Bird et al., 2012). Temperature affects the viscosity of both liquid and gas phases but pressure affects normally the viscosity of the gas phase. Viscosity of different amines increases exponentially with temperature by Arrhenius correlation which is given by as under.

$$\mu(mPa.s) = A \exp\left(\frac{E}{RT}\right) \quad (2.6)$$

A is the Arrhenius constant and E is the activation energy for flow in the above equation.

The viscosity of aqueous amine solutions is important for the measurement of the diffusivities. Viscosity of aqueous amine solutions can be correlated to diffusivity by modified Stokes-Einstein relation (Versteeg et al., 1998).

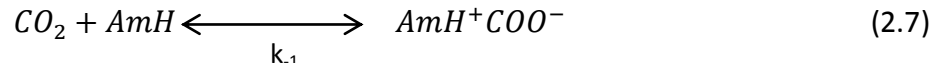
Viscosity of aqueous solutions of AMP (loaded and unloaded) and PZ were measured at different temperatures and compositions. The experimental procedure and results from the measurements are shown in the following chapter 3.

2.2 Kinetics of alkanolamines

The reaction between alkanolamines and CO₂ has significant importance particularly in the manufacture of H₂ from natural gas, treating NGL (natural gas liquids) and thermal power plants. The absorption of CO₂ into the aqueous solution of amine follows three mechanisms i.e. Zwitterion mechanism, termolecular mechanism and base catalyzed hydration (Versteeg et al., 1998). Primary, secondary and sterically hindered amines follow the zwitterion mechanism while reaction of tertiary amines with CO₂ follows base catalyzed hydration mechanism.

2.2.1 Zwitterion mechanism

This mechanism which consists of two steps, was originally proposed by Caplow (Caplow, 1968) and later reintroduced by Danckwerts (Danckwerts, 1979). In the first step, the reaction between CO₂ and the amine (AmH) proceeds through the formation of zwitterion as an intermediate.



The second step is the formation of carbamate due to de-protonation of zwitterion complex by a base B.



By the application of the pseudo steady state condition to the zwitterion intermediate, then the rate of reaction between CO₂ and aqueous solution can be expressed by the equation 2.9.

$$r = \frac{k_1(CO_2)(AmH)}{1 + \frac{k_{-1}}{k_B(B)}} \quad (2.9)$$

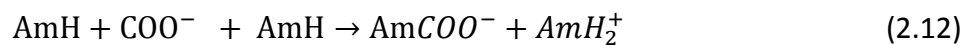
The reaction rate being expressed in equation 2.7 depicts a fractional order of reaction w.r.t amine concentration. If the protonation of zwitterion is instantaneous and reaction of zwitterion formation can be considered as rate determining step, then $1 \gg \frac{k_{-1}}{\sum k_b[B]}$. The rate of reaction now becomes as equation 2.10.

$$r = k_1 (CO_2)(AmH) \quad (2.10)$$

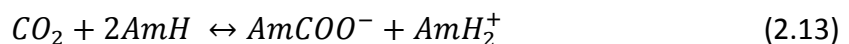
The equation now suggests a first order rate dependency with respect to both amine and CO₂ concentrations. If the zwitterion deprotonation is the rate determining step, then $k_{-1} \gg k_b[B]$ and equation 2.10 becomes:

$$r = \frac{k_1 \sum k_b[B]}{k_{-1}} (CO_2)(AmH) \quad (2.11)$$

The above expression suggests the fractional reaction order between one and two with respect to amine concentration. If the amine itself is the base B, then carbamate formation can be expressed as follows:



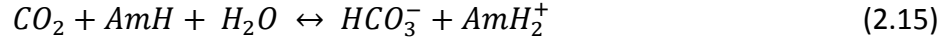
The overall rate of reaction in case of carbamate formation can be then represented by the sum of the reactions in equations 2.7-2.12.



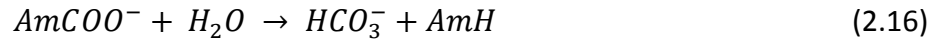
Bicarbonate formation occurs if the amine is sterically hindered because zwitterion reacts more rapidly with water than AmH.



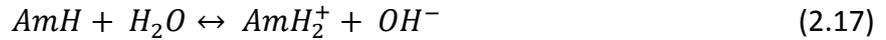
The overall rate of reaction in case of bicarbonate formation is represented by sum of the reactions in equations 2.7-2.14 as follows:



Steric effect lowers the stability of carbamate formation (Sharma). Carbamates of sterically hindered amine readily undergo hydrolysis and forming carbonates. The free amine molecule again react with CO₂ and formation of more bicarbonates takes place. In this way, lower carbamate formation occurs.



There are some more reactions that may take place in an aqueous solution of amine which are as follows:



The overall rate of all reactions between CO₂ and amine solutions is represented by the sum of all reactions given by equation 2.9, 2.19 and 2.20.

$$r_{overall} = \left[\frac{(k_1)(CO_2)(AmH)}{1 + \frac{k_{-1}}{k_B(B)}} \right] + \{ [k_{H_2O}(H_2O) + k_{OH^-}(OH^-)](CO_2) \} \quad (2.21)$$

2.2.2 Termolecular mechanism

Crooks and Donnellan (Crooks et al., 1989) developed termolecular mechanism and this mechanism was reintroduced by da Silva and Svendsen (da Silva et al., 2004). The method assumes that an amine reacts simultaneously with one mole of CO₂ and molecule of a base. The initial product is not zwitterion but a loosely bound encounter complex.



This loosely bound complex breaks up to give reactant molecules again while a few of them reacts with a second molecule of amine or water molecule to give ionic products. Da Silva and Svendsen reviewed this mechanism by ab initio calculations and a solvation model. According to their results, the most probable mechanism was similar as suggested by Crooks and Donnellan (Crooks et al., 1989). The other alternative could be that CO₂ forms a bond to amine with solvent molecule stabilizing the zwitterion like intermediate with hydrogen bonds.

The forward rate of reaction for this mechanism is given by the following equation:

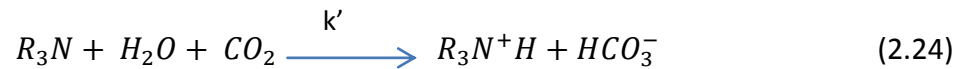
$$r = k_{obs}(CO_2)$$

Where k_{obs} is given by

$$k_{obs} = [k_{H_2O}(H_2O) + k_{OH^-}(OH^-) + k_{AmH}(AmH)](AmH) \quad (2.23)$$

2.2.3 Base-catalyzed hydration mechanism

Donaldson and Nguyen suggested the mechanism in which tertiary alkanolamines cannot react directly with CO₂. These amines have a base-catalytic effect in the hydration of CO₂. This was confirmed by Versteeg and Van Swaaij (Versteeg et al., 1988b) by the absorption of CO₂ into a water free solution of MDEA and ethanol. They concluded that CO₂ was only physically absorbed and which agrees with the proposed reaction mechanism (Versteeg et al., 1988).



At higher pH values (pH =13), a direct reaction between CO₂ and tertiary amine has been reported by Jørgensen and Faurholt (1954). However, the rate of this reaction can be neglected at lower pH values (pH < 11) (Versteeg et al., 1988).

The overall rate of reaction for all CO₂ reaction in aqueous amine solutions can be represented by the sum of all the reactions given by equation 2.19, 2.20 and 2.24.

$$r_{overall} = [k_{H_2O}(H_2O) + k_{OH^-}(OH^-) + k'(R_3N)](CO_2) \quad (2.25)$$

k_{obs} is given by :

$$k_{obs} = [k_{H_2O}(H_2O) + k_{OH^-}(OH^-) + k'(R_3N)] \quad (2.26)$$

And k_{ap} is given by:

$$k_{ap} = k'(R_3N) \quad (2.27)$$

2.3 Mass transfer with a chemical reaction

The rate of absorption of CO₂ into aqueous amine solution will increase if the mass transfer is accompanied by chemical reaction. The absorption flux can be calculated as under:

$$N_A = \frac{1}{\frac{1}{E_A k_l} + \frac{RT}{H k_g}} (C_A^* - C_{A,b}) \quad (2.28)$$

E_A is the enhancement factor which may be defined as the ratio of liquid side mass transfer coefficient with chemical reaction to the mass transfer coefficient without chemical reaction.

The absorption flux can be simplified in two ways:

1. For very low CO₂ loadings, the concentration of solute(CO₂) in the liquid bulk will be zero and equation for absorption flux can be reduced to:

$$N_A = \frac{1}{\frac{1}{E_A k_l} + \frac{RT}{H k_g}} C_A^* \quad (2.29)$$

2. Acid-side mass transfer resistance can be neglected if pure CO₂ is used and absorption flux equation reduces to:

$$N_A = E_A k_l C_A^* \quad (2.30)$$

E_A is an important parameter when mass transfer is accompanied by chemical reaction. Enhancement factor can be determined from equations based on mass transfer models like film model, penetration theory and surface renewal model. The reaction order with respect to amine concentration varies from 1-2 and concentration of amine is large as compared to CO₂, so a model can be simplified by choosing the pseudo first order irreversible approach. All the models are described one by one as under.

2.3.1 Two-Film Model

The film model put forward by Whitman and Lewis (Whitman, 1923) is based on the assumption that a stationary film exists at the liquid and gas interface. It is also assumed

that mass transfer takes place by steady molecular diffusion through the film. This model predicts mass transfer rate on the basis of first power dependence.

The mass transfer rate without chemical reaction is determined from the mass balance of the solute (CO₂) at steady state as:

$$D_A \frac{\partial^2 C_A}{\partial x^2} = 0 \quad \text{for } 0 \leq x \leq \delta \quad (2.31)$$

Boundary Conditions:

$$X=0, C_A = C_{A,i}$$

$$X=\delta, C_A = C_{A,b}$$

The mass transfer flux of solute through the gas liquid interface will be then:

$$N_A = k_l(C_{A,j} - C_{A,b}) \quad (2.32)$$

k_l is the mass transfer coefficient for liquid side and is equal to $\frac{D_A}{\delta}$.

Hatta (Hatta, 1932) proposed the analytical solution for the mass transfer through a film.

Mass balance for the solute is given as under:

$$D_A \frac{\partial^2 C_A}{\partial x^2} = k_l C_A \text{ for } 0 \leq x \leq \delta \quad (2.33)$$

Boundary Conditions:

$$X=0, C_A = C_{A,i}$$

$$X=\delta, D_A \left[\frac{\partial C_A}{\partial x} \right]_{\delta}$$

Enhancement factor is given by:

$$E_{A, film} = \frac{Ha}{\tanh(Ha)}$$

If $Ha \gg 1$, then $E_{A, film} \cong Ha$.

2.3.2 Penetration theory

The penetration theory proposed by Higbie (Higbie, 1935) is based on the assumption that gas-liquid interface is made up of small liquid elements, which are continuously brought to the surface from the bulk of the liquid. These liquid elements are considered as stagnant. When element reached the surface, the dissolved gas concentration in the element is considered equal to the liquid bulk concentration.

The residence time of all these liquid elements at the interface is the same and mass transfer takes place by unsteady molecular diffusion. Mass transfer is determined by mass balance of solute.

$$D_A \frac{\partial^2 C_A}{\partial x^2} = \frac{\partial C_A}{\partial t}$$

Initial and Boundary Conditions:

$$C_A(x, 0) = 0$$

$$C_A(0, t) = C_{A,i}$$

$$C_A(\infty, t) = C_{A,b}$$

The mass transfer rate with above conditions gives a solution:

$$N_A = k_l(C_{A,i} - C_{A,b})$$

k_l is the mass transfer coefficient and is equal to $2\sqrt{\frac{D_A}{\pi t^*}}$.

The enhancement factor for pseudo first order irreversible reaction can be expressed as:

$$E_{A,pen} = \left[\left\{ 1 + \frac{\pi}{8Ha^2} \operatorname{erf} \left[\sqrt{\frac{4Ha^2}{\pi}} \right] + \frac{1}{2Ha} \exp \left(\frac{4Ha^2}{\pi} \right) \right\} \right] \quad (2.34)$$

If $Ha \gg 1$, then $E_{A,pen} \cong Ha$.

2.3.3 Surface renewal model

Surface renewal model for mass transfer was proposed by Danckwerts (Danckwerts, 1951) as extension of penetration theory. It is based on the assumption that the liquid elements do not stay on the surface (gas-liquid contact) at the same time.

The absorption rate at the surface can be expressed by Danckwerts' age function which is given below:

$$N_A(t) = \sqrt{D_A(k_1 + s)C_{A,i}} = \sqrt{D_A \left(k_1 + \frac{k_l^2}{D_A} \right) C_{A,i}} = k_l C_{A,i} \sqrt{1 + \frac{k_l D_A}{k_1^2}} \quad (2.35)$$

And the enhancement factor is given by:

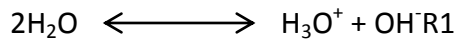
$$E_{A,surf} = \sqrt{1 + \frac{k_l D_A}{k_1^2}} = \sqrt{1 + Ha^2} \quad (2.36)$$

If $Ha \gg 1$, then $E_{A,surf} \cong Ha$.

2.4 Reaction mechanism

Chemical equilibria (CO₂ – AMP – H₂O) system:

Water Dissociation



Dissociation of CO₂ from gas phase to liquid phase



Hydrolysis of dissolve CO₂



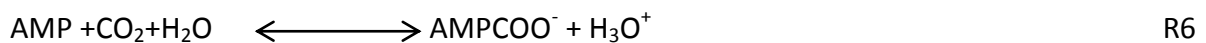
Dissociation of carbonate ion



Amine protonation



Carbamate formation of AMP



Chemical equilibria (CO₂ – PZ – H₂O) system

Dissociation of water



Dissociation of CO₂ from gas phase to liquid phase



Hydrolysis of dissolve CO₂



Dissociation of carbonate ion



Amine protonation



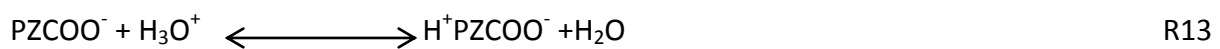
Di-protonation of PZ



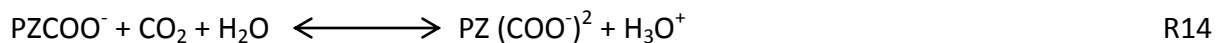
Carbamate formation



Protonated carbamate formation



Dicarbamate formation



2.5 Reaction regime

The ratio of Hatta number and enhancement factor is used to determine the reaction regime. Reaction regime can be determined from Hatta number and the ratios of Hatta number and the $E_{A\infty}$ (the infinite enhancement factor) or by the relative rates of diffusion and reaction (Astarita et al., 1983).

$$\phi = \frac{\text{Diffusion time}}{\text{Reaction time}}$$

Different cases of reaction regimes depending on Hatta number and enhancement factor are as follows:

1. Slow reaction regime

Hatta number is less than 0.3 for this case and no enhancement of mass transfer in the presence of chemical reaction. The absorption flux depends on the physical mass transfer coefficient (**Hartono, 2009**). The absorption flux will depend on liquid flow rate as mass transfer coefficient is strongly liquid flow rate dependent.

2. Fast reaction regime

The condition of $3 < Ha \ll E_{A\infty}$ applies for this regime. Mass transfer is enhanced by weak to strong in the presence of chemical reaction. The absorption flux is independent of physical mass transfer coefficient and liquid flow rate.

3. Instantaneous reaction regime

The condition of $3 < E_{A\infty} \ll Ha$ applies for this reaction regime. The absorption flux is limited by diffusion of reagents.

The reaction regime on the basis of relative reaction rates and diffusion are as follows:

1. Slow reaction regime: If $\phi \ll 1$, then $E_A=1$. There will be no enhancement in diffusion rate with the occurrence of chemical reaction.
2. Fast reaction regime: If $\phi \gg 1$, then $E_A= \sqrt{\phi}$. There will be no significant effect on mass transfer rate as reaction is fast. Reaction proceeds at finite rate and equilibrium is not established instantaneously.
3. Instantaneous reaction regime: $\phi \rightarrow \infty$, $E_A= E_{A\infty}$. No resistance to mass transfer due to reaction and chemical equilibrium is established instantaneously.

2.6 Liquid film mass transfer coefficient

It is important to have the gas film resistance as small as possible while measuring the liquid film mass transfer coefficient. Sherwood (Sherwood et al., 1975) proposed a correlation (presented by equation 2.37) for wetted wall columns by fixing the power of Reynold's number and Schmidt number to 1/2 and 1/3 respectively. Pacheco (Pacheco et al., 2000) also proposed a correlation as shown in equation 2.38.

$$Sh_l = 1.4731 Sc_l^{1/3} Re_l^{1/2} \quad (2.37)$$

$$Sh_l = 1.2723 (Sc_l Re_l \frac{d}{h})^{0.4915} \quad (2.38)$$

$$Sh_l = \frac{k_l^o d}{D_{CO_2}^{sol}} \quad (2.39)$$

Equation 2.39 was used to calculate the liquid film mass transfer coefficient k_l^o .

Liquid side film mass transfer coefficient for string of discs contactor can be determined by the correlation given by Stephens and Morris (Stephens et al., 1951).

$$\frac{k_l}{D} = \alpha \left(\frac{4\Gamma}{\mu} \right)^n \left(\frac{\mu}{\rho D} \right)^{0.5}$$

Where $\alpha = 308.5$, $n = 1.1$, Γ is the wetting rate of the apparatus and D is the diffusivity of the solute in the liquid phase.

2.7 Gas film mass transfer coefficient

The gas film mass transfer coefficient for the wetted wall column can be estimated by the correlations given by Sherwood and Pacheco. These correlations are given in the following equations respectively.

$$Sh_g = 0.6655 Sc_g^{1/3} Re_g^{1/2} \quad (2.40)$$

$$Sh_g = 2.0006 (Sc_g Re_g \frac{d_h}{h})^{0.4123} \quad (2.41)$$

$$Sh_g = \frac{k_g d}{D_{CO_2}^{N_2}} \quad (2.42)$$

Stephens and Morris (Stephens et al., 1951) also proposed the correlation for gas side mass transfer coefficient in the strings of disc contactor which is given as under.

$$\frac{k_G P}{v \rho_d} = 0.3281 \Gamma^{0.13} \left(\frac{v d \rho}{\mu} \right)^{-0.33} \left(\frac{\mu}{\rho D} \right)^{-0.56} \left(\frac{P}{P_i} \right)$$

ρ_d is the density of the solute gas, v (the gas velocity), d (the equivalent diameter for gas flow), P (the total pressure) and P_i is the partial pressure of solute gas.

2.8 Gas side resistance

The soluble gas in a mixture of soluble and insoluble gases must diffuse through the insoluble gas to reach the interface. That is why the partial pressure of the soluble gas at the interface is less than that in the bulk. The gas film resistance may be defined as the stagnant film of finite thickness of gas across which soluble gas is transferred by molecular diffusion only and the bulk of the gas has uniform composition (Danckwerts, 1970). The mass balance of the soluble gas for both the liquid and gas film at steady state condition is given by:

$$N_A = k_g(p_A - p_{A,i}) = E_A k_l(C_{A,i} - C_{A,b})$$

By applying the Henry's law ($p_{A,i} = HC_{A,i}$) at the liquid interface, the absorption flux is given as under:

$$N_A = K_g(p_A - HC_{A,b}) = K_l\left(\frac{p_A}{H} - C_{A,b}\right)$$

Where

$$\frac{1}{K_G} = \frac{1}{k_g} + \frac{H}{k_l} \quad (2.44)$$

And

$$\frac{1}{K_L} = \frac{1}{k_l} + \frac{1}{Hk_g} \quad (2.45)$$

The above two equations 2.44 and 2.45 give the overall resistance as the sum of the resistances in the films. The values of k_g and k_l vary from point to point.

2.9 Soft Model

The soft model was used to calculate the CO₂ backpressure in the loaded AMP solutions and this model can be fitted with the vapor liquid equilibrium measurements. The following equation was used in the soft model:

$$P_{CO_2} = \exp\left(1.8 * \ln x + K_1 + \frac{10}{(1 + K_2 \cdot \exp(-K_3 \cdot \ln x))}\right)$$

Where $K_1 = A_1 \cdot \ln\left(\frac{1}{T}\right) + A_2$, $K_2 = \text{Exp}\left(A_3 \cdot \frac{1}{T} + A_4\right)$, $K_3 = A_5 \left(\frac{1}{T}\right) + A_6$

T is in K and x is the weight fraction of the solution.

2.10 Kinetic rate constant

The overall rate of reaction for absorption of CO₂ into aqueous amine solution can be presented as follows:

$$r_{obs} = r_{CO_2-AmH} + r_{CO_2-OH^-} \quad (2.46)$$

The apparent kinetic rate constant (K_{ap}) can be expressed as:

$$k_{ap} = k_{obs} - k_{OH}^*[OH^-] \quad (2.47)$$

The apparent kinetic rate constant for the single-step termolecular mechanism is given by:

$$k_{ap} = \{k_{AmH}(AmH) + k_{H_2O}(H_2O)\}(AmH) \quad (2.48)$$

The apparent kinetic rate constant for the zwitterion mechanism can be found from the following equation:

$$k_{ap} = k_2 (AmH) \quad (2.49)$$

$$k_{ap} = \frac{(AmH)}{\frac{1}{k_2} + \frac{1}{\{k_{AmH}(AmH) + k_{H_2O}(H_2O)\}}} \quad (2.50)$$

The kinetic parameters (k_{AmH}, k_{H_2O}) for single step termolecular mechanism can be calculated by two methods:

1. By graphical method: If the concentration of water can be assumed constant for low amine concentrations, then the slope of the plot between $\frac{k_{ap}}{(AmH)}$ and (AmH) will give the value for k_{AmH} and the intercept of the plot will give the value of k_{H_2O} .
2. By non-linear regression: If the concentration of water cannot be assumed to be constant, then a non-linear regression method is used to determine the kinetic parameters.

Both of the above methods can also be applied to Zwitterion mechanism to find out the kinetic parameters.

2.11 Activity based rate constant

Kinetics constants are not real constants at a given temperature and depend upon the concentration and types of the ions in the solution (Pinsent et. al., 1956). The kinetic expression based on activity can be expressed by the equation 2.51.

$$r = k_2^Y C_A C_B \gamma_A \gamma_B \quad (2.51)$$

In the above expression, k_2^Y should be independent of concentration and depends only on the temperature. The distribution of CO₂ between the vapor and liquid phase is modeled based on Henry's law constant at infinite dilution.

$$\varphi_{CO_2}(T, P, y) y_{CO_2} P = \hat{\gamma}_{CO_2}(T, P, x) x_{CO_2} H_{CO_2}^{\infty*}(T) \exp\left\{\frac{\bar{v}_{CO_2}((P - P_{H_2O}^{sat}))}{RT}\right\} \quad (2.52)$$

Apparent Henry's constant is used to measure the concentration of species for calculation of kinetic rate constant. Apparent Henry's law constant is given by equation 2.53.

$$H_A^{App} = \frac{P_{A,i}}{C_{A,i}} \quad (2.53)$$

Comparing equation (2.52) and (2.53), we have:

$$H_A^{App} x_A = x_A \gamma_A H_A^{\infty*}$$

Mass transfer equation on the basis of activity can be expressed by equation 2.53 and overall gas side mass transfer coefficient by equation (2.54):

$$N_A = E^Y k_L^o (a_{A,i} - a_{A,b}) \quad (2.54)$$

$$K_{ov,G} = \frac{1}{\frac{1}{k_G} + \frac{H_{CO_2}^{\infty*}/C_{tot}}{E^Y k_L^o}} = \frac{1}{\frac{1}{k_G} + \frac{H_{CO_2}^{\infty*}}{E^Y k_L^o}}$$

The rate of reaction can be calculated by film theory for irreversible first order reaction given in equation 2.55 and Hatta number by equation (2.56):

$$r = a_A k_1^Y = k_1^Y \gamma_A C_A \quad (2.55)$$

$$Ha^Y = \frac{\sqrt{k_1^Y \gamma_A D_A}}{k_L^o} \quad (2.56)$$

First order kinetic constant based on activity can be calculated by equation 2.57 and second order rate constant by equation (2.58):

$$k_1^Y = \frac{H_A^{\infty 2} \gamma_A}{\left(\frac{1}{K_{ov,G}} - \frac{1}{k_g}\right)^2 D_A} \quad (2.57)$$

$$k_2^Y = \frac{k_1^Y}{C_{BYB}} \quad (2.58)$$

The VLE model must be able to estimate the apparent Henry's law constant correctly so that a consistency is achieved between component activity based on Henry's law constant and activity from VLE model (Knuutila, 2009).

Chapter 3

Materials and Experimental Methods

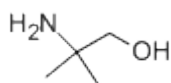
3.1 Chemicals

The solvents selected for measurements of kinetics study of CO₂ absorption are sterically hindered amine 2-amino-2-methyl-1-propanol (AMP) and Piperazine. The following table shows some properties of both the solvents used for the measurements.

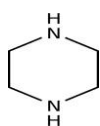
Table 3.1 Amine solvents used in the present work

Chemical	CAS No.	Manufacturer	Purity	Molecular Weight(g/gmol)	Molecular Formula
2-methyl 2-amino 1-propanol	124-68-5	Sigma Aldrich	>99.99%	89,14	C ₄ H ₁₁ NO
Piperazine	110-85-0	Sigma Aldrich	>99%	86,14	C ₄ H ₁₀ N ₂
Nitrogen		YaraParaxair AS	>99.99%	28	N ₂
Carbon dioxide		YaraParaxair AS	>99.99%	44	CO ₂

Molecular structure of 2-amino 2-methyl 1-propanol (AMP)



Molecular structure of Piperazine (PZ)



3.2 Amine and CO₂ analyses of liquid samples

All liquid samples were analyzed for amine and CO₂ concentrations by precipitation titration method. The apparatuses used for amine and CO₂ concentrations are shown in the figure 3.1 (a) and 3.1 (b) respectively.

3.2.1 Amine analysis

50ml of liquid sample was collected in sampling bottles during the experiments. Titration apparatus used was Mettler Toledo G-20 as shown in the figure 3.1(a). High concentration samples were analyzed by using 0.2N H₂SO₄ as titrant and low concentration samples were analyzed by using 0.02N H₂SO₄. There was no hard and fast rule for low concentrations of the samples. If the titrant used is very low and less 2ml then remaining low concentration samples were analyzed using other titrant of low concentration. The advantage of this apparatus is that one can save time by placing 9 samples at one time and it works automatically.



Figure 3.1(a) Mettler Toledo G-20 setup for amine analysis

Preparation of sample for analysis

60 ml of distilled water was added to sampling beaker, tare it and 0.2- 0.4ml of sample was added depending upon the estimated sample concentration. The weight of the sample was noted. Nine samples were prepared and put into the sampling rotating rack. Parallel samples were prepared for each point.

How to run the program

LabX software program was used for determination of the amine concentrations of by titration. Weighed quantities of the sample are filled there and program was started. Results were obtained for amine concentration in mol/Kg.

3.2.2 CO₂ analysis

The weighed amount of sample (0.9-1.3ml) was added to a 250 cm³ Erlenmeyer flask containing 50 cm³ sodium hydroxide (NaOH, 0.1 N) and 25 cm³ barium chloride (BaCl₂, 0.1 N) solutions. The Erlenmeyer flask was heated to enhance the barium carbonate (BaCO₃) formation and then cooled to ambient temperature. Then the solution was filtered with a 0.45 μm Millipore paper and washed with deionized water. The filter cake formed on the filter paper was transferred to a 250 cm³ beaker. 50 cm³ of deionised water was added into the 250 cm³ beaker and 40-50 ml of hydrochloric acid (HCl, 0.1 N) was also added to dissolve the BaCO₃ cake. The remaining amount of HCl that was not used to dissolve BaCO₃, was then titrated with 0.1 N NaOH in an automatic titrator (Metrohm 809 Titrando) with an end point of pH 5.2. The Metrohm 809 Titrando is shown in the figure 3.1(b).



Figure 3.1(b) Metrohm 809 titrando setup for CO₂ analysis

A blank sample without adding liquid sample was also analyzed with the same procedure in order to take into account of CO₂ in the atmosphere. The twelve samples can be analyzed in this apparatus at a time. LabX software program was used to determine the CO₂

concentration. Amount of NaOH used during the titration was noted and applied the following equation to calculate the CO₂ in the sample:

$$CO_2 \left(\frac{mol}{kg} \right) = \frac{1}{20} \frac{HCL(gm) - NaOH(ml) - [Blank HCL(gm) - blank NaOH(ml)]}{Sample (gm)}$$

$$CO_2 \left(\frac{mol}{litre} \right) = CO_2 \left(\frac{mol}{kg} \right) * \rho_{sol} \left(\frac{kg}{liter} \right)$$

3.3 Density measurements

Density of all solutions of AMP and piperazine were measured by Anton Paar DMA 4500M apparatus as shown in the figure 3.2. A measured volume of the sample equal to 9.5ml was filled in the test vial and covered the vial with a cap. Temperature was set to the desired value and started the measurement.



Figure 3.2 Density meter (Anton Paar DMA 4500M)

3.4 Viscosity measurements

The rheometer (Physica MCR 100) was used for the viscosity measurements of different AMP and Piperazine solutions. This apparatus is controlled by US 200 Software. First of all, opened the software window and correctly chose the measuring system (DG 26.7) and measuring cell (TEK 150P-C). Set the temperature value to the desired temperature. Then removed the protection white cylinder and fitted the measuring system as shown in the figure 3.3.

The bottom cylinder was filled with 4ml of solution. The upper cylinder fixation piece was pulled up to be coupled to the motor. The marks on motor and upper cylinder piece should

be aligning. After this, pressed the measuring position button on the software and waited for the temperature to be stabilized. Then reset the NF to zero and started the measurement. 25 data points were selected for most of the cases to observe the shear stress and shear rate. Newton1 method was used to measure the viscosity of aqueous solutions (loaded and unloaded) with assumption of amines as being Newtonian fluids. The data points were averaged to one value and that value was recorded as viscosity of the given solution. Same procedure was adapted for rest of the temperatures and concentrations.



Figure 3.3 Physica MCR 100 rheometer setup for viscosity measurements

3.5 Solubility measurements

N₂O solubility was measured in apparatus containing a stirred jacketed glass vessel with volume $1 \cdot 10^{-3} \text{ m}^3$ and a stainless steel gas holding vessel with a calibrated volume of $1.17 \cdot 10^{-3} \text{ m}^3$. Absorption flask was ensured dry and free of impurities by injecting N₂ and vacuum. Vacuum was generated by using vacuum pump upto pressure less than 2 KPa. The solution was weighed before injecting into the absorption vessel. Firstly, the vacuum was

generated inside by vacuum pump and the solution injecting line was filled with solution to ensure that there was no solution already in the line. Then the solution equal to the half of the level of the glass vessel was injected. The remaining solution in the flask was weighed and difference was calculated. This difference gave the exact amount of the solution added into the glass vessel. The solution was degassed by vacuum up to around 20 mbar and at ambient temperature. The glass vessel was equipped with outlet condenser and cooling medium using a Julabo F25 water bath to minimize the solvent losses. It was ensured that temperature of the Julabo F25 was about 4⁰C before degassing. When the temperature was stabilized, the cooling system and gas outlet were closed. The stirrer was switched on to ensure homogeneous mixing and to attain the equilibrium and it was set to 500RPM. The temperature of stirred glass vessel was maintained by a heating medium Lauda E300 glycol bath.



Figure 3.4 Experimental setup for solubility measurements

The solubility measurements were performed at different temperatures starting from 25⁰C and up to 120⁰C. The commercial N₂O gas was supplied by AGA Gas GmbH with a purity

of 99.999%. N₂O was injected to the glass vessel by opening the valve to the steel gas holding vessel at a maximum pressure of 600 kPa. Before the injection of N₂O, T_v (initial temperature) and P_v (initial pressure) of the glass vessels were recorded. The amount of N₂O injected was calculated from the difference in pressure of the gas supply vessel before and after feeding N₂O. Pressure and temperature of glass vessel and temperature of the gas were recorded after the temperature and pressure of the glass vessel were stabilized. Pressure was measured by two pressure transducers (Druck PTX 610 and PCE28) and temperature was measured by two K type thermocouples.

The experimental measurements were monitored in Labview computer program. All the readings were recorded in the excel sheet. The added amount of N₂O was calculated from the difference in pressure of the gas supply vessel before and after feeding N₂O as: (Hartono, 2009).

$$n_{N_2O}^{added} = \frac{V_V}{RT_V} \left[\frac{P_{v1}}{z_1} - \frac{P_{v2}}{z_2} \right]$$

P_v, T_v, z₁, z₂ and R are the pressure, temperature of gas holding vessel, compressibility factor of gas at initial and final conditions and universal gas constant respectively. The compressibility factor was calculated by using Peng Robinson equation of state.

The N₂O quantity in the gas phase of the vessel can be estimated by the following equation 3.1:

$$n_{N_2O}^{gas} = \frac{P_{N_2O}(V_R - V_S)}{zRT_R} \quad (3.1)$$

Here P_{N₂O} is the partial pressure of N₂O which is calculated by the following equation:

$$P_{N_2O} = P_R - P_S^o \quad (3.2)$$

Here P_R is the total pressure of jacketed glass vessel and P_S^o, the solvent vapor pressure.

V_s in equation (3.1) is the volume of the solvent. V_s is measured by density of the solvent.

The amount of N₂O in the liquid phase can be measured by:

$$n_{N_2O}^{liq} = (n_{N_2O}^{added}) - (n_{N_2O}^{gas}) \quad (3.3)$$

The N₂O concentration is calculated as follows:

$$C_{N_2O} = \frac{(n_{N_2O}^{liq})}{V_S} \quad (3.4)$$

The solubility of N₂O can be calculated by Henry's law constant relation:

$$P_{N_2O} = H_{N_2O} C_{N_2O} \quad (3.5)$$

3.6 Kinetics measurements

Kinetics measurements for CO₂ absorption in AMP and piperazine were performed on string of discs contactor and wetted wall column. These are described in the following section.

3.6.1 String of discs apparatus (SDC)

The absorption rates of CO₂ into aqueous amine solutions were measured using string of discs contactor as shown in the figure 3.4. It comprises an arrangement of 43 discs each with diameter ($d = 1.5 \times 10^{-2} \text{m}$) and thickness ($w = 4.0 \times 10^{-3} \text{m}$). Channel 3 for CO₂ has a capacity of 200NmL/mint and channel 2 of 20NmL/mint). CO₂ analyzer having a range of 0-10% was used for all the experiments. The active mass transfer area is 226.15cm² calculated by the following equation 3.6 (Hartono, 2009) and characteristic active length is 64.5cm.

$$A_{active}(m^2) = \left\{ 2 \cdot \pi \left(\frac{d}{2} \right)^2 + \pi d w - 2 w^2 \right\} \cdot n_d \quad (3.6)$$

Start-Up Procedure of SDC

Calibration Mode

First of all, valves of CO₂ and N₂ cylinders were opened followed by turning on the fan and fan regulator. Valves of MFC CO₂ were switched to the calibration mode. Flow of condensate water was opened. Experiment valve was closed in order to do the calibration. Main panel containing power supply for analyzers of MFC's of N₂ and CO₂ was switched on. Fan regulator was adjusted to get the desired gas flow rate.

The Labview program "co2 Kinetikk-manuell-hoved_V2" was opened from the computer desktop which was the control panel of apparatus for the data input and reading. Analyzer was chosen within the range of 0-10% CO₂ and saved the log file of the experiment.

Leakage test was done in the start by opening of 6% valve of N₂ MFC. Bubbles were seen in the gas outlet cylinder and indicated that there is no leakage. But there should not be any

bubbles in the gas secondary outlet cylinder. If any leakage found then it was removed by adjusting the fan regulator.

Afterwards, calibration was started by firstly setting the zero reading of CO₂ analyzer at 100% N₂ MFC opening. Different openings of MFC CO₂ using channel 2 and channel 3 were used (starting from 68% for channel 3 and channel 2 from 100% up to 10%). Five minutes were given for each opening and waited for the point to get stable. These points were recorded in the sheet. Channel 3 was calibrated first and channel 2 afterwards.

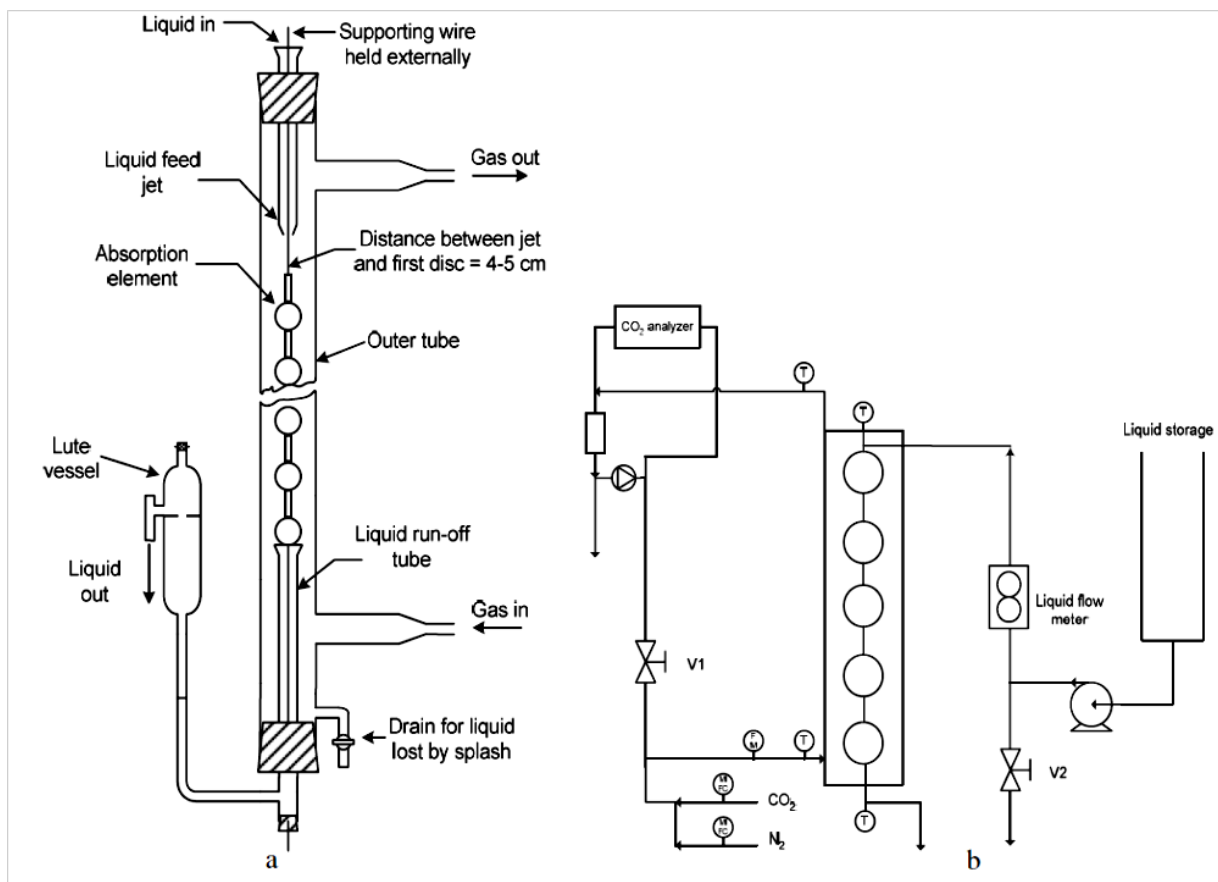


Figure 3.5 Experimental set-up of string of discs contactor apparatus

Experimental Mode

After finishing the calibration, switched the valves to experiment mode and closed the calibration valve. The bottle of 5L for liquid inlet was filled with the desired solution, turned on the heating element and adjusted the set point for temperature. Five K-type thermocouples were used to register the 4 inlet and outlet gas/liquid temperatures and the temperature inside the chamber (Ma'mun, 2005). Some of the liquid solution was drained from the inlet of the pump in order to avoid the air in the pump inlet. Firstly, 200 mL of

solution was drained out after passing through the string of discs contactor. Opening of N₂ MFC was changed to 6% and this value was used throughout all the experiments. This value of MFC N₂ opening was verified by performing an experiment. It was concluded from the experiment that if N₂ was opened more than this then it would not affect the flux anymore. It was waited for liquid and gas temperatures to get stable at the desired set point. Set the liquid flow rate to a value (50mL/mint) above which increasing the flow rate didn't affect the flux of CO₂ and it was verified by performing an experiment. Liquid flow rate was controlled by peristaltic liquid pump (EHPromass 83). CO₂ partial pressure was adjusted on analyzer (Fisher-Rosemount BINOS 100 NDIR CO₂ analyzer) to 1 KPa by setting the opening of CO₂. All the experiments were performed at 1 KPa of CO₂ using channel3 and channel 2. It was waited for the reading to get stable at 1 KPa of CO₂ partial pressure at the desired temperature for more than 5 minutes. After recording the readings, temperature was changed to higher desired value and kept close the flow of liquid and gas until the temperature was stabilized at the desired temperature. Liquid and gas flows were opened after the stabilizing of temperature. Experiment was repeated in the same way up to 70°C. When 5 liter of solution was finished in the first run, then the solution from the outlet bottle was shifted to the inlet solution bottle.

Shut Down Procedure

Stop button was pressed on the Labview program and closed the main screen window of Labview program. Liquid inlet valve, gas flow (N₂ and CO₂), and experiment valves were closed. Temperature was set to 25°C again and then closed the fan regulator and fan. At the end, cylinders valves of CO₂ and N₂ were closed.

The flux of CO₂ can be calculated by applying the solute balance over the entire system. The difference between CO₂ flow rate in the system and CO₂ out of the system gives the absorption flux of CO₂(Ma'mun, 2007, Hartono, 2009 and Aronu, 2011).

$$r_{CO_2}^{abs} \left(\frac{kmol}{s} \right) = Q_{CO_2}^{in} - Q_{CO_2}^{out} \quad (3.7)$$

The amount of CO₂ which is going out of the system can be calculated from:

$$Q_{CO_2}^{out} = Q_{N_2}^{in} \frac{y_{CO_2}^{out}}{1 - \left(\frac{P_{solution}}{P} \right) - y_{CO_2}^{out}} \quad (3.8)$$

Here $Q_{N_2}^{in}$ represents nitrogen flow rate into the system. $P_{solution}$ is measured using Raoult's law.

3.6.2 Wetted Wall Column (WWC)

The experimental setup for wetted wall is shown in the figure 3.6.

Start-up procedure of WWC

N₂ and CO₂ cylinders valves were opened and condensate water flow was also opened. Power supply for analyzers, gas pump of analyzer and computer was switched on. The two yellow valves in the main loop were closed. Labview program from computer desktop was run and saved the log file for the experiment. Fan and fan regulator were turned on. Leakage test was done by the opening of N₂ and bubbles were seen in the gas outlet bottle.

Calibration Mode:

Calibration was started by N₂ opening set to 1000NmL/mint on MFC and waited for the CO₂ analyzer reading to be zero. Two MFC's of CO₂ (Bronkhorst HIGH-TECH) having different capacities (0.2NI/min and 1NI/min) and CO₂ analyzer (Rosemount Binos 100) within the range of 0-10% were used during all the experiments. MFC B has a capacity of 200 nmL/mint and MFC C of 1nL/mint..After zero reading of CO₂ analyzer, set the opening of MFC B of CO₂ to 108NmL/mint. It was waited for reading to get stable for five minutes and repeated the same procedure for the different openings of MFC CO₂ up to 10%.

Experimental mode

The bottle of 5L for liquid inlet was filled with solution of desired solvent. The yellow valves in the main loop were opened and heating element was turned on. Temperature was adjusted to the desired value. Fan regulator was adjusted to get the desired gas flow rate and MFC N₂ was set to 100NmL/mint. The main gas circulation was provided by Rietschleside channel blower and measured by a calibrated orifice flow meter with a Foxboro differential pressure transmitter. The gas side pressure was monitored by a Drück pressure transmitter while the temperatures of liquid and gas (inlet and outlet) were monitored by four Pt-100 RTD transmitters.

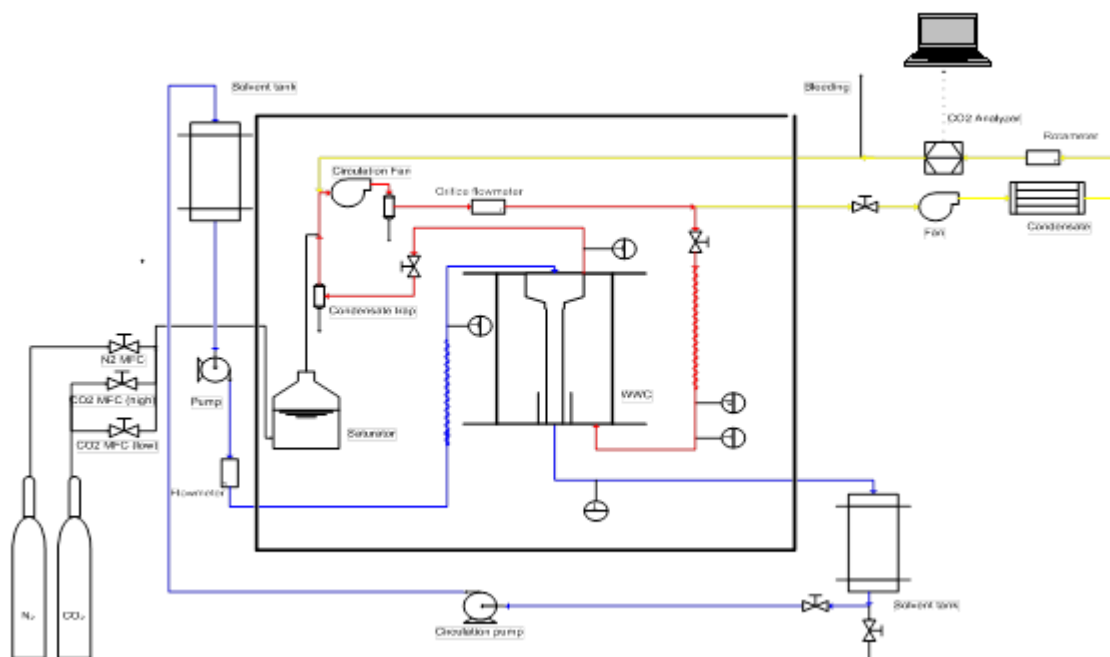


Figure 3.6 Experimental set-up of wetted wall column

Liquid flow rate was adjusted so that there were no fluctuations in the liquid film and film wetted the whole column. Liquid level was adjusted inside the column by using the valve. A flow rate of 50 mL/min for liquid inlet was used. Liquid pumped into the apparatus by gear pump (Micropump GA 180). 200 mL solution was drained out from the pump inlet in order to avoid any air at the pump inlet. MFC of CO₂ was set to a value and liquid flow rate was opened. It was waited to get the desired value of CO₂ partial pressure and be stable for five minutes. This point was recorded and repeated the same procedure for different partial pressures of CO₂. Liquid solution was recirculated by switching in the circulation pump. The same experimental procedure was adapted for measurements at other temperatures.

Shut-down procedure

The liquid level was lowered inside the column. The liquid and gas flow rates were stopped by setting the pump and MFC's of CO₂ to zero. Liquid in the storage bottle was transferred back to liquid inlet bottle with the help of circulation pump. Sample was collected after each experiment. CO₂ and N₂ cylinders valves were closed at the end.

CHAPTER 4

RESULTS AND DISCUSSION

4.1 Density measurements

The experimental measured densities of aqueous solutions of AMP, PZ and 3M CO₂-loaded (0.15/0.22/0.29/0.35) AMP at different temperatures (20-80°C) and concentrations are listed in the table A1, A2 and A3 in appendix A and results are shown in the figure 4.1(a), 4.1(b) and 4.2 respectively. The parallel measurements were done for each point to ensure the reproducibility of the data. The uncertainty in the measurements was approximately less than $\pm 0.1\%$ (see tables in appendix A) which shows the accuracy of the measurements and apparatus. The density of deionized water was also measured to ensure the apparatus working efficiency.

The equation 4.1 was applied in model for the density calculation of AMP aqueous solutions at all temperatures and concentrations while equation 4.2 was used to calculate the density of loaded AMP and piperazine aqueous solutions. The parameters K1, K2, K3, K4 and K5 are given in the table A4 in appendix A.

$$\rho\left(\frac{g}{cm^3}\right) = \left(1 + K_1 \cdot \frac{X}{T} + \frac{K_2}{T^2}\right) \cdot Exp\left[\frac{K_3}{T} + \frac{K_4}{T^2} + K_5 \cdot \frac{X}{T^3}\right] \quad (4.1)$$

$$\rho\left(\frac{g}{cm^3}\right) = \left(1 + K_1 \cdot \frac{X}{T} + \frac{K_2}{T^2}\right) \cdot Exp\left[\left(\frac{K_3}{T}\right) + K_4 \cdot \left(\frac{X}{T}\right)^{0.5}\right] \quad (4.2)$$

ρ = density (g/cm³), X = mass fraction, T = T in K

Effect of temperature and concentration on density

It can be observed from the figure 4.1(a), 4.1(b) and 4.2 that the density decreases as temperature and concentration increases. Density decrease was high at higher temperatures. At low temperatures (20-30°C), the difference between the densities of any two concentrations of the AMP and PZ was very small and this difference becomes large as temperature was increased. The parallel measurements (tables A1, A2 and A3 in appendix A) showed that the density values at 80°C were having the highest error but within the

range of $\pm 0.1\%$. The density values for DI water at 80°C are not in good agreement with the literature. It might be showing the apparatus sensitivity at high temperatures (80°C). But in case of loaded solutions, the change in volume due to addition of CO₂ affects the density at different temperatures.

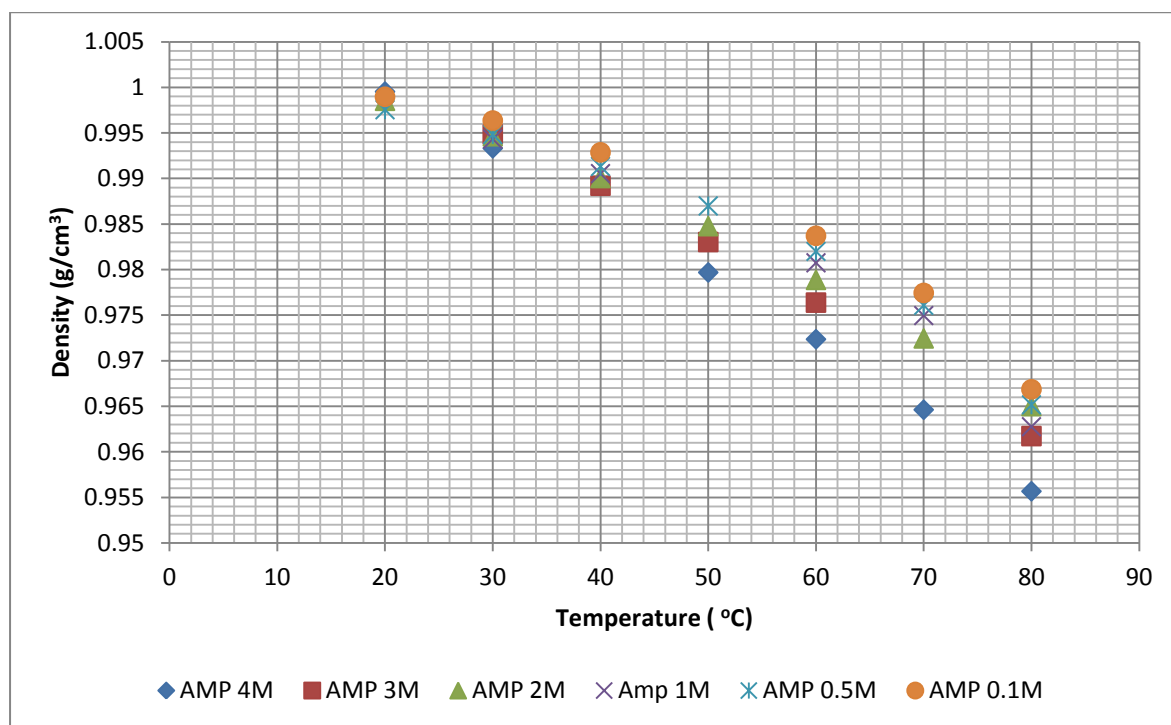


Figure 4.1(a) Experimental measured densities of AMP solutions at different temperatures (20-80°C)

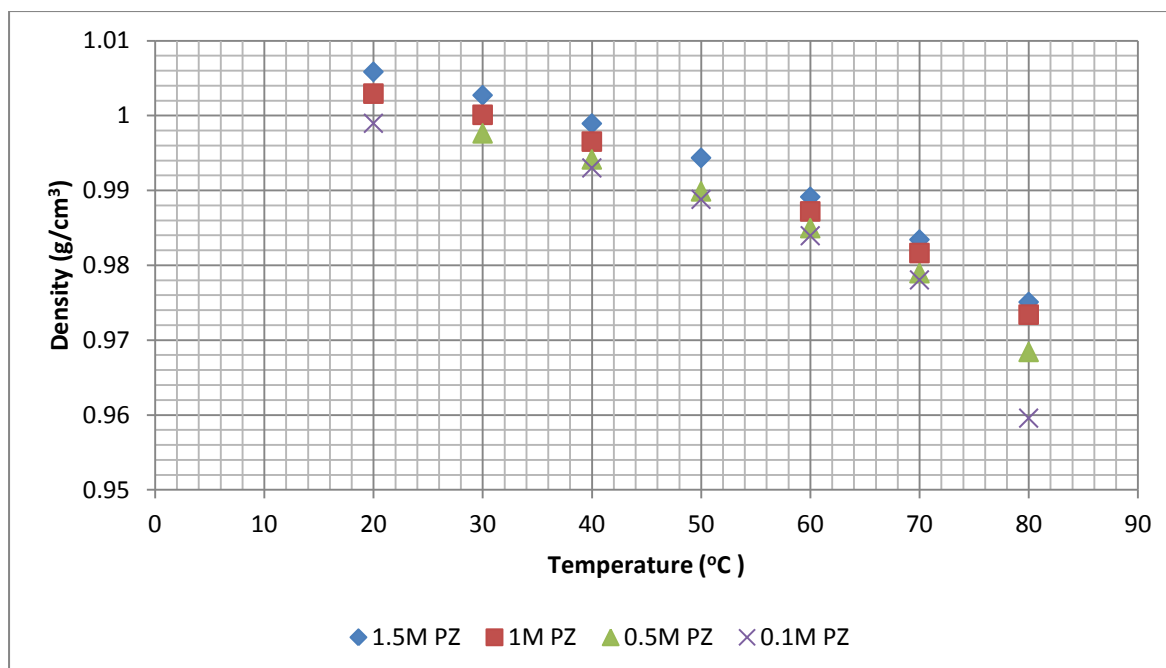


Figure 4.1(b) Experimental measured densities of piperazine solutions at different temperatures (20-80°C)

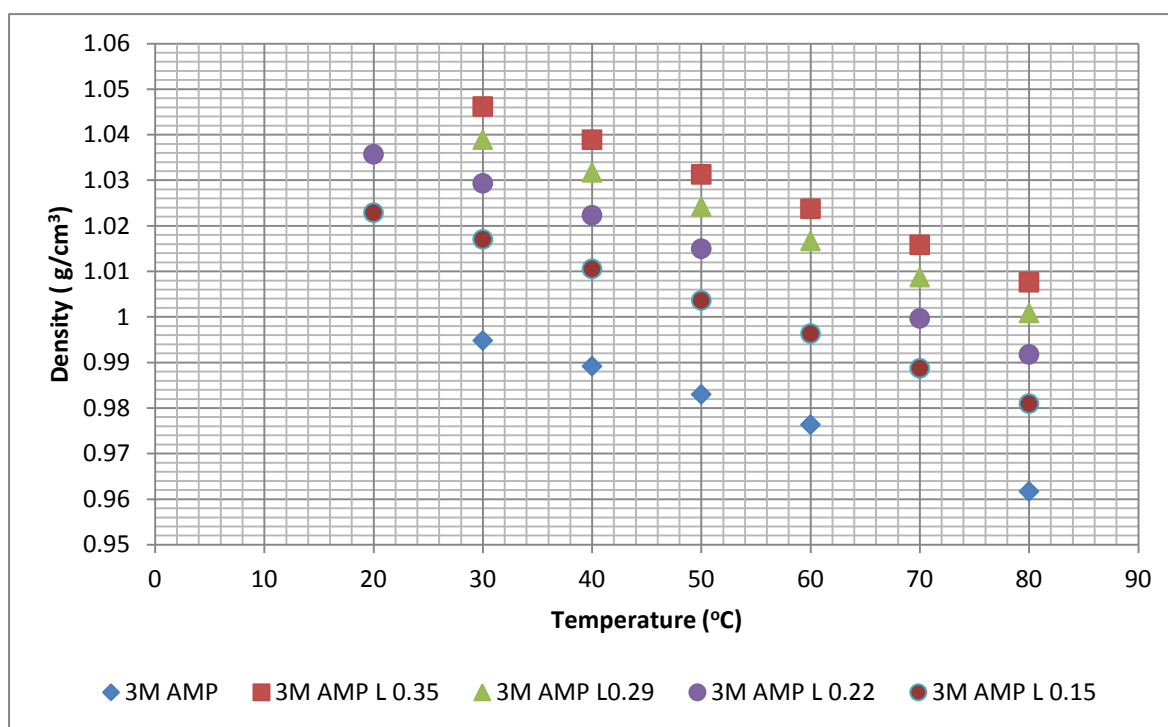


Figure 4.2 Densities of 3M AMP solution with different CO₂ loadings (L=loading)

Effect of loading

The effect of loading on the density of solution can be seen from the figure 4.2 in which density profiles of 3M AMP with loadings 0.15, 0.22, 0.29, 0.35 of CO₂ are plotted. The densities of loaded solutions are greater than the unloaded solution of AMP. The reason is the change in volume due to addition of CO₂. The density of solution with 0.35 loading of CO₂ is high among all and decreases with decrease in CO₂ loading.

4.2 Viscosity measurements

The viscosity data for AMP unloaded solutions with concentrations of 0.1/0.5/1/2/3/4 mole/liter, 3M AMP with CO₂ loadings of 0.15/0.22/0.29/0.35 and piperazine with concentrations of 0.1/0.5/1/1.5 mole/liter within temperature range of 20-80°C were presented in the table A5, A6 and A7 respectively. The graphical representation of the viscosity data of AMP unloaded, piperazine and 3M AMP loaded with CO₂ are shown in the figure 4.3, 4.4 and 4.5 respectively.

The following equation was used in the model to calculate the viscosity of all the unloaded and loaded solutions.

$$\mu(\text{mPa s}) = \left(1 + \frac{k_1 x}{T} + k_2 \left(\frac{x}{T}\right)^2\right) * \text{Exp}\left(\frac{k_3}{T} + \frac{k_4}{T^2} + \frac{k_5 x^2}{T^3}\right)$$

'X' is the mass fraction of amines and 'T' is the temperature in K. The parameters k_i were listed in the table A8 in the appendix A.

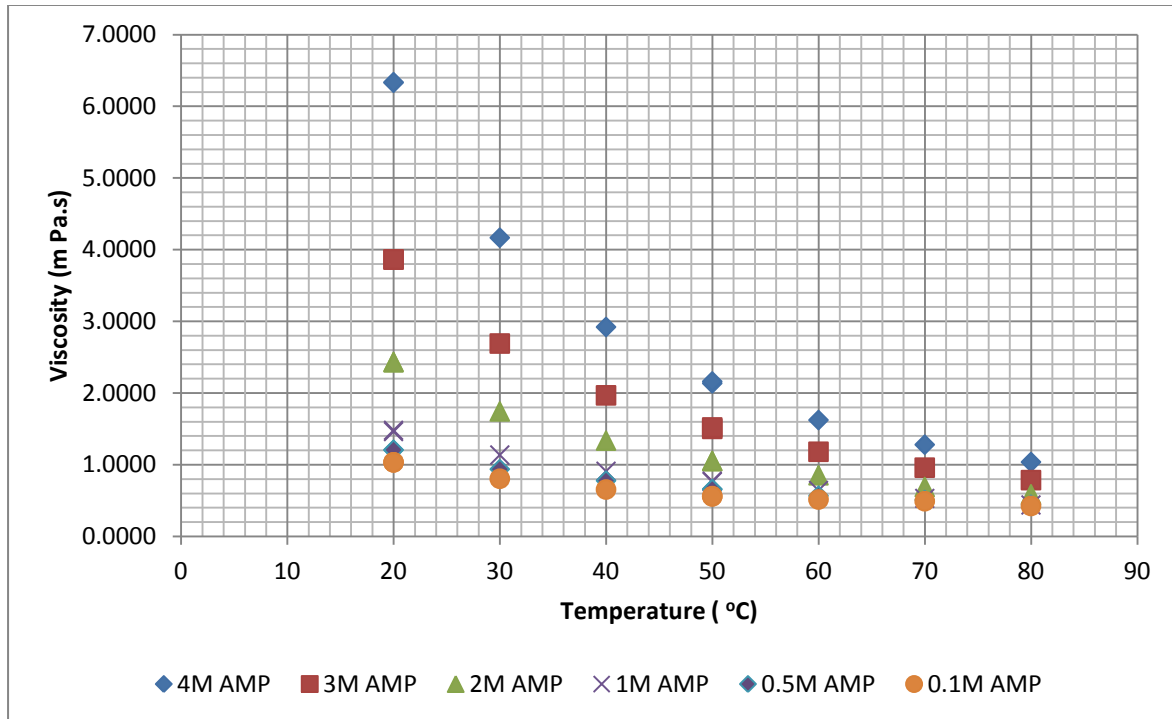


Figure 4.3 Experimental viscosity data of 4/3/2/1/0.5/0.1M AMP at different temperatures (20-80°C)

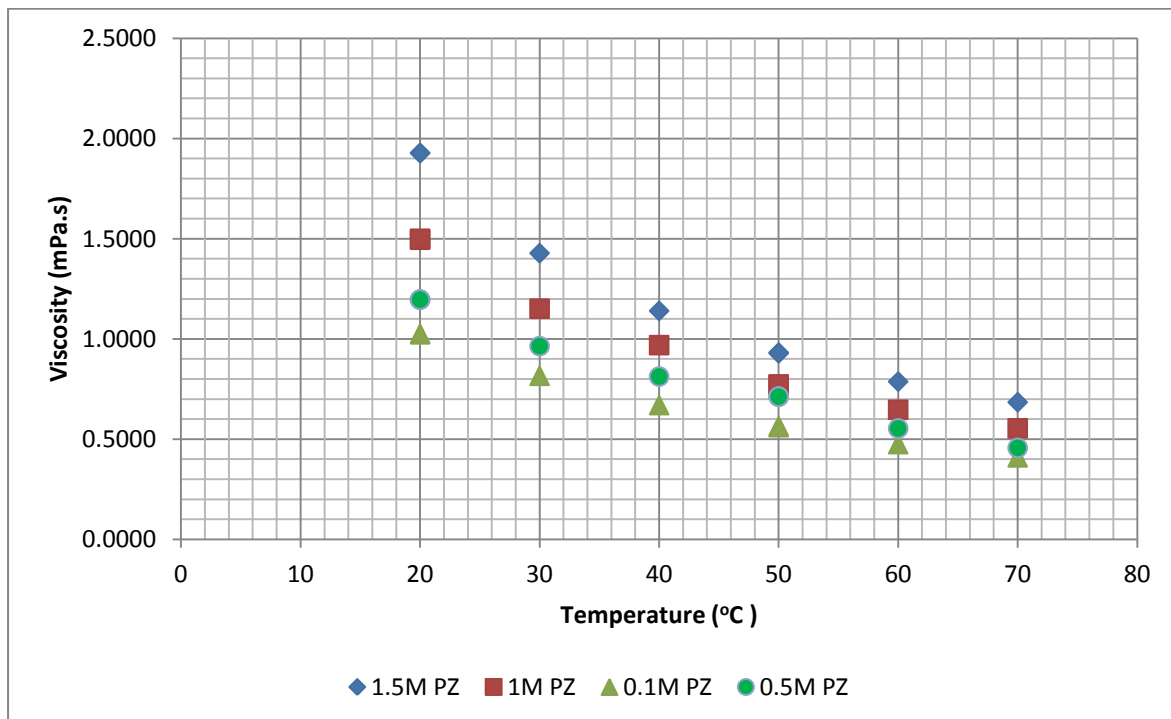


Figure 4.4 Experimental data for viscosities of piperazine solutions at different temperatures (20-70°C)

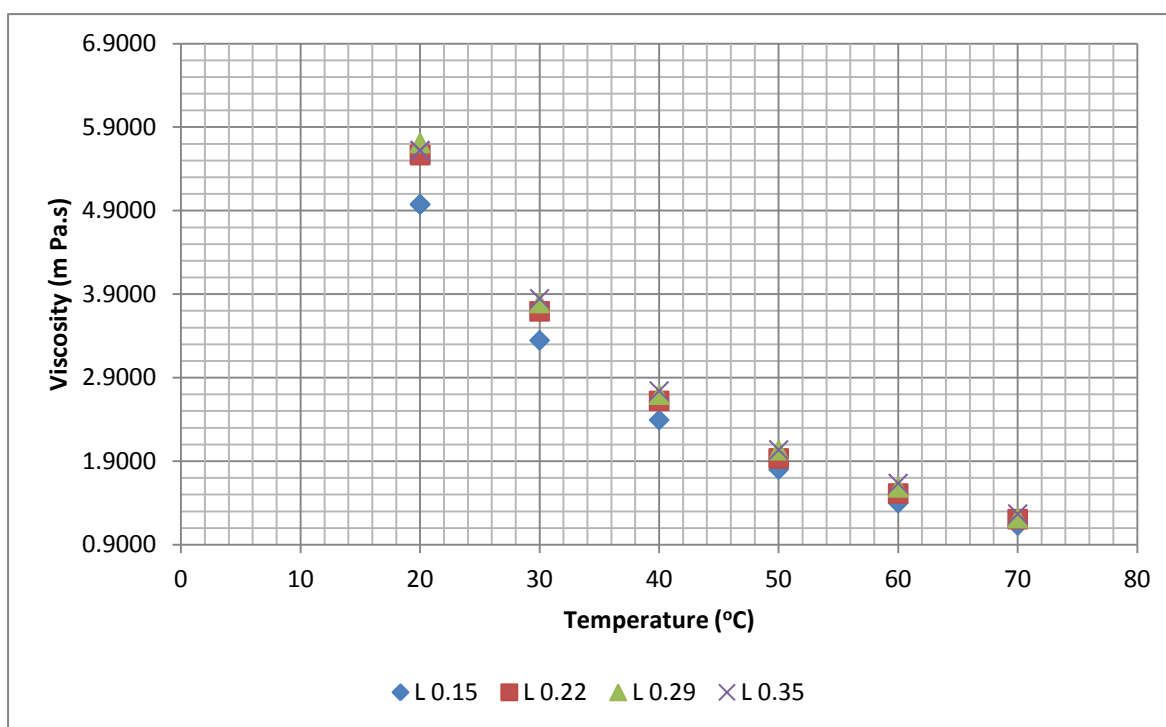


Figure 4.5 Experimental viscosities of 3M AMP Loaded solutions at temperatures (20-70°C); L=loading

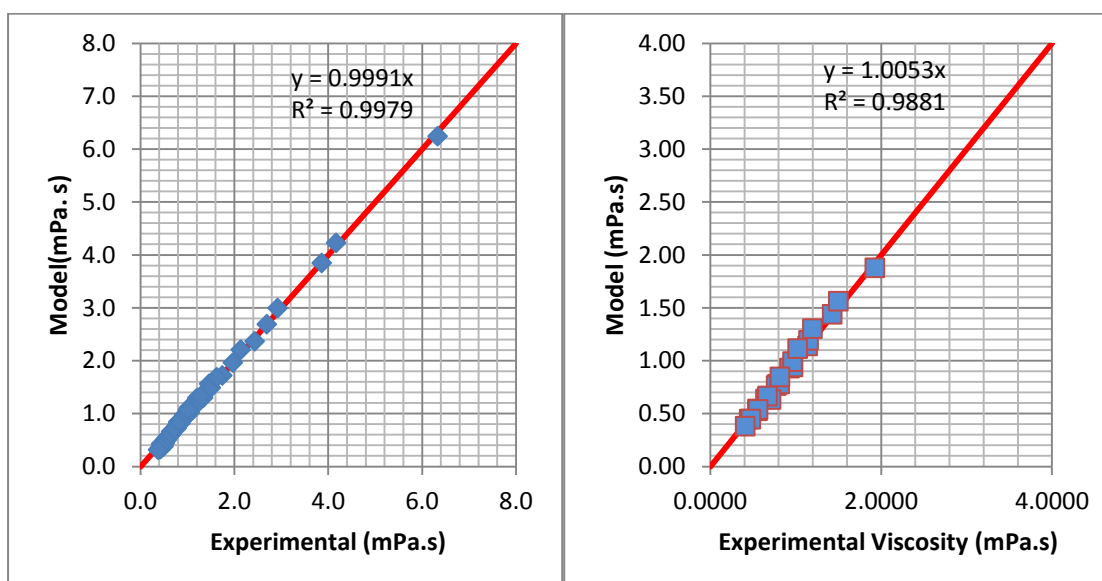


Figure 4.6 Comparison of experimental and model data points for AMP (left) and PZ (right)

Effect of temperature on viscosity

From the figure 4.3, 4.4 and 4.5, it can be seen that the viscosity of the solution decreases with the increase in temperature at all concentrations of AMP and PZ. The differences in the viscosities of solutions are less at higher temperatures (70 and 80°C) and even close values of viscosities at 70 and 80°C can be seen. This effect is due to the increase in the kinetic

energy of molecules with increase in the temperature and hence the relative motion of the molecules which decrease the resistance to flow.

Effect of concentration

The figures 4.3 and 4.4 presenting the graph between temperature and viscosity for different concentrations of AMP and PZ solutions show that viscosity is higher for higher concentration at constant temperature and vice versa. The apparatus did not give good results at a viscosity lower than 0.5 (mPas). The viscosity of 0.1/0.5M AMP and 0.1MPZ at 70°C was less than 0.5mPas and it gave different results in parallel measurements. That's why the results for the viscosity are a bit uncertain at a value lower than 0.5mPas.

Effect of loading of CO₂

The viscosity data for 3M AMP solutions with CO₂ loadings of 0.15/0.22/0.29/0.35 with temperature range of 20-70°C are represented in the figure 4.5. The figure 4.5 showed that viscosity increases with increase in the loading of CO₂ in the solution due to the more ionic presence in the system but decreases with increase in temperature.

Comparison with the model

The experimental data for AMP and piperazine were also compared with the model in the figure 4.6. The model fitted well for both AMP and PZ with % error of ± 1 for AMP and piperazine.

4.3 Solubility measurements

The measured Henry's constants in AMP, PZ and AMP (loaded with CO₂) aqueous solutions for the temperatures (25, 40, 60, 80 and 100°C) were presented in table A9, A10 and A11 in appendix A and graphically represented by figures 4.7, 4.8 and 4.9 respectively. The measured solubilities were for AMP concentrations of 0.1/0.5/1/2/3/4 mole/liter, 3M AMP with CO₂ loadings of 0.15/0.22/0.29/0.35 and PZ concentrations of 0.5/1.5 mole/liter. The solubility measurements for unloaded AMP solutions were done by another master student while loaded AMP solutions and piperazine solutions Henry's constants were measured in the present work.

N₂O solubility in AMP and PZ solutions were predicted by the Redlich-Kister equation (equation 2(a)) mentioned in chapter 2. The parameters for the equation are shown in the table A12 in appendix A.

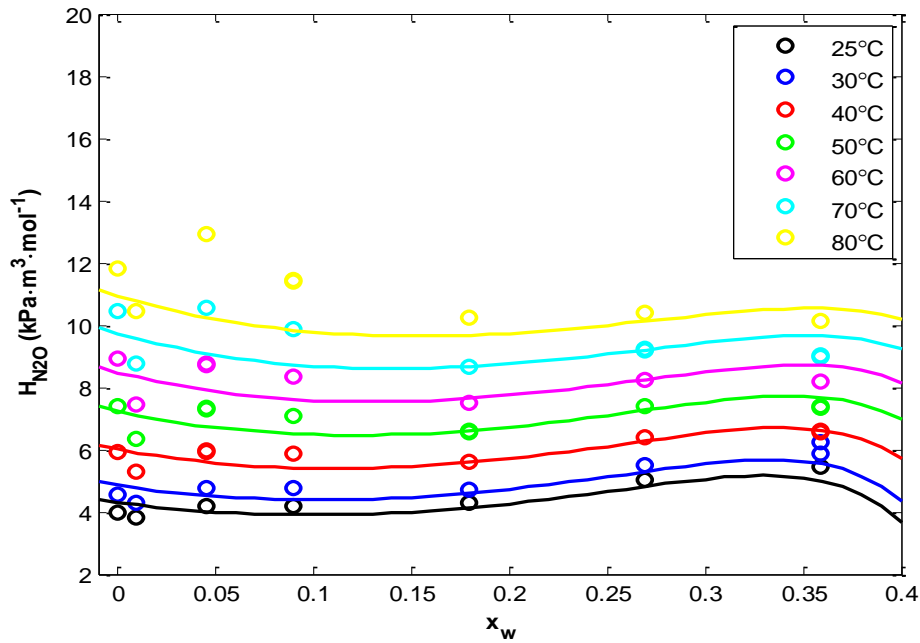


Figure 4.7 Henry's constant for different concentrations of AMP at temperature range of 25-80°C; 0.358 $x_w/4M$, 0.268 $x_w/3M$, 0.179 $x_w/2M$, 0.089 $x_w/1M$, 0.044 $x_w/0.5M$, 0.0089 $x_w/0.1M$

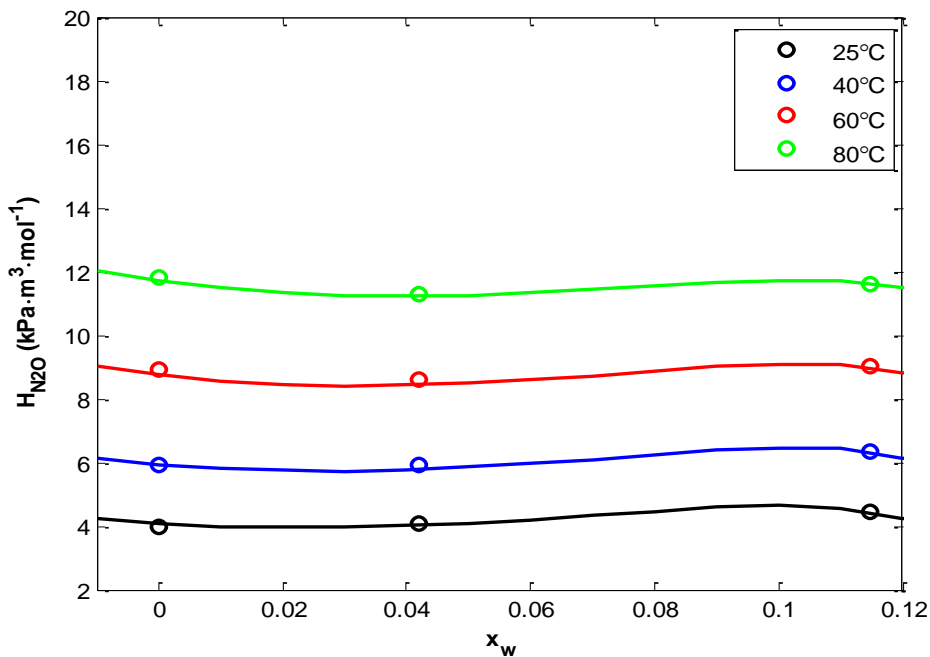


Figure 4.8 Henry's constant for different concentrations of PZ at temperature range of 25-80°C; 0.11 $x_w/1.5M$, 0.0419 $x_w/0.5M$

The values of Henry's constant are very important in order to predict the kinetics of amine.

The following equation was used in the model to predict the Henry's constants:

$$H(KPa\ m^3/mol) = \left(1 + \frac{k_1 x}{T} + k_2 \left(\frac{x}{T}\right)^2\right) * \text{Exp}\left(\frac{k_3}{T} + \frac{k_4}{T^2} + \frac{k_5 x^2}{T^3}\right)$$

X is the mass fraction and T is the temperature in K. The parameters k_i are listed in the table A12 in appendix A.

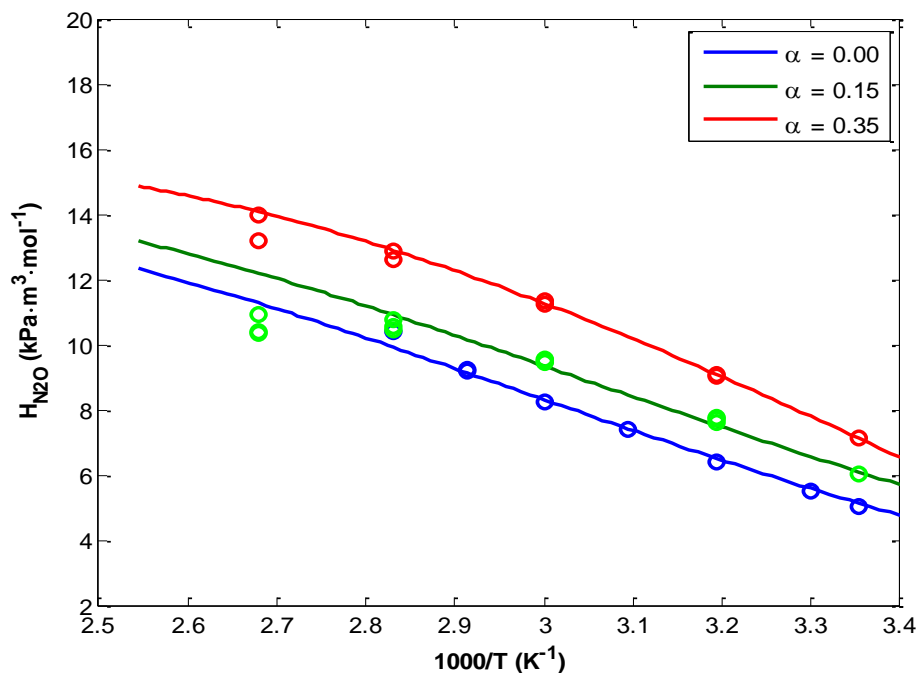


Figure 4.9 Henry's constant for 3M AMP with 0.15 and 0.35 CO₂ loadings (α) at temperature 25-100°C

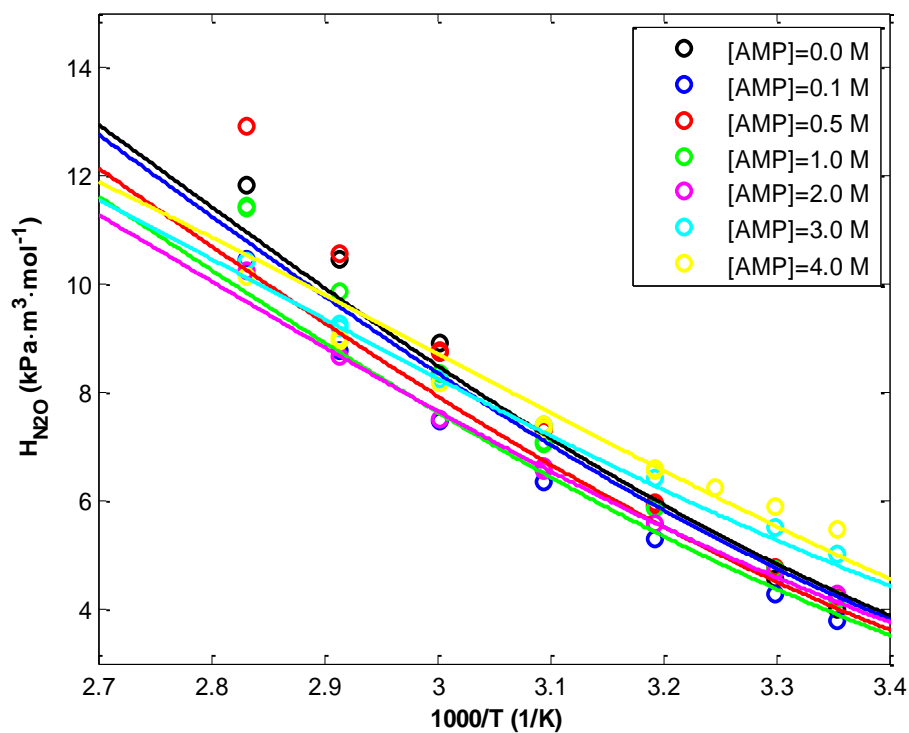


Figure 4.10 Temperature dependencies of Henry's constants for different concentrations of AMP

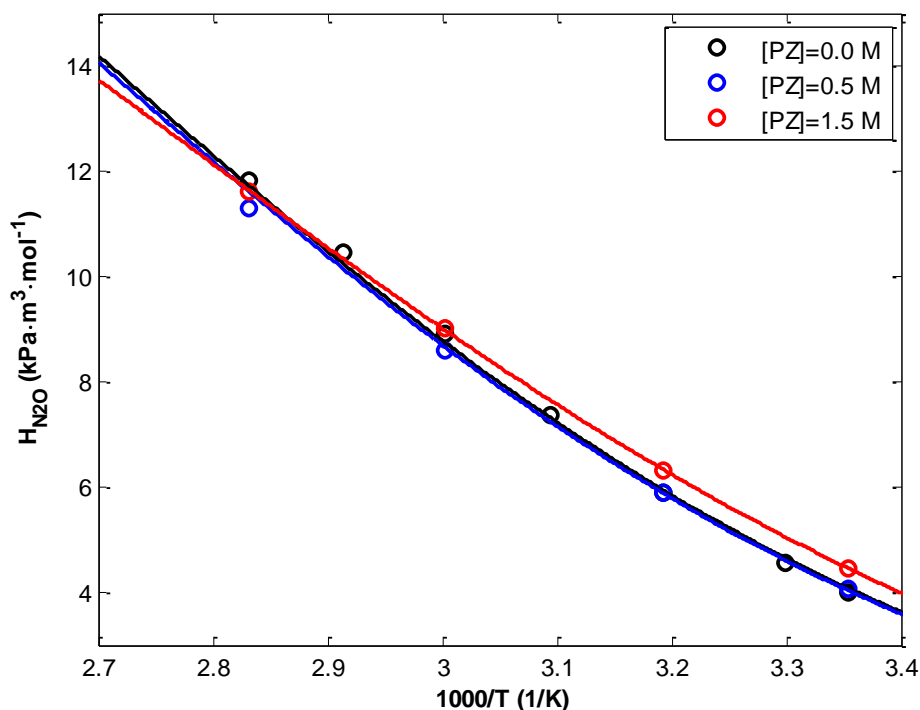


Figure 4.11 Temperature dependency of Henry's constants for different concentrations of PZ

Effect of concentration

From the figure 4.10, the model over predicted for 4, 3 and 2M AMP at 25, 30 and 80°C. The model didn't catch the lower concentration (<0.5M) points and the data seemed to be scattered at 80°C. Henry's constant is a strong function of concentration and temperature. The results for solubility measurements for AMP presented in the figure 4.7 also showed that the solubility firstly decreases up to 17% weight fraction (2mole/liter) then increases up to 35.6% weight fraction (4 mole/liter). Similar trends were seen for the piperazine in figure 4.8 and the model fits well for piperazine.

Effect of temperature and CO₂ loadings

The Henry's constants are directly temperature dependent and the results shown in the figures 4.10 and 4.11 showed the similar trends. Henry's constant were the highest at higher temperatures and low at lower temperature. The model over predicted in case of loaded AMP and under predicted in case of unloaded AMP at temperatures of 70 and 80°C. The Henry constant increases with increase in the loading of CO₂. At temperatures of 60 and 70°C, the model over predicts for CO₂ loadings of 0.15 and 0.35

4.4 Liquid flow rate

Experiments were performed to observe the effect of liquid flow rate on CO₂ absorption flux in AMP using string of discs contactor. The results obtained from the experiment are shown in the figure 4.12 in which liquid flow rate is plotted against CO₂ absorption flux. 1M AMP solution was used and experiments were run at 25 and 50°C for different liquid flow rates (5-100mL/min) at a constant gas flow rate of 3.63Kg/hr. From the figure 4.12, the CO₂ absorption flux is independent of liquid flow rate above 50 mL/min at both the temperatures 25 and 50°C. Liquid flow rate doesn't change so much from 40-50 mL/min. The absorption flux for 25°C is high than 50°C up to 30mL/min of liquid flow because fresh solution was not used for the experiment. So, on the basis of these results, the whole experiments on SDC (string of discs) were performed with 50mL/min of liquid flow rate.

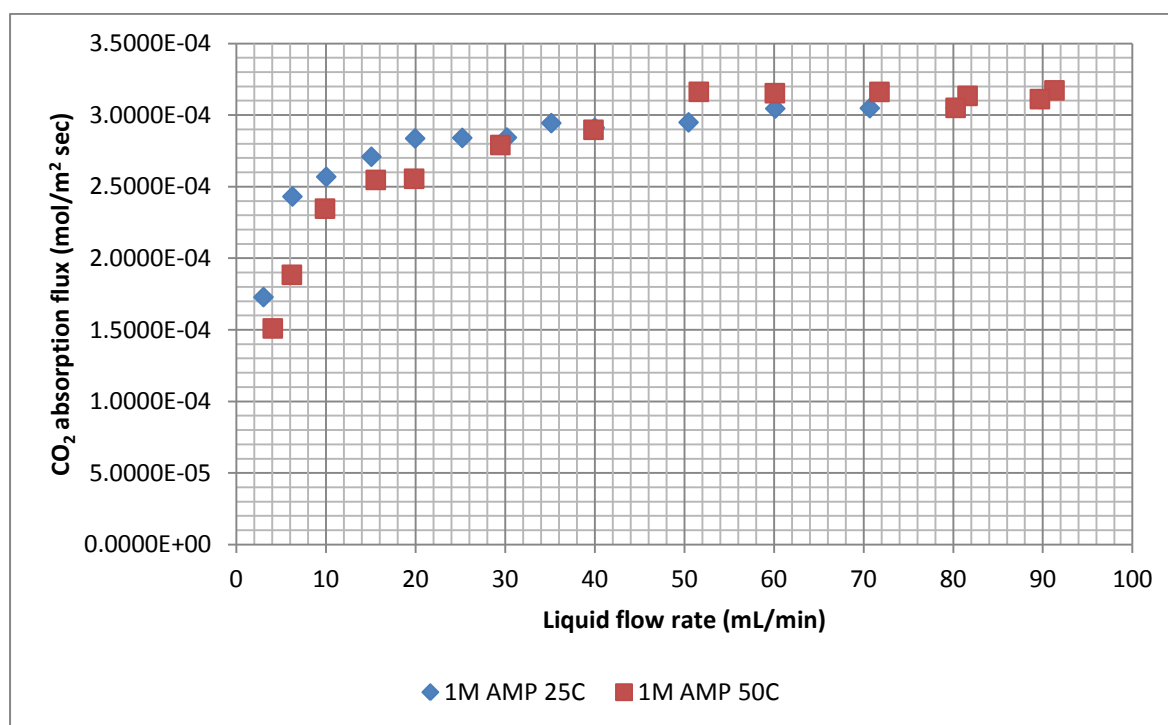


Figure 4.12 CO₂-Absorption fluxes for different liquid flow rates

4.5 Nitrogen flow rate

Different nitrogen flow rates were tested for AMP (0.5M) to see the effect of N₂ flow rate on the mass transfer resistance. The experiment was measured on string of discs contactor. The results were plotted in figure 4.13 where nitrogen flow rate were plotted against mass transfer resistance. The results showed that increasing the nitrogen flow rate

above 0.04 mol/sec doesn't affect the mass transfer resistance. So, 0.04 mol/sec was used as nitrogen flow rate for the whole experiments on string of discs contactor.

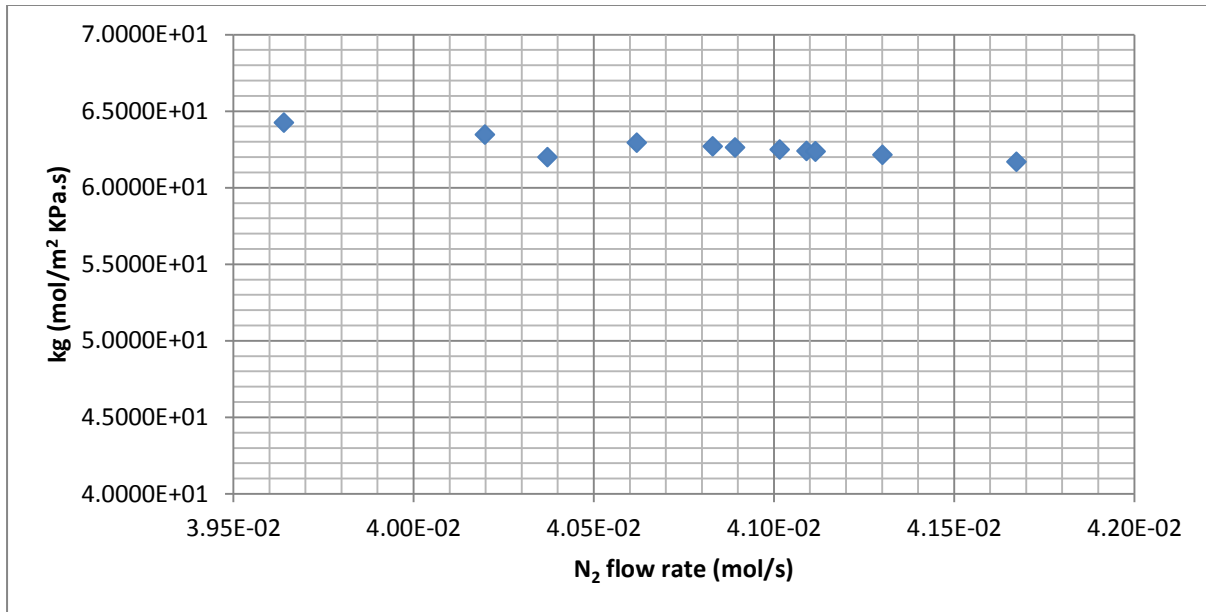


Figure 4.13 Mass transfer resistances for different nitrogen flow rates

4.6 Gas circulation rate

The experimental data points for different gas circulation rates against the absorption flux have been shown in the figure 4.14. The experiment was performed on 5M MEA solution at 25°C in string of discs contactor. Gas circulation rate should be high enough so that there is no back pressure in the system and smaller mass transfer resistance. The gas circulation rates from 0.00498-0.0354 mol/sec were observed and there is the highest CO₂ absorption flux at 0.0354 mol/sec. So, it was recommended as gas circulation rate for whole range of experiments on SDC (string of discs).

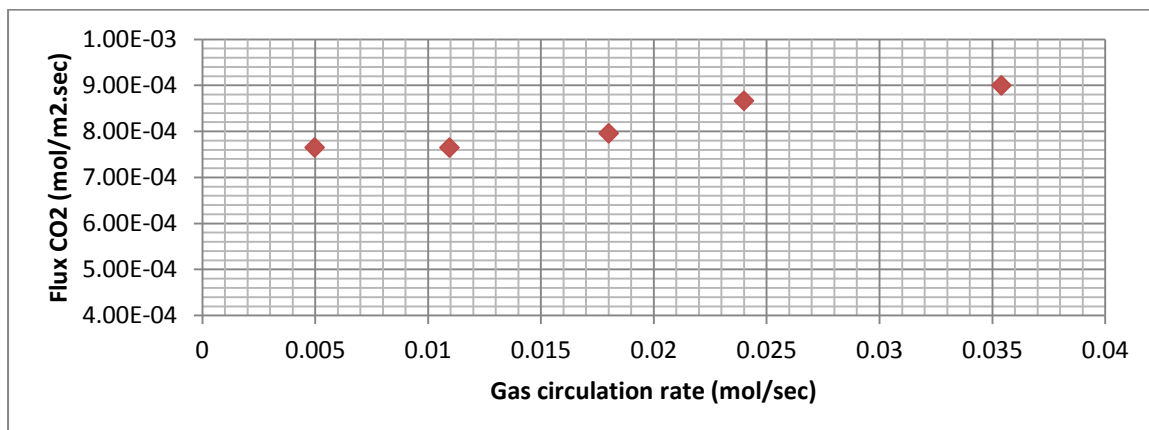


Figure 4.14 Experimental data of gas circulation rates

Kinetics of CO₂ absorption in AMP aqueous solutions

4.7 Absorption flux dependency over temperature and concentration

The kinetics measurements for AMP were measured on the string of discs apparatus at different temperatures, concentrations and loadings of CO₂. All the measurements for unloaded AMP solutions were carried out at 1KPa of CO₂ partial pressure. Low partial pressure of CO₂ (1KPa) was chosen because of AMP quite slow reaction with CO₂ and to ensure the better accuracy in CO₂ flux. The results for CO₂ absorption flux at temperature range of (25-70°C) for concentrations of 0.1/0.5/1/2/3/4M are plotted in the figure 4.15.

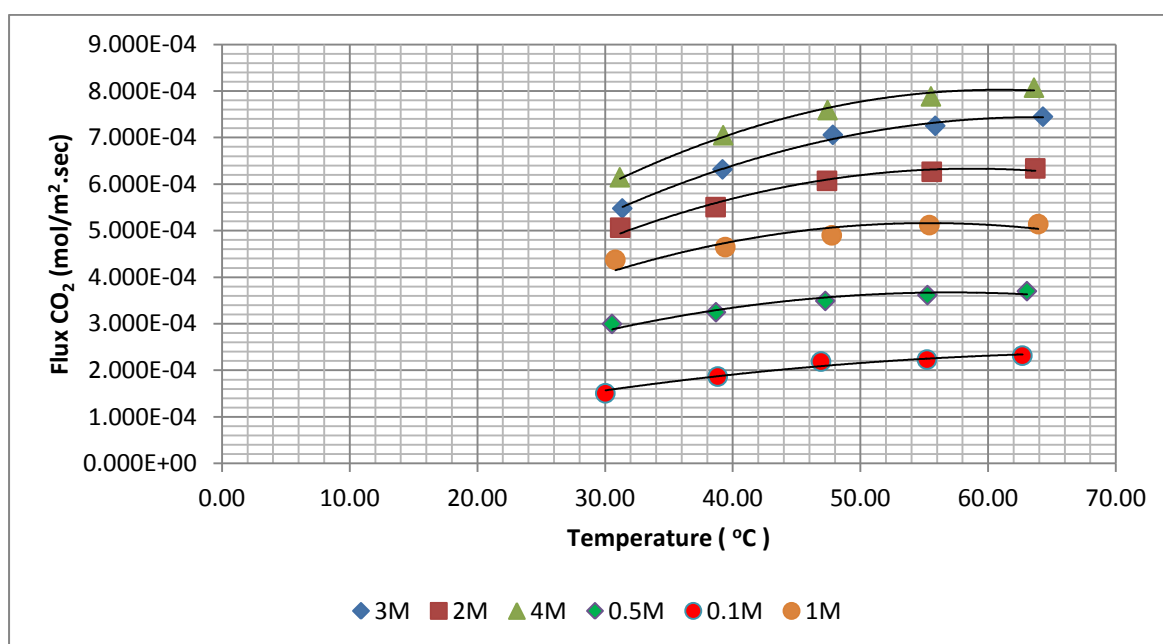


Figure 4.15 Experimental data for absorption flux of CO₂ for all AMP solutions at temperatures (25-70°C)

From the experimental data in figure 4.15, it can be seen that rate of CO₂ absorption increases with increase in the temperature. But the increase in absorption flux at 60-70°C is not so much as compared to lower temperatures (<60°C). The reason for this may be the solution becomes saturated with CO₂ when reach at high temperatures and it cannot absorb more CO₂. The fresh solution was being used in the start of every experiment on string of discs contactor and solution had to be recirculated after 5 liter was finished. The absorption flux showed maximum at 70°C for all the temperatures. The temperature was averaged for liquid inlet and outlet because the temperatures achieved during the experiments were not exactly 25 or 30°C. The fact for this poor temperature control is that when liquid goes out in the discharge storage tank, it remains outside under ambient conditions until 5L is finished.

When this liquid is recirculated back to inlet liquid tank then temperature of the solution doesn't remain the same. It became lower than it was.

From the figure 4.15, it can also be observed that absorption flux increases as concentration of solution increases. The absorption flux has direct dependence of concentration (partial pressure). The CO₂ absorption flux is of the order: 4M>3M>2M>1M>0.5M>0.1M. The experimental data shows that the absorption flux difference between 4 and 3M is less than between 0.5 and 1M due to the changes in the physiochemical properties (density, viscosity and solubility) of the solution at different temperatures.

4.8 Reproducibility of the data

To ensure the experimental data points for different concentrations of AMP and at temperature range of (25-70°C), the three experiments for 4, 3 and 2M of AMP at different temperatures were repeated. The data points obtained for absorption flux of CO₂ in 4, 3 and 2M AMP at temperature range of 25-70°C are plotted in the figure 4.16. It can be analyzed from the figure 4.16 that the data points are accurate with a standard deviation of 7.375e-5/7.653e-5/5.002e-5 for 4/3/2M AMP respectively.

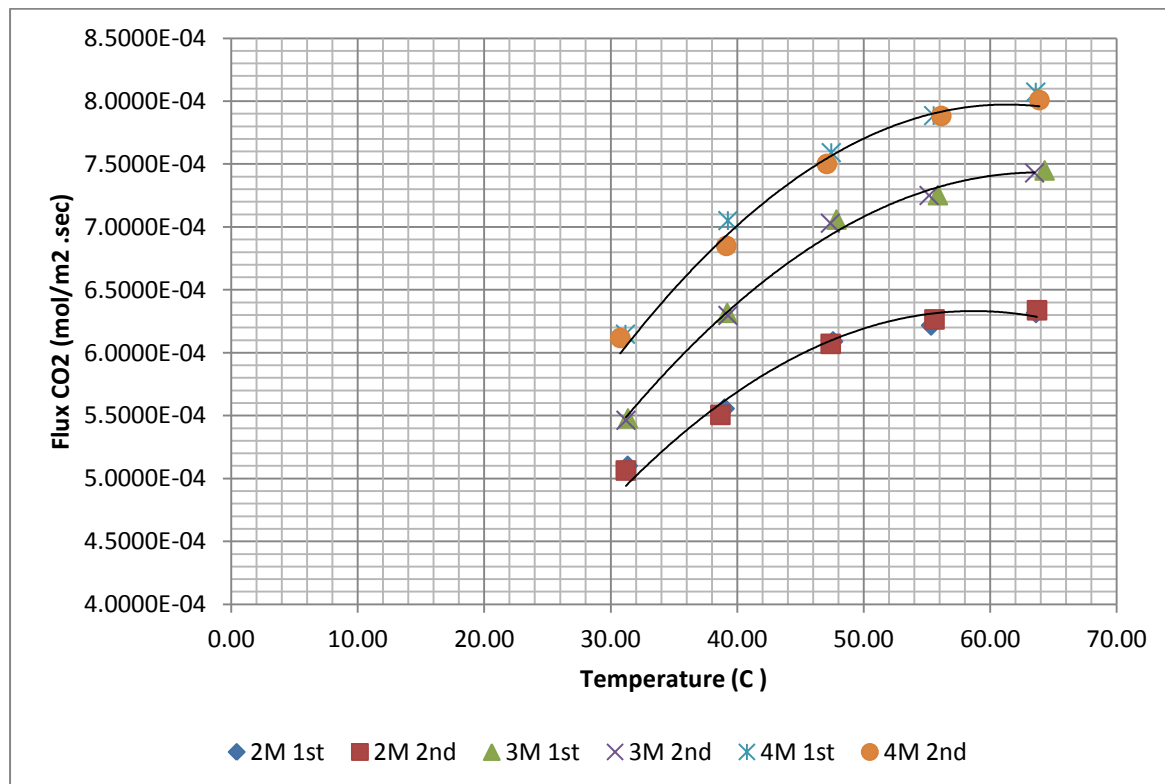


Figure 4.16 Reproducibility of the data for (4,3 and 2M) AMP solutions on string of discs

4.9 Overall mass transfer coefficient

The overall mass transfer coefficient for different concentrations of AMP and at temperature range of (25-70°C) are graphed in the figure 4.17. The overall mass transfer coefficient increases with increase in the temperature. The results also show that overall mass transfer coefficient increases with increase in concentration of the solution. It means that there is more ease for the mass transfer at higher concentrations than at lower concentrations.

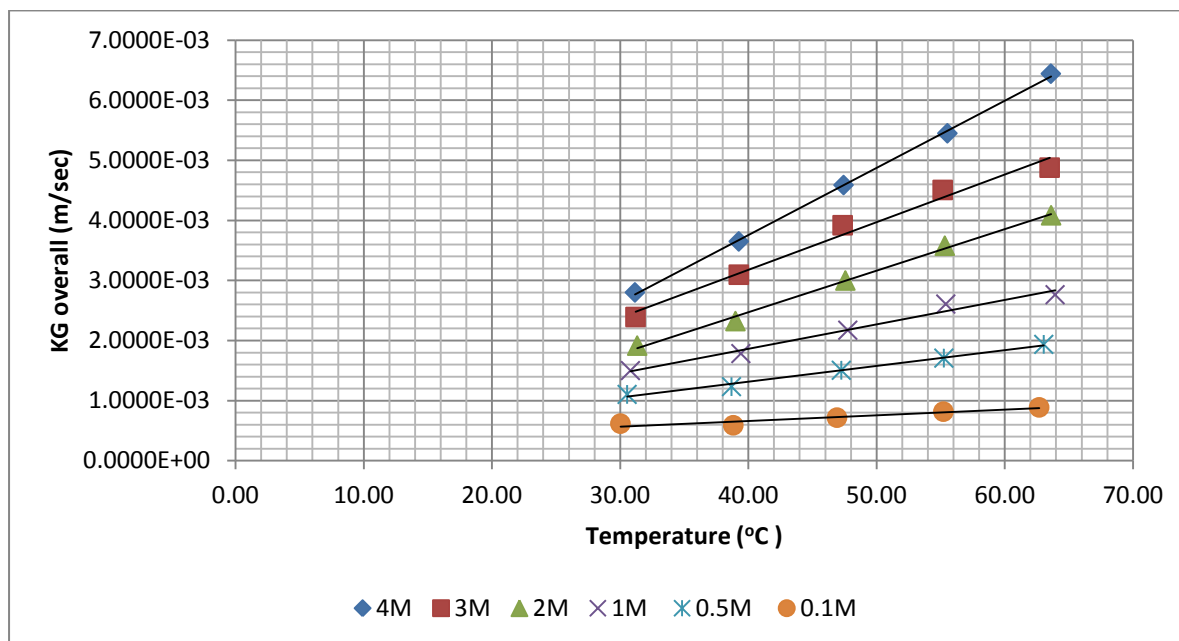


Figure 4.17 Gas side mass transfer coefficient at different temperatures and concentrations of AMP

4.10 Second order rate constant

The Arrhenius type of second order rate constants for AMP concentrations of 0.1/0.5/1/2/3/4M was plotted in the figure 4.18. The trends showed that there was direct dependency of the rate constant over temperature and concentration.

The trend lines for K_2 values were linear but the slightly difference in linearity is due to the results of physiochemical properties. The values for the rate constants at lower concentrations and temperatures are very close with very small difference among them. The reason for this was the results for very close physiochemical properties at lower temperatures and lower concentrations which affects the K_2 values. The solubility affects the K_2 values more than density and viscosity. The other reason could be the very low flow rates of CO₂ on MFC were used during experiments on SDC to get 1KPa pressure and that creates the uncertainty in flux.

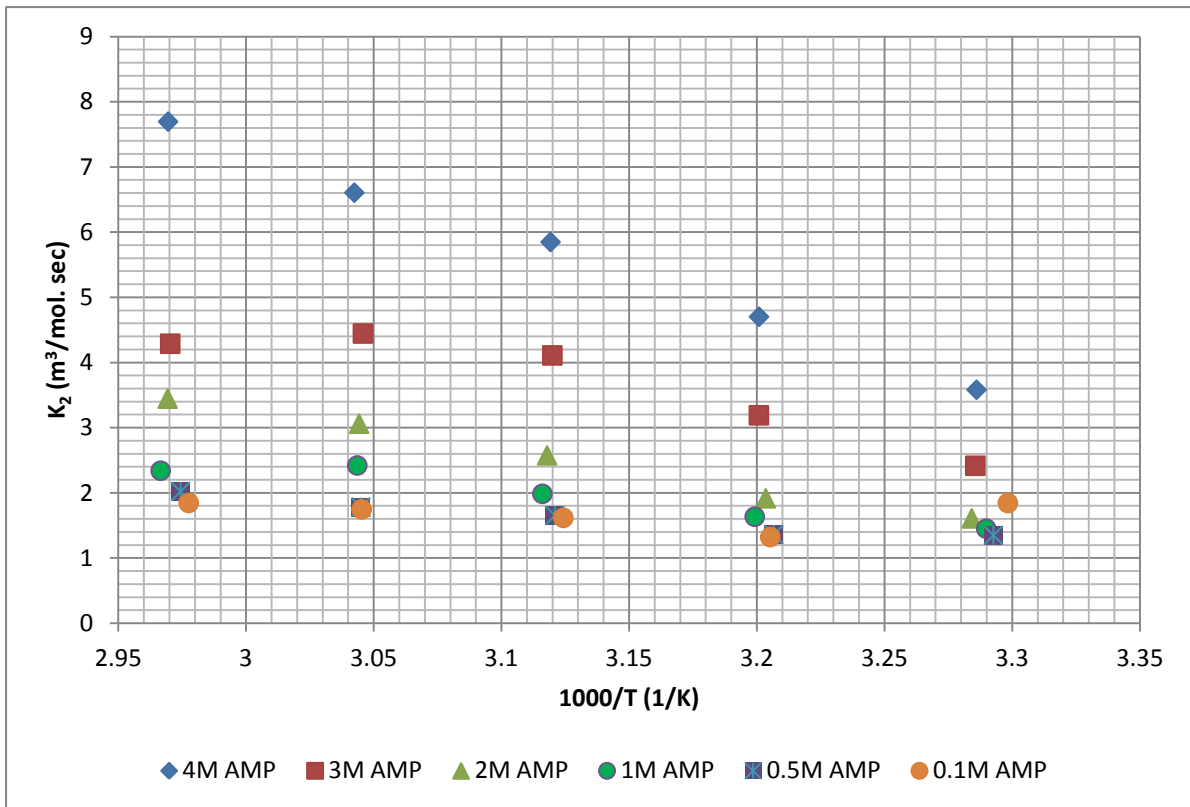


Figure 4.18 Arrhenius type temperature dependency of second order rate constant for AMP solutions

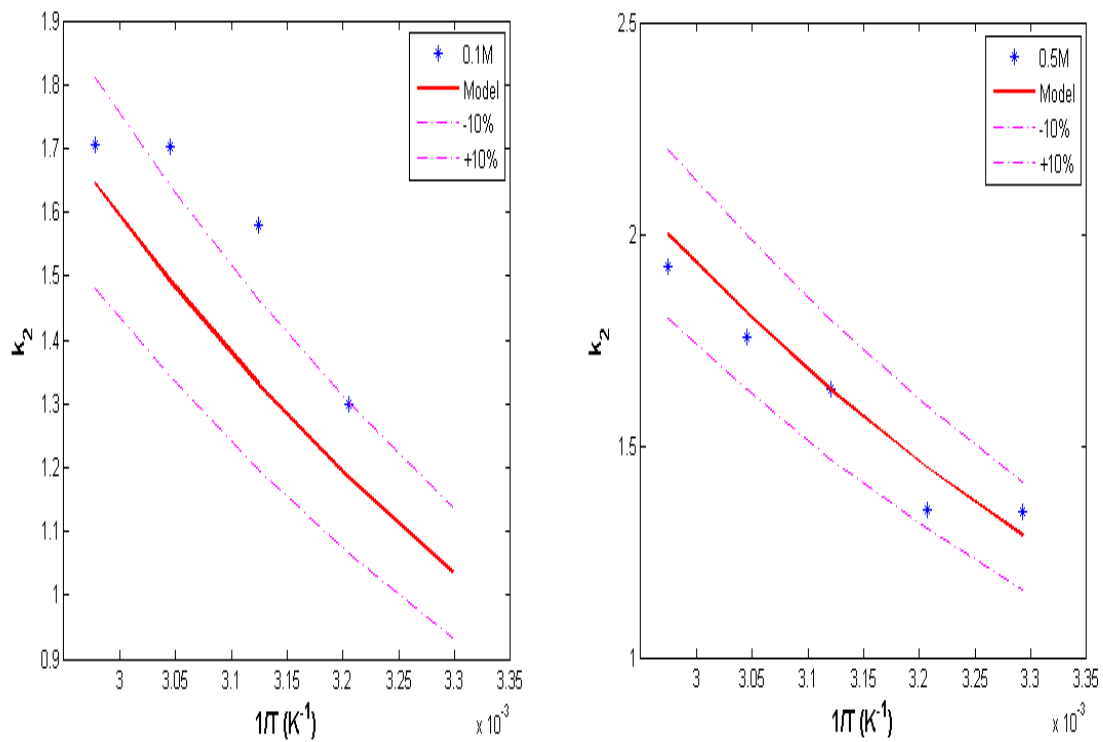


Figure 4.18(a) Arrhenius type second order rate constant for 0.1M AMP (left) and 0.5M AMP (right)

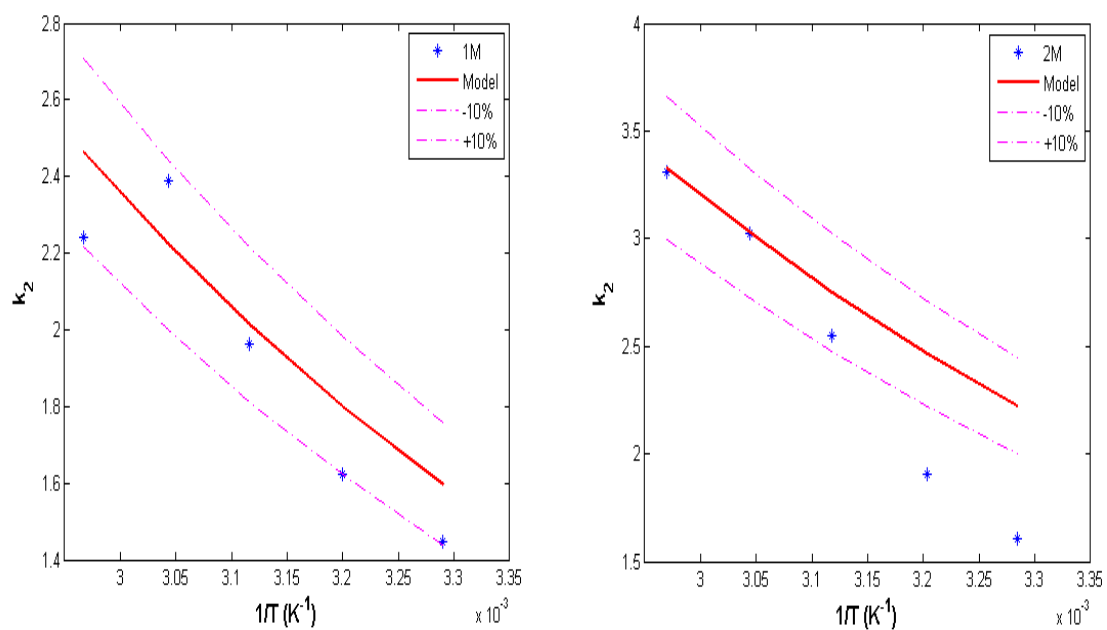


Figure 4.18(b) Arrhenius type second order rate constant for 1M AMP (left) and 2M AMP (right)

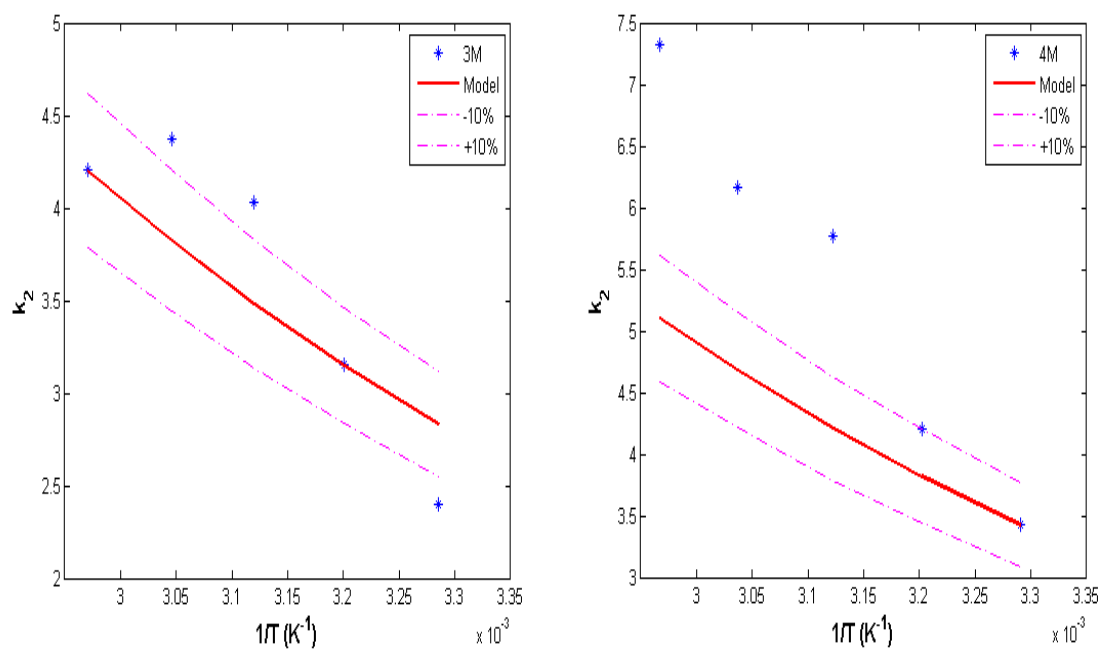


Figure 4.18(c) Arrhenius type second order rate constant for 3M AMP (left) and 4M AMP (right)

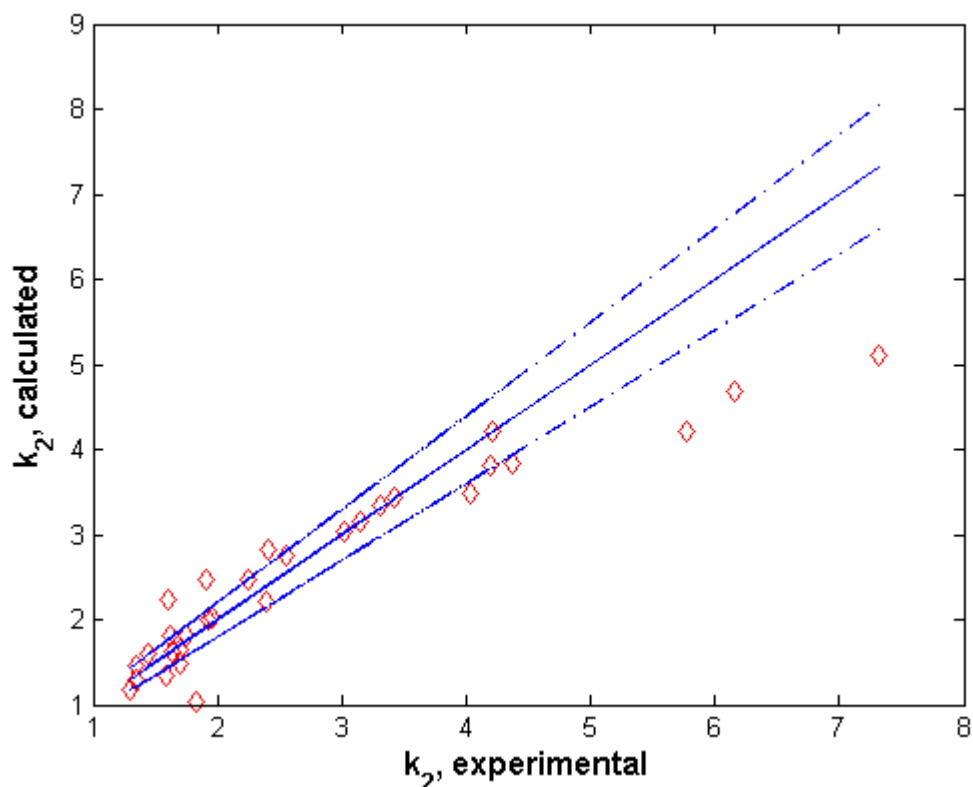


Figure 4.18(d) Comparison of experimental and calculated second order rate constant for AMP

The experimental measured data of second order rate constants of AMP at different concentrations were also plotted in the figures 4.18(a, b, c). The experimental data was fitted in the model and results for experimental and calculated second order rate constant were shown in the figure 4.18(d). The figure 4.18 (d) showed that the model fits the lower concentrations well and data was more scattered at higher concentrations (3 and 4M). The second order constant involves many parameters and physiochemical properties affect the K_2 value. The equation 4.4 was used to calculate the second order rate constant in the model. The K_2 in equation 4.4 equals $K_{obs}/(AmH)$. The termolecular mechanism was applied considering pseudo first order assumption. The (OH^-) were neglected as its concentration was very low as compared to H_2O and AMP.

$$K_2 = \left(A * \exp\left(\frac{B}{T}\right) * (AMP) \right) + \left(C * \exp\left(\frac{D}{T}\right) * H_2O \right) \quad (4.4)$$

Where $A = 0.033036299$, $B = -1171.8529$, $C = 0.0025321695$, $D = -1505.0385$

The AARD was calculated by using the following formula and AARD was 11.8491% for fitting the model with experimental data which is quite reasonable. The reason to this was the measured solubilities for AMP.

$$Error = \left(\frac{K_{2c} - K_{2e}}{K_{2e}} \right)$$

$$AARD = \text{sum} \left(\frac{\text{abs}(err)}{\text{Length } T} \right) * 100$$

Where length (T) = number of experiments = 30

Kinetics of CO₂ absorption in loaded AMP solutions

4.11 Flux dependency over loading and temperature

The experimentally determined absorption flux of CO₂ for 3M AMP with CO₂ loadings of 0.15/0.22/0.29 at a temperature range of 25-70°C is shown in the figure 4.19. The experiments for the 3M AMP loaded solutions were performed on the string of discs contactor.

The LMPD was calculated by the following equation:

$$LMPD = \frac{P_{co_2,bulk}^{in} - P_{co_2}^{*,in} - P_{co_2,bulk}^{out} - P_{co_2}^{*,out}}{\ln \frac{P_{co_2,bulk}^{in} - P_{co_2}^{*,in}}{P_{co_2,bulk}^{out} - P_{co_2}^{*,out}}}$$

The results showed that the flux of CO₂ increases with the increase in the temperature and driving force (partial pressure of CO₂). But at the higher temperature (60 and 70°C) for all loadings, the flux becomes negative which means that there was high back pressure of CO₂ from the bulk solution as compared to the partial pressure at the interface. This was the discrepancy in the model for the loaded solutions. So, model needs to be modified for the loaded aqueous amine solutions.

The back pressure of CO₂ from the solution was calculated by using Soft model as described in chapter 2(Section 2.9). At a specific constant temperature, the flux increases with the decrease in the loading. The absorption of CO₂ in aqueous AMP solution is higher at lower loadings due to lower back pressure from the CO₂ present in the bulk solution and solution

can still absorb more CO₂. When the soft model will be accurate then all negative fluxes will go to zero point.

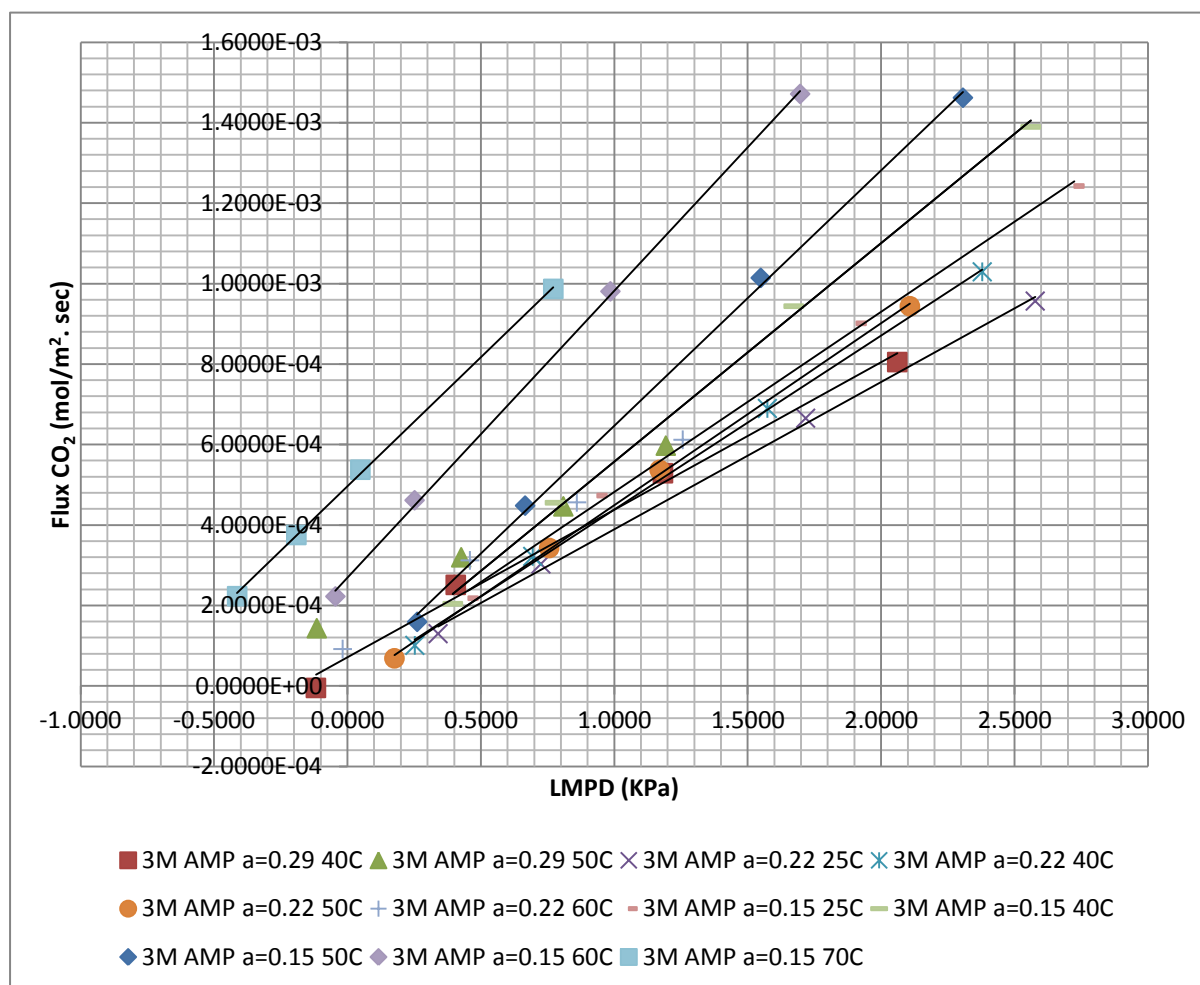


Figure 4.19 Experimental measured data of 3M AMP solutions with CO₂ loadings of $a=0.15/0.22/0.29$

Kinetics of CO₂ absorption in Piperazine

The experimental measurements for kinetics study of aqueous piperazine solutions were carried out in a wetted wall column as described in chapter 3. Different experiments were performed for 0.1/0.5/1/1.5M Piperazine solutions at a temperature range of 25-70°C and driving forces ranging from 3-9KPa. The results are shown in the following section.

4.12 Absorption flux dependency over concentration

The absorption flux for 1.5, 1.0, 0.5 and 0.1M aqueous solutions of piperazine at a temperature range (25-70°C) and driving forces of CO₂ partial pressure (1,3,7 and 9kPa) are represented in the figure 4.20, 4.21, 4.22 and 4.23 respectively.

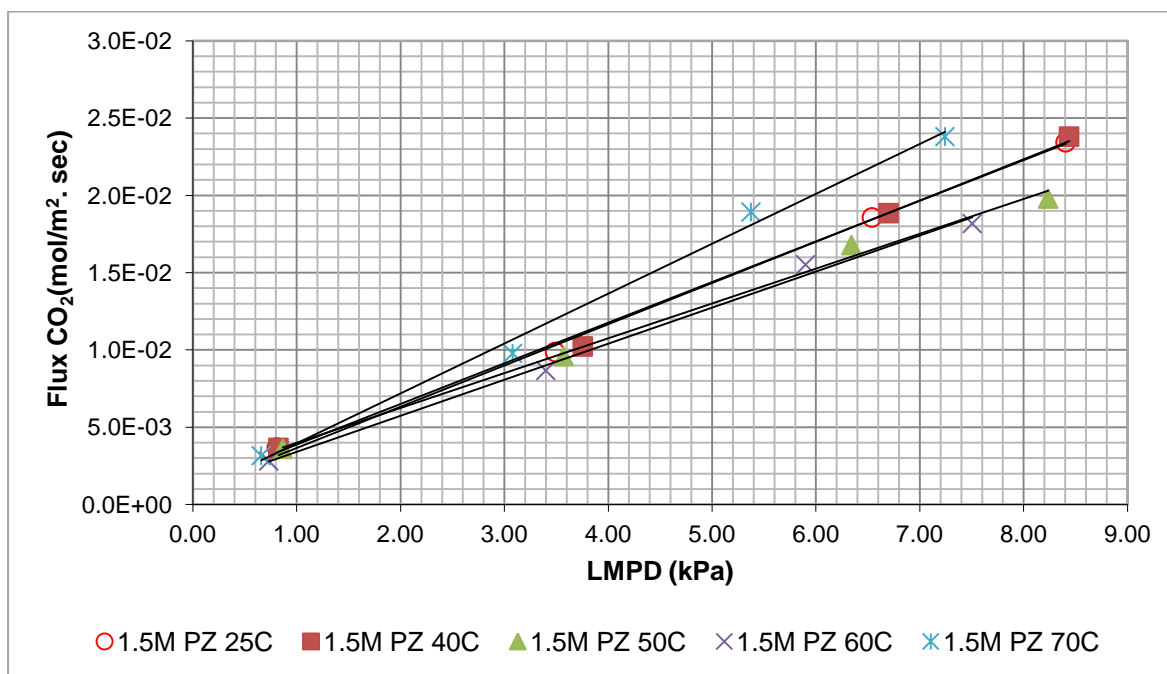


Figure 4.20 Experimental measurements of 1.5M PZ at temperature range of 25-70°C

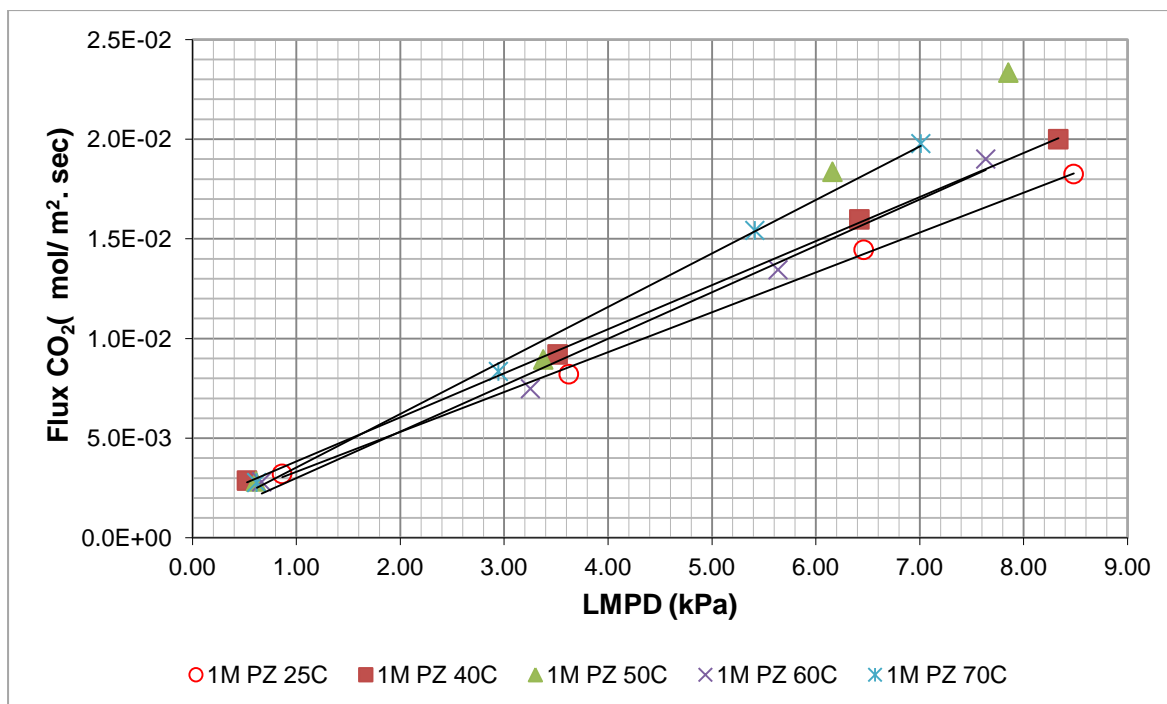


Figure 4.21 Experimental measurements of 1.0M PZ at temperature range of 25-70°C

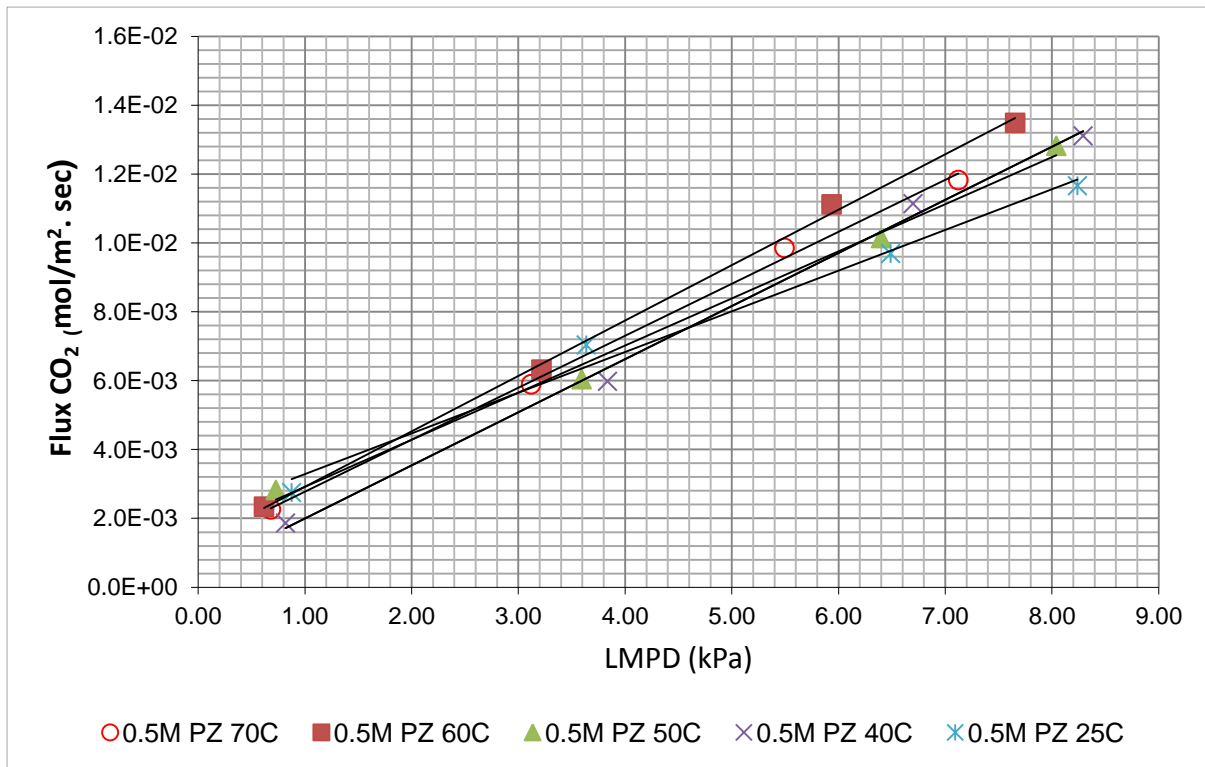


Figure 4.22 Experimental measurements of 0.5M PZ at temperature range of 25-70°C

The data points are scattered over different temperatures. Flux should be increased with the increase in the temperature and partial pressure of CO₂ as a driving force. At temperature of 25°C in figure 4.20 (for example), the first two points at 1 and 3KPa are not consistent with points at 7 and 9KPa because two CO₂ mass flow controllers of 0.2NL/mint and 1NL/mint capacity were used for the measurements. The opening of mass flow controller of 0.2NL/mint could be set within a range of 10-200Nml/mint while of the mass flow controller of 1NL/mint could be set between 5-1000Nml/mint. For low partial pressure of CO₂, the mass flow controller of 1NL/mint was used because it was not possible to get the 1 and 3KPa partial pressure as a driving force with 0.2NL/mint due to its range. The lower limit of 0.2NL/mint flow controller was 10 and it was not possible to get pressure lower than 3KPa for low concentrations of piperazine with this controller. Then the low pressures were obtained by setting an opening of 5-7Nml/mint of 1NL/mint flow controller. These two controllers were the only available mass flow controllers.

The reason for strange behavior of absorption flux at different temperatures in figure 4.20, 4.21, 4.22 and 4.23 could be the change in the loading of the solution during the experiment. It was assumed that the loading does not change so much because of the less contact time between liquid and gas. The liquid samples taken after each measurements

were analyzed in the end and loading was changed to 0.4-0.8 (molCO₂/mol Am). The other reason for these scattered data could be the non-wetting liquid film on the column. It was observed during the measurements that liquid coming from the top doesn't wet completely the whole column and liquid film was not proper particularly at low concentrations (0.1 and 0.5M PZ). Liquid distributor design was not proper because the liquid didn't fall equally through it. The inlet pipes to the distributor were having different lengths and liquid in one side was taking more time to fall down due to which liquid film was not proper.

There was also the problem with handling of the level of the liquid inside the column. The liquid level in the outer column was adjusted with the help of pressure column. The surface area was not supposed to be constant due to change in the pressure of the column.

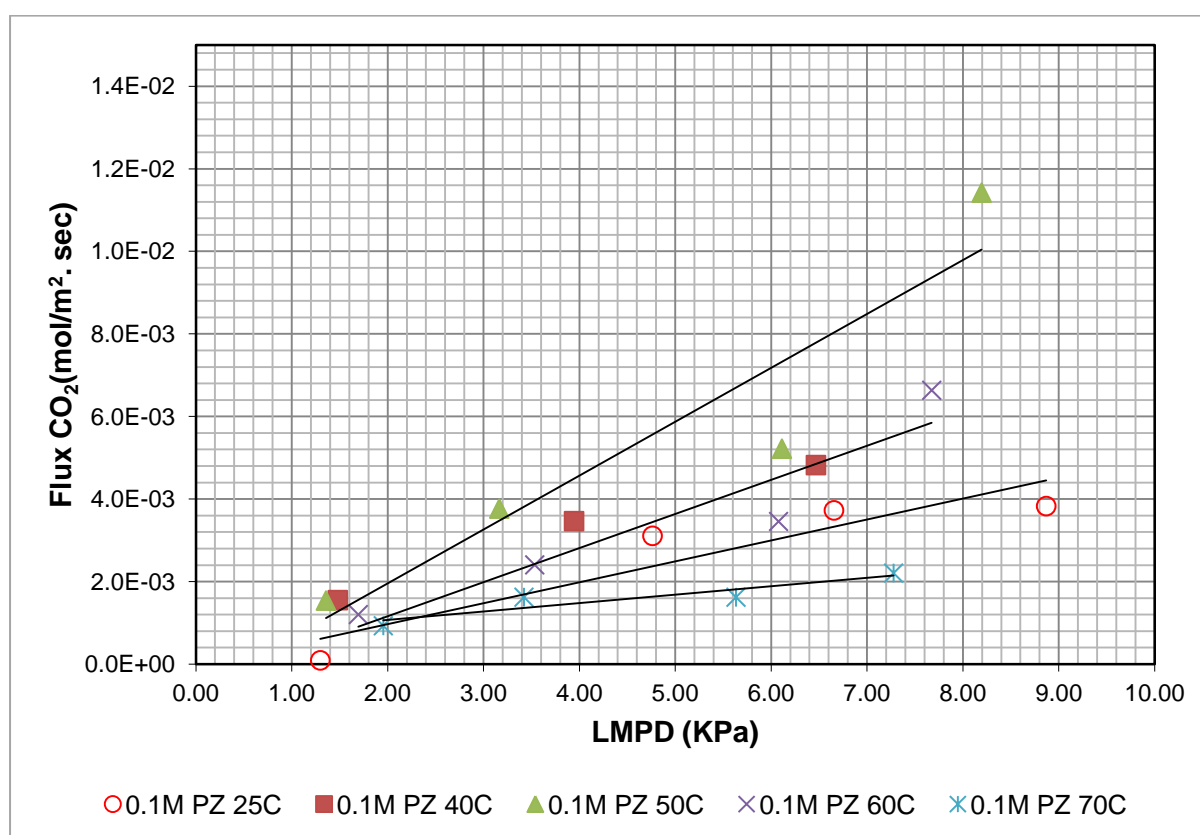


Figure 4.23 Experimental measurements of 0.1M PZ at temperature range of 25-70°C

4.13 Comparison of physiochemical properties data with literature

The experimental measurements should be analyzed and verified by comparing it with the literature data. The following section covers the comparison of physiochemical properties and kinetics measurements for AMP and piperazine solutions.

4.13.1 Density

The graphs had been plotted between the experimental measured densities and literature data in the figures 4.24 and 4.25 for AMP and PZ aqueous solutions. The literature data for loaded solutions of AMP was not available. The density of unloaded AMP solutions and PZ were compared with the literature data. The literature data reported was listed in the table 4.1.

The figures 4.24 and 4.25 showed that the experimental data of present work matches with the literature data with a deviation of less than 0.1% which showed the accuracy of the data (A1, A2 and A3 in Appendix A). The slightly difference was due to minute different concentrations (weight fractions) of AMP and PZ used in present work and literature.

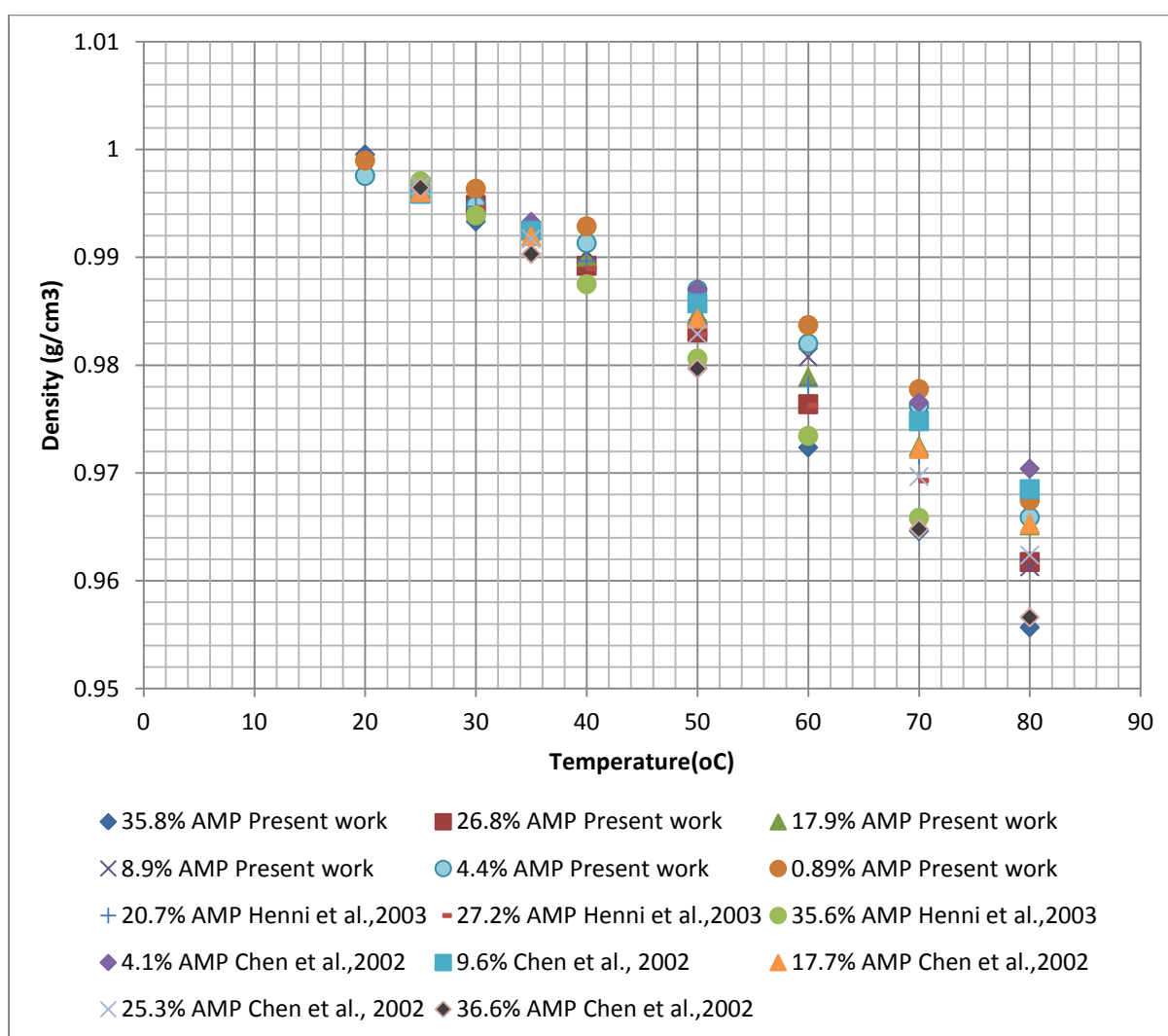


Figure 4.24 Comparison of density data of AMP with literature

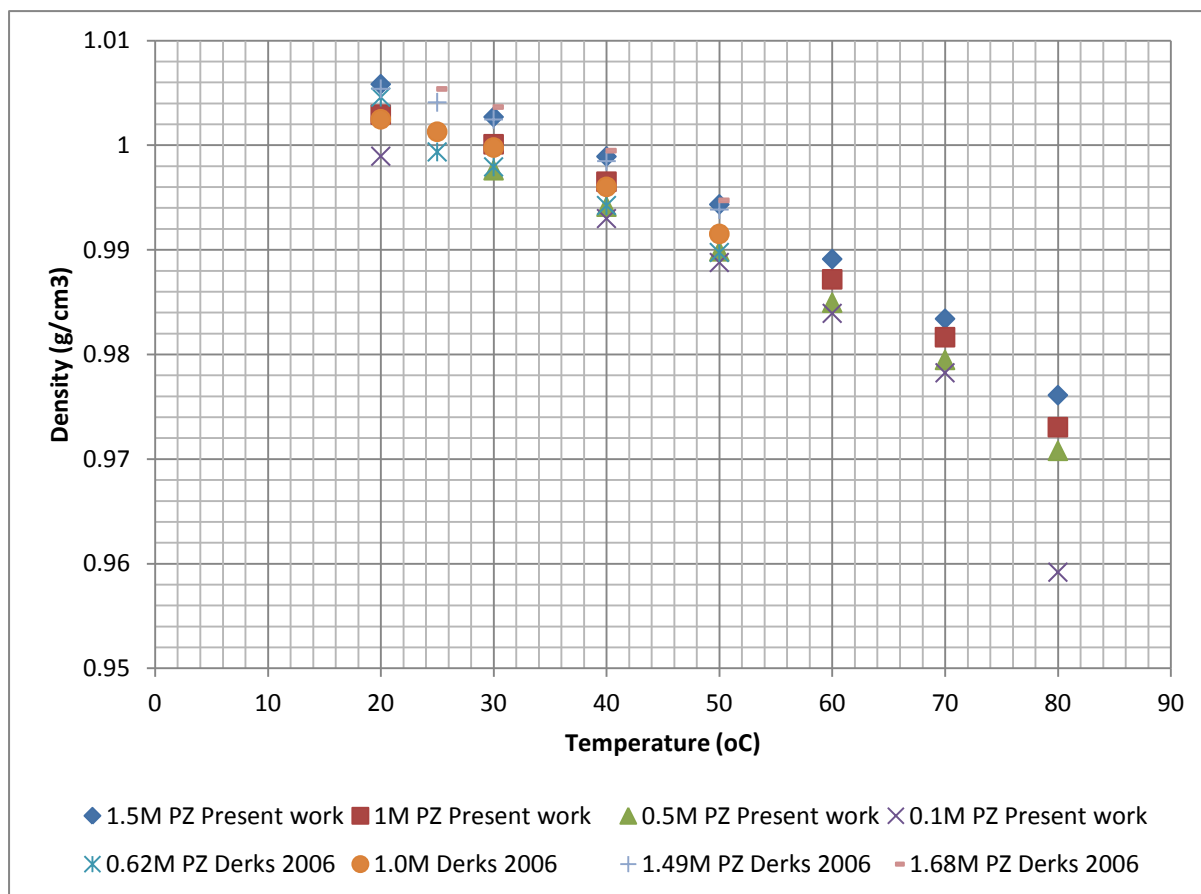


Figure 4.25 Comparison of density data of PZ with literature

Table 4.1 Literature data reported for AMP and PZ

Temperature Range(°C)	Concentration	Source	Solvent
25-80	9.6-36.6 weight %	Chan et al., 2002	AMP
25-70	20.7-35.6 weight %	Henni et al.,2003	AMP
20-50	0.62-1.68 M	Derk, 2006	PZ

4.13.2 Viscosity

The viscosity data of Henni et al., 2003 and Chan et al., 2003 were compared with the present work measurements as shown in the figure 4.26.

The data points for 35%, 26% and 17%AMP are in good agreement with the literature. The minute difference is due to the different weight fractions used in literature and present work.

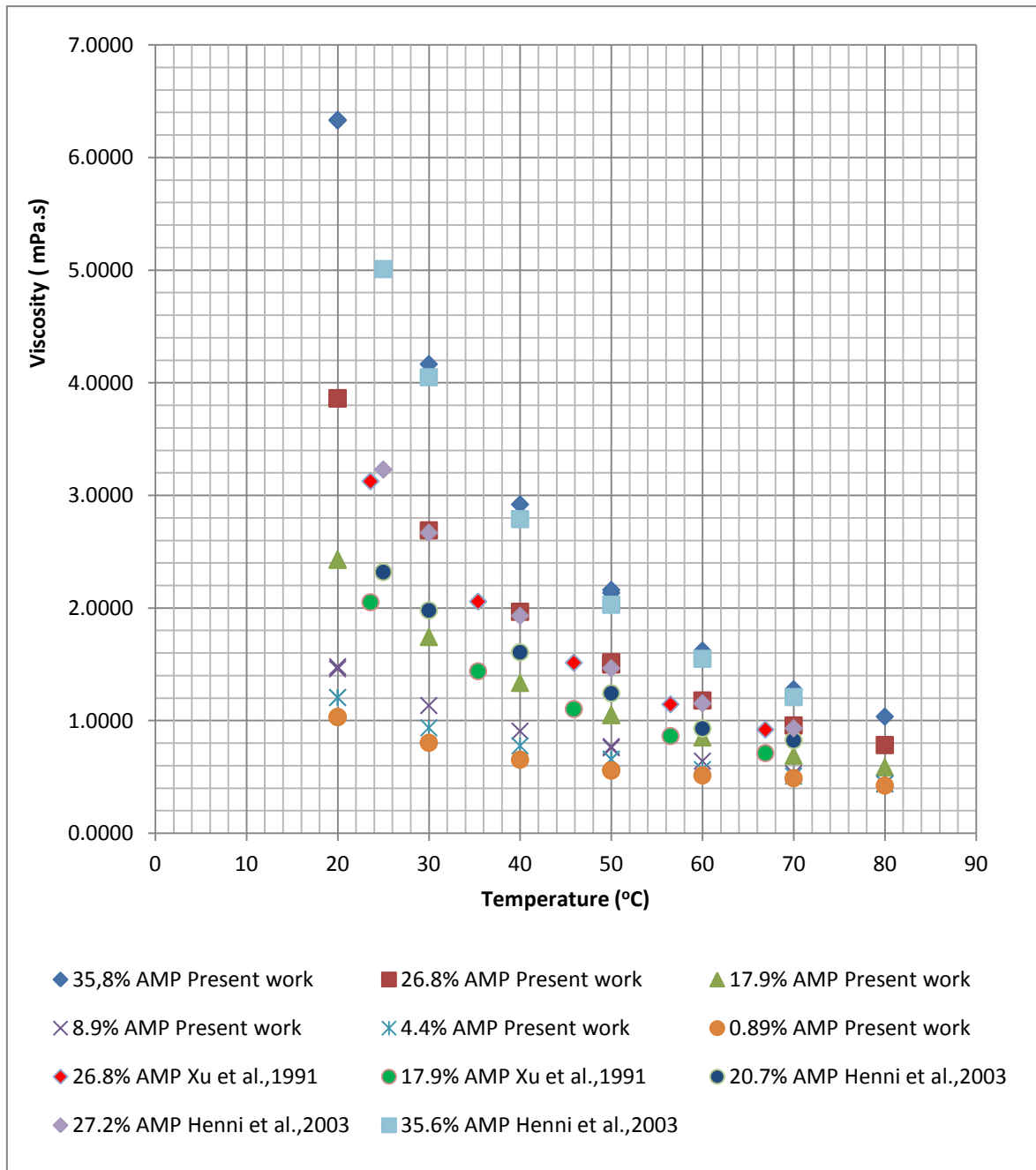


Figure 4.26 Comparison of experimental viscosity data of AMP with literature

The viscosity of PZ was also compared with literature in figure 4.27 and found good agreement with literature with $\pm 3\%$ for 1.5M and $\pm 1\%$ deviation for rest of the concentrations of PZ.

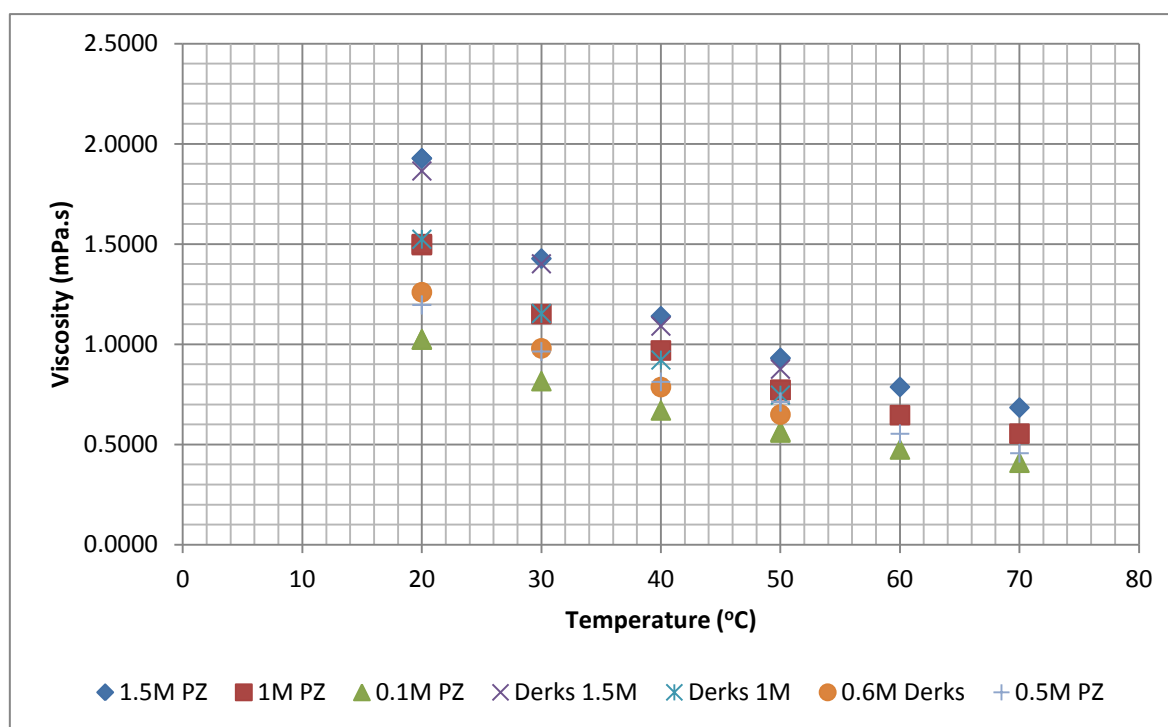


Figure 4.27 Comparison of experimental viscosity data of PZ with literature

4.13.3 Solubility

The solubility data for AMP concentrations of 0.1/0.5/1/2/3 and 4M are compared with the literature data. The table (4.2) showed the literature data available for AMP and piperazine. The literature data of viscosity was not available for loaded AMP solutions.

Table 4.2 Comparison of experimental solubility data of AMP and PZ with reported literature

T (°C)	Concentration of AMP (mol/liter)	Reference	Solvent
20-45	0.5-2.0	Saha et al., 1993	AMP
25-60	2-3	Xu et al., 1991	AMP
25	0-2.5	Bosch et al., 1990	AMP
20-40°C	0.2-1.4	Samanta et al., 2007	PZ

The figure 4.28 showed the comparison between the literature data and experimental data for different concentrations of AMP. The solubility measured by Saha et al., 1993 was less than the present work at 25 and 30°C while the solubility data of Xu et al., 1991 was consistent with the present work at 25°C but higher at 50 and 60°C. The Henry's constant calculated by Bosch (1990) was higher than present work at 25°C. The Henry's constants calculated by Saha (1993) and Xu (1991) was based on the concentration and temperature. The equation used by Saha (1993) was more concentration dependent than Xu (1991) because of the multiplying factor with the concentration. The model used in the present

work was also temperature and concentration dependent. The difference in the measurements for Henry's constant may be the experimental error because equilibrium established for some time during the measurements and it changed suddenly. So, measurements should be recorded until steady state condition was achieved for at least 30 minutes.

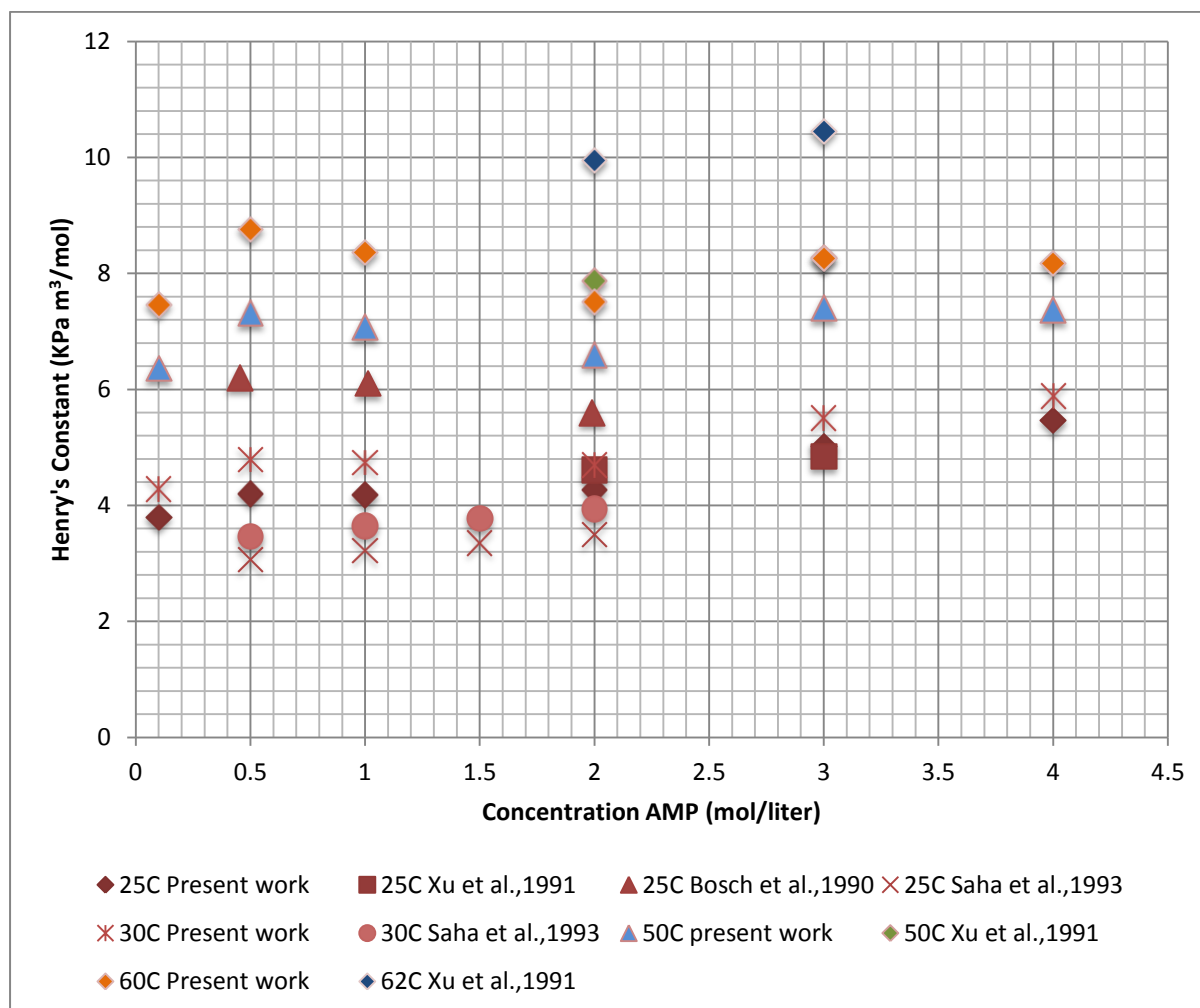


Figure 4.28 Comparison of experimental data of AMP with reported literature

The Henry's constants for piperazine solutions were compared with the present work in the figure 4.29. The results indicated that the solubility data of present work were consistent with the Samanta (2007) data and trendlines were the same. The difference in data points at one temperature was due to the different concentrations of the solution and Henry's constant is concentration dependent. The Henry's constants are very close so it can be said that the data was precise.

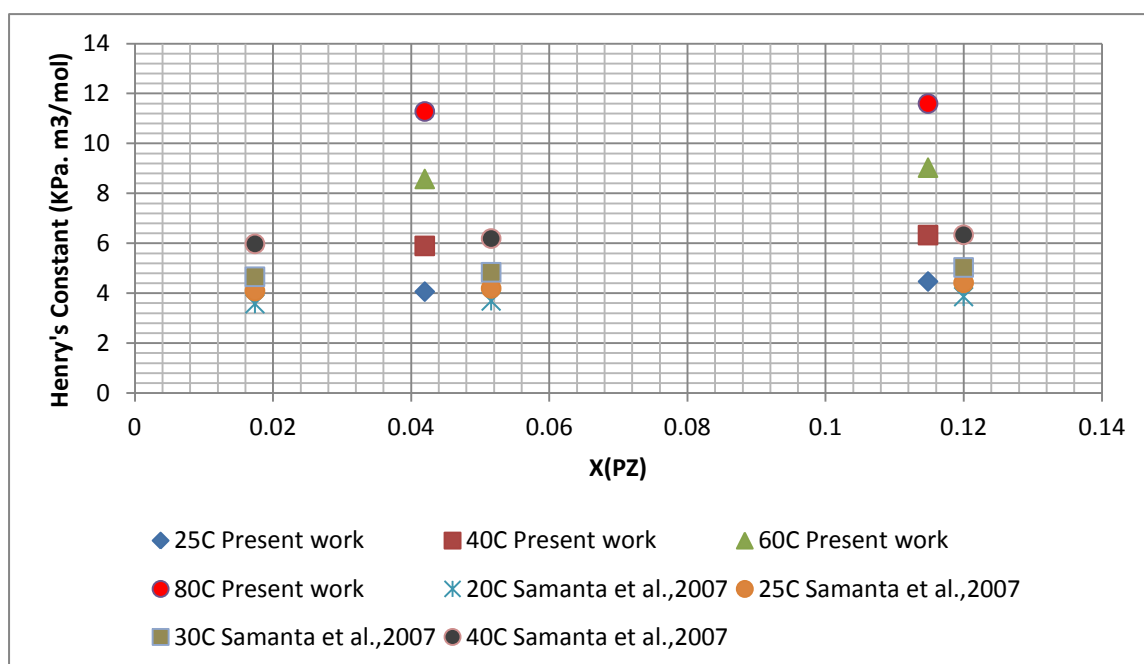


Figure 4.29 Comparison of experimental data of PZ with reported literature

4.14 Comparison of second order rate constant with literature

The literature data reported for AMP are listed in the table 4.3. The comparison of second order rate constants of AMP with literature data was shown in the figure 4.30. The Arrhenius type of plot between temperature and second order rate constant showed that the second order rate constants measured during the present study are quite large than reported data. The data was investigated using wetted wall column, stopped flow technique and stirred vessel by Saha (1995), Alper (1990) and Bosch (1989) respectively. The string of disc contactor was used for the present study. Disc contactor has the large contact time and large mass transfer area as compared to other techniques. The K_2 values also depend upon the interpretation of the data.

Table 4.3 Literature data for second order rate constants of AMP

Temperature (°C)	Reference
14.8-25	Alper, 1990
25	Bosch et al.,1989
20.8-44.8	Saha et al.,1995

The K_2 values are two times greater than the values measured by Alper, Bosch and Saha.

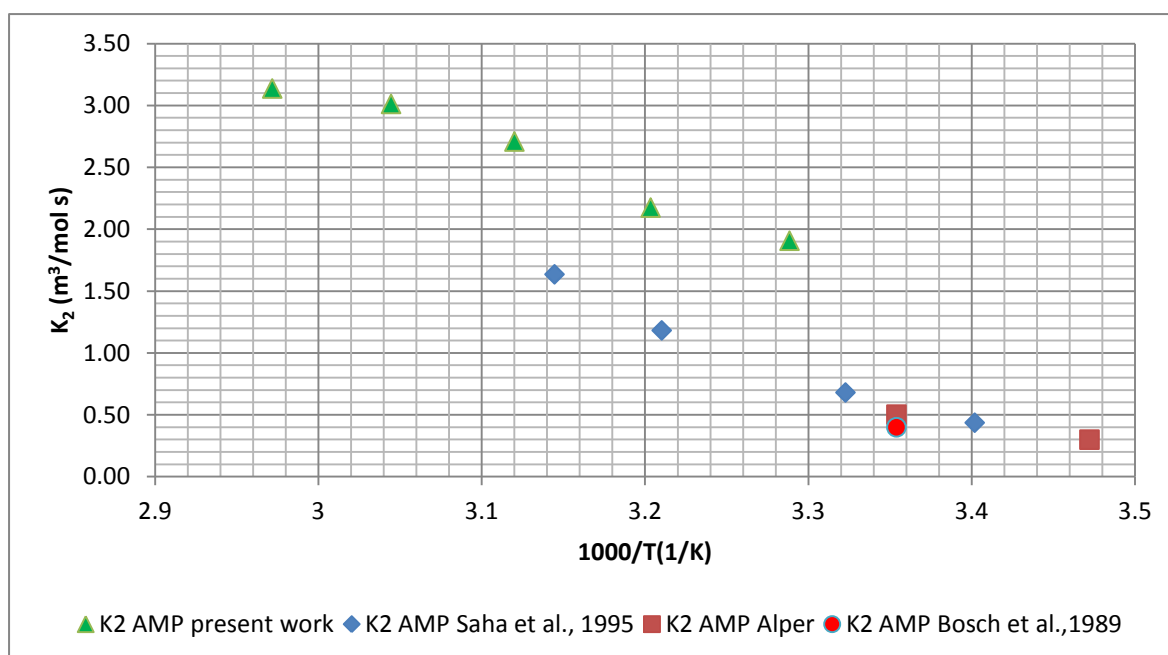


Figure 4.30 Comparison of K₂ values of AMP with the literature

4.15 Comparison of AMP with MEA

The MEA data was calculated at the experimental temperatures by Versteeg (1988) correlation for second order rate constant. The Arrhenius type plot in figure 4.31 showed that the second order rate constant of MEA was 4-10% large than the AMP. The carbamate formation in case of AMP is very low and carbamate stability constant is less than 0.1 for AMP due to which rate constants are low for AMP.

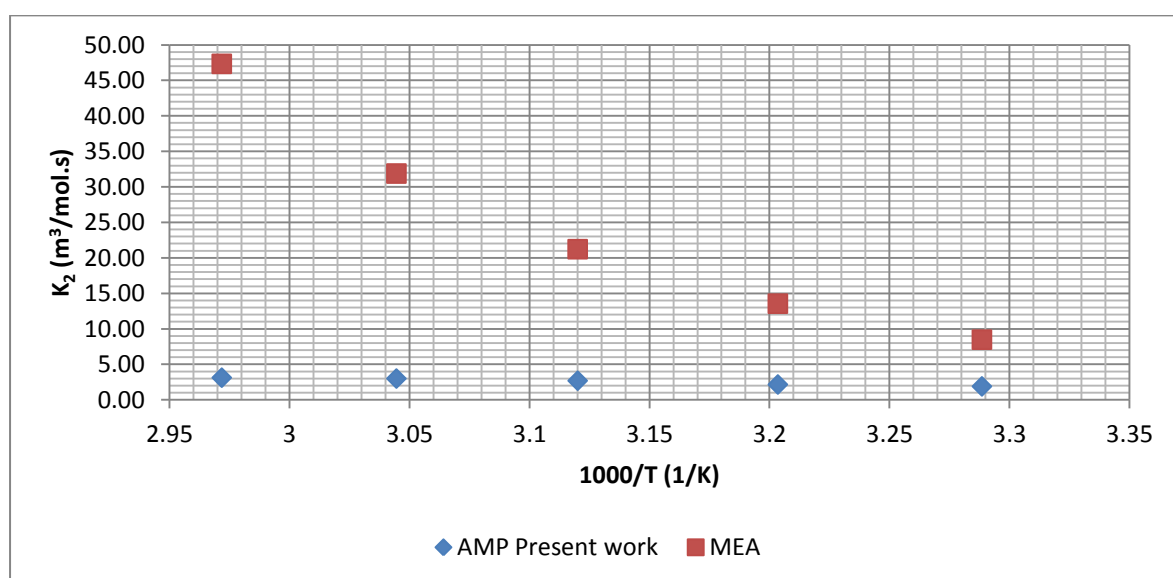


Figure 4.31 Comparison of second order rate constants of AMP with MEA

Conclusions and Recommendations

The kinetics of the CO₂ absorption in AMP and CO₂-loaded solution of AMP were investigated using a string of discs contactor while kinetics of piperazine was studied using wetted wall column apparatus. The kinetics study of AMP and PZ was done at a temperature range of 25-70°C and concentration range of 0.1-4mol/liter while the kinetics of loaded 3M AMP solutions with CO₂ loadings 0.15, 0.22, 0.29 was investigated. The average values of second order rate constants for AMP (0.1-4 mol/L) was found to be 2042/2355/2965/3344/3607 (m³/K-mol s) at temperatures 30.48/39.08/47.38/55.32/63.40 °C respectively. The model was fitted on the basis of termolecular mechanism and considering pseudo first order reaction. Model was fitted with the experimental measured data with AARD of 11.48%. The absorption flux of CO₂ in AMP is 4-10% less than MEA at all measured temperatures and concentrations.

The second order rate constant was predicted on the basis of concentration and it is recommended to predict it on the basis of activity as a future work.

The solubility should be measured accurately as it affects the second order rate constant much of all.

The samples should be collected after each run of 5L of solution and analyze them to see the exact effect of the CO₂ absorption.

The fresh solutions should be prepared for each experiment because loading may change.

Bibliography

Abanades, J. Carlos, Akai, Makoto, Benson, Sally, "IPCC Special Report, Carbon Dioxide Capture and Storage", (2005)

Alper, Erdogan, "Reaction Mechanism and Kinetics of aqueous solutions of 2-amino-2-methyl-1-propanol and carbon dioxide", *Ind.Eng.Chem.Res.*, 1725-1728, (1990)

Aronu, E. Ugochukwu, Hartono, A., Hallvard F. Svendsen, "Density, Viscosity and N₂O Solubility of aqueous amino acid salt and amine amino acid salt solution", *Journal of Chemical Thermodynamics*, (2011)

Astarita, G., Savage, D. W., Bisio, A., "Gas Treating with Chemical Solvent", John Wiley & Sons., New York, (1983)

Bird, R. B., Stewart, W.E., Lighfoot, E. N., "Transport phenomena", (2002), 2nd, John Wiley & Son, Inc., New York

Bird, R. B., Stewart, W.E., Lighfoot, E. N., "Transport phenomena", 2nd edition, John Wiley & Son, Inc., New York, (2002)

Bosch, h., versteeg, g. F., van swaaij, w. P. M., "Kinetics of the reaction of CO₂ with the sterically hindered amine 2-amino-2-methylpropanol at 298 K", *Chemical engineering science*, vol 45, pp1167-1173, (1990)

Caplow, M., "Kinetics of Carbamate Formation and Breakdown", *J. Am. Chem Soc.*, 90, 6795-6803 (1968)

Chan, C., Maham, Y., Mather, A.E., Mathonat, C., "Densities and volumetric properties of the aqueous solutions of 2-amino-2-methyl-1-propanol, n-butyl diethanolamine and n-propylethanolamine at temperatures from 298.15 to 353.15 K", *Elsevier, Fluid phase equilibria*, 239-250, (2002)

Clarke, J. K. A., "Kinetics of Absorption of Carbon Dioxide in Monoethanolamine Solutions at Short Contact Time", *Ind. Eng. Chem. Fundam.*, 3, 239-245, (1964)

Crooks, J. E.; and Donnellan, J. P., "Kinetics and Mechanism of the Reaction between Carbon Dioxide and Amine in Aqueous Solution", *J. Chem. Soc., Perkins Trans., II*, 331-333, (1989)

da Silva, E. F., and Svendsen, H. F., "Ab Initio Study of the Reaction of Carbamate Formation from CO₂ and Alkanolamines", *Ind. Chem. Eng. Res.*, 43, 3413-3418, (2004)

Danckwert, P.V., "The Reaction of CO₂ with Ethanolamine, Chem. Eng. Sci., 34,443-446 (1979)

Danckwerts, P. V., "Gas-Liquid Reaction", (1970) McGraw-Hill, New York

Davison, J.; P. Freund, A. Smith, "Putting Carbon Back Into the Ground", IEA Greenhouse Gas R&D Programme, (2011)

Derks, P. W. J., Kleingeld, T., van Aken, C., Hogendoorn, J. A., Versteeg, G. F., "Kinetics of Absorption of Carbon Dioxide in Aqueous Piperazine Solutions, Chem. Eng.Sci., 61, 6837-6854,(2006)

Derks, P.W. J., "Carbon dioxide absorption in Piperazine activated NMethyldiethanolamine", PhD Thesis, University of Twente, The Netherlands, (2006)

DIPPR 801," Information and Data Evaluation Manager for the Design Institute for Physical Properties", Version 4.1.0, (2004)

Edwards, T. J.; Newman, J.; Prausnitz, J. M., "Thermodynamics of Aqueous Solutions Containing Volatile Weak Electrolyte Solutions", AIChE J.,21, 248–259, (1975)

GCEP Energy Assessment Analysis, "An Assessment of Carbon Capture Technology and Research Opportunities", Spring (2005)

Hakka L. R., "Integrated regenerable SO₂ and CO₂ capture", IEA GHG Absorption Network, May 24-25, IFP, Lyon, France, (2007)

Hartono, A., Juliussen, O., Svendsen, H. F., "Solubility of N₂O in Aqueous Solution of Diethylenetriamine (DETA)", J. Chem. Eng. Data., 53 (11), 2696–2700, (2008)

Henni, Amr., Hromek, J.J., Tontiwachwuthikul, Paitoon, Chakma, A., "Volumetric Properties and Viscosities for Aqueous AMP Solutions from 25 °C to 70 °C", J.Chem.Eng.Data, 551-556,(2003)

Higbie, R., "The Rate of Absorption of a Pure Gas into a Still Liquid during Short Periods Exposure", Trans.Am.Inst.Chem.Eng.31, 365-389, (1935)

IEA Energy Technology Essentials,"CO₂ Capture & Storage", Dec (2006)

IPCC, 2005, "IPCC Special Report on Carbon dioxide Capture and Storage", Chapter No.3, (2005)

Knuutila,H., "Carbon dioxide capture with carbonate systems", Doctoral thesis, National university of science and technology, Trondheim, NTNU:2009:115, (2009)

Laddha, S. S., Diaz, J. M., Danckwerts, P. V., "The N₂O Analogy: the Solubilities of CO₂ and N₂O in Aqueous Solutions of Organic Compounds", Chem. Eng. Sci., 36, 228-229 (1981)

Little, R.J., Versteeg, G. F., van Swaaij, P.M., "Solubility and diffusivity for the absorption of COS, CO₂ and N₂O in amine solutions", J.Chem.Eng.Data, 37(1),49-55, (1992)

- Ma'mun, S., " Selection and characterization of new absorbents for carbon dioxide capture, Norwegian University of Science and Technology: Trondheim, (2005)
- Pacheco, M. A., Kaganoi, S., Rochelle, G. T., "CO₂ absorption into aqueous mixtures of diglycolamine and methyldiethanol amine", Chem.Eng.Sci.,5125-5140, (2000)
- Pinsent, B. R. W., Pearson, L., Roughton, F. W. J., " The Kinetics of Combination of Carbon Dioxide with Hydroxide Ions", Trans. Faraday Soc., 52, 1512-1520, (1956)
- Prakash D. Vaidya; Eugeny Y. Kenig, "CO₂-Alkanolamine Reaction Kinetics: A Review of Recent Studies", Chem. Eng. Technol., 30, No. 11, 1467–1474, (2007)
- Prausnitz J. M.; Lichtenthaler, R. N.; de Azevedo, E. G., " Molecular Thermodynamics of Fluid-Phase Equilibria", 3rd ed.; Prentice Hall Inc: Upper Saddle River, NJ, (1999)
- Prausnitz, J. M., Lichtenthaler, R. N., and de Azevedo, E. D., "Molecular Thermodynamics of Fluid-phase Equilibria", (3rd ed.), Prentice Hall PTR; New Jersey, (1999)
- Prausnitz, J. M.; Lichtenthaler, R. N.; and de Azevedo, E. D., " Molecular Thermodynamics of Fluid-phase Equilibria", (3rd ed.), Prentice Hall PTR; New Jersey (1999)
- R.J. Little; W.P.M. van Swaaij en G.F. Versteeg, "Kinetics of carbon dioxide with tertiary amines in aqueous solution", AIChE Spring National Meeting, Orlando, FL, USA, (1990)
- Saha, K., Asit, Bandyopadhyay, S.S., " KINETICS OF ABSORPTION OF CO₂ INTO AQUEOUS SOLUTIONS OF 2-AMINO-2-METHYL-1-PROPANOL", Chemical Eng.Sci., vol 50, pp3587-3598, (1995)
- Saha, K., Asit, Bandyopadhyay, S.S., " Solubility and Diffusivity of N₂O and CO₂ in Aqueous Solutions of 2-Amino-2-methyl- 1 –propanol", J.Chem.Eng.Data, pp78-82, (1993)
- Samanta, A., Roy, S., Bandyopadhyay, S.S., " Physical Solubility and Diffusivity of N₂O and CO₂ in Aqueous Solutions of Piperazine and (N-Methyldiethanolamine + Piperazine)", J.Chem.Eng.Data, pp1381-1385, (2007)
- Stephens, E. J.; Morris, G. A., "Determination of Liquid-Film Absorption Coefficient: A New Type of Column and Its Application to Problems of Absorption in Presence of Chemical Reaction". Chem. Eng. Prog. 47, 232-242, (1951)
- Tiepel, E.W.; Gubbins, K. E.; Can. J., " Theory of gas solubility in mixed solvent systems", Chem. Eng. 1972, 50, 361–365, (1972)
- TORP A. T., BERGER, B., STEENEVELDT R., "CO₂ CAPTURE AND STORAGE Closing the Knowing–Doing Gap", (2006)

Versteeg, G. F., van Swaij, W. P. M., "Solubility and Diffusivity of Acid Gases (CO₂, N₂O) in Aqueous Alkanolamines Solutions", J. Chem. Eng. Data., 33, 29-34, (1988)

Versteeg, G. F.; van Swaij; W. P. M., "Solubility and Diffusivity of Acid Gases (Carbon Dioxide and Nitrous Oxide) in Aqueous Alkanolamine Solutions", J. Chem. Eng. Data, 33, 29-34, (1988)

Whitman, W. G., "The two-film theory of gas absorption, Chem. Met. Eng., 29 (4), 146–148, (1923)

Wong, S.; R.Bioletti, "Carbon Dioxide Separation Technologies", Alberta Research Council (2002)

Wu, Yuxiang, Zhou, Qing, Chan, Christine W., "A comparison of two data analysis techniques and their applications for modeling the carbon dioxide capture process", (2010)

Xu, S., Otto, D.F., Mather, E.A., "Physical properties of aqueous AMP solutions", J.Chem.Eng.Data., 36, pp71-75, (1991)

Appendices

Appendix A

Physiochemical Properties

Table A1 Experimental density data of AMP solutions at temperatures 20-80°C

Temp	Concentration	Weight fraction	Density		Difference
°C	mol/l		(g/cm ³)		(g/cm ³)
80	4	0,3587	0,95567	0,95567	0
80	3	0,26874	0,96173	0,96174	-0,0010398
80	2	0,17936	0,96502	0,96525	-0,0238337
80	1	0,08975	0,96276	0,95982	0,3053721
80	0,5	0,04479	0,96516	0,9666	-0,1491981
80	0,1	0,008975	0,96686	0,96805	-0,1230788
70	4	0,3587	0,96462	0,96461	0,0010367
70	3	0,26874			
70	2	0,17936	0,97245	0,97246	-0,0010283
70	1	0,08975	0,97496	0,9749	0,0061541
70	0,5	0,04479	0,97608	0,97642	-0,0348332
70	0,1	0,008975	0,97744	0,97809	-0,0665002
60	4	0,3587	0,97236	0,97235	0,0010284
60	3	0,26874	0,97638	0,97637	0,0010242
60	2	0,17936	0,97887	0,97887	0
60	1	0,08975	0,98075	0,98076	-0,0010196
60	0,5	0,04479	0,982	0,982	0
60	0,1	0,008975	0,98371	0,98371	0
50	4	0,3587	0,97969	0,97968	0,0010207
50	3	0,26874	0,98303	0,98303	0
50	2	0,17936	0,98477	0,98477	0
50	1	0,08975			
50	0,5	0,04479	0,98699	0,98699	0
50	0,1	0,008975			
40	4	0,3587			
40	3	0,26874	0,98921	0,98921	0
40	2	0,17936	0,99005	0,99005	0

Kinetics study of CO₂ absorption in AMP and PZ solutions

40	1	0,08975	0,99054	0,99054	0
40	0,5	0,04479	0,99132	0,99132	0
40	0,1	0,008975	0,99287	0,99287	0
30	4	0,3587	0,99332	0,99332	0
30	3	0,26874	0,99485	0,99485	0
30	2	0,17936	0,99464	0,99464	0
30	1	0,08975	0,99433	0,99433	0
30	0,5	0,04479	0,99482	0,99482	0
30	0,1	0,008975	0,99636	0,99635	0,0010037
20	4	0,3587	0,99954	0,99954	0
20	3	0,26874			
20	2	0,17936	0,99853	0,99853	0
20	1	0,08975			
20	0,5	0,04479	0,99755	0,99755	0
20	0,1	0,008975	0,99897	0,99897	0

Table A2 Experimental density data of PZ solutions at temperatures 20-80°C

Temp	Concentration	Weight Fraction	Density		Difference
			(g/cm ³)	(g/cm ³)	
C	mol/l		(g/cm ³)	(g/cm ³)	(g/cm ³)
80	1,5	0,11485	0,97508	0,97612	-0,10666
80	1	0,07961	0,9734	0,97306	0,034929
80	0,5	0,04199	0,96842	0,9708	-0,24576
80	0,1	0,00869	0,95957	0,9592	0,038559
70	1,5	0,11485	0,98342	0,98342	0
70	1	0,07961	0,98163	0,98166	-0,00306
70	0,5	0,04199	0,97894	0,97949	-0,05618
70	0,1	0,00869	0,97804	0,97826	-0,02249
60	1,5	0,11485	0,98913	0,98913	0
60	1	0,07961	0,98719	0,98719	0
60	0,5	0,04199	0,98496	0,98496	0
60	0,1	0,00869	0,98394	0,98394	0
50	1,5	0,11485	0,99435	0,99435	0
50	1	0,07961			
50	0,5	0,04199	0,98987	0,98987	0
50	0,1	0,00869	0,9888	0,9888	0
40	1,5	0,11485	0,99893	0,99893	0
40	1	0,07961	0,99652	0,99652	0
40	0,5	0,04199	0,99414	0,99414	0
40	0,1	0,00869	0,993	0,993	0
30	1,5	0,11485	1,00271	1,00271	0
30	1	0,07961	1,0001	1,0001	0
30	0,5	0,04199	0,99762	0,99762	0
30	0,1	0,00869			

Kinetics study of CO₂ absorption in AMP and PZ solutions

20	1,5	0,11485	1,00584	1,00584	0
20	1	0,07961	1,00293	1,00294	-0,001
20	0,5	0,04199			
20	0,1	0,00869	0,99896	0,99896	0

Table A3 Experimental density data of AMP solutions loaded with CO₂ at temperatures 20-80°C

Temp	Concentration	Weight Fraction	Loading	Density		Difference
C	mol/l		(nCO ₂ /nAm)	(g/cm ³)	(g/cm ³)	g/cm ³
80	3	0,26874	0,15	0,981	0,981	0
80	3	0,26874	0,22	0,99181	0,99182	-0,0010083
80	3	0,26874	0,29	1,0009	1,00091	-0,0009991
80	3	0,26874	0,35	1,00765	1,00784	-0,0188558
70	3	0,26874	0,15	0,98875	0,98875	0
70	3	0,26874	0,22	0,99971	0,99971	0
70	3	0,26874	0,29	1,00876	1,0877	-7,8254491
70	3	0,26874	0,35	1,01586	1,01587	-0,0009844
60	3	0,26874	0,15	0,99637	0,99638	-0,0010036
60	3	0,26874	0,22			
60	3	0,26874	0,29	1,0167	1,0167	0
60	3	0,26874	0,35	1,02377	1,02375	0,00195356
50	3	0,26874	0,15	1,00365	1,00365	0,00098953
50	3	0,26874	0,22	1,015	1,015	0,00097814
50	3	0,26874	0,29	1,02426	1,02426	0,00193844
50	3	0,26874	0,35	1,03132	1,03132	0,00385012
40	3	0,26874	0,15	1,01058	1,01057	0,00098323
40	3	0,26874	0,22	1,02235	1,02234	0,00388591
40	3	0,26874	0,29	1,03176	1,03174	-0,0028875
40	3	0,26874	0,35	1,03893	1,03889	0,00286749
30	3	0,26874	0,15	1,01706	1,01705	0,00098323
30	3	0,26874	0,22	1,02936	1,02932	0,00388591
30	3	0,26874	0,29	1,03896	1,03899	-0,0028875
30	3	0,26874	0,35	1,04621	1,04618	0,00286749
20	3	0,26874	0,15	1,02291	1,02291	0
20	3	0,26874	0,22	1,03573	1,03574	-0,0009655
20	3	0,26874	0,29	1,04554	1,0453	0,02295465
20	3	0,26874	0,35	1,05276	1,05276	-0,4274479

Table A4 Parameters used in equations 4.1 and 4.2

Solvent	Parameters				
	K1	K2	K3	K4	K5
AMP	-8.36933	-71295.9	-53.2191	15769.1	2.4736e+007

Kinetics study of CO₂ absorption in AMP and PZ solutions

Piperazine	58.46924	286129.33396	-430.13623	-0.00976	-
Loaded AMP	126.04904	181209.61880	-331.03895	0.01878	-

Table A5 Experimental viscosity data of AMP solutions at temperatures 20-80°C

Temperature	Viscosity (m Pa.s)_AMP					
	4M	3M	2M	1M	0.5M	0.1M
20	6,329302	3,860664	2,43323598	1,4612253	1,205586	1,032987
20	6,335319	3,86427399	2,42862264	1,47957837	1,20618783	1,03248555
30	4,17E+00	2,690279	1,74E+00	1,13518251	0,93714	0,80416
40	2,92E+00	1,97E+00	1,34E+00	0,9078552	0,776886456	0,653840655
50	2,14E+00	1,50E+00	1,05E+00	0,770608	0,657621588	0,557031
50	2,161049	1,52E+00	1,050939	0,7597168	0,657621588	0,560952057
60	1,62E+00	1,17981156	8,52E-01	0,641124	0,566227311	0,514176801
70	1,27919895	9,58E-01	0,689012358	0,529902273	0,507467	0,490
80	1,04E+00	0,784177539	0,587107689	0,437876169	0,441195768	0,424116381

Table A6 Experimental viscosity data of PZ solutions at temperatures 20-70°C

Temperature	Viscosity (mPa. Sec) (PZ)			
	1.5M	1.0M	0.5M	0.1M
20	1,928376	1,495424	1,19666028	1,02566583
20	1,927574	1,50003753	1,19666028	1,0239609
30	1,43E+00	1,151329	9,64E-01	0,81666147
40	1,14E+00	9,69E-01	8,13E-01	0,6704186
50	9,33E-01	7,73E-01	7,12E-01	0,565736
50	0,928575	7,72E-01	0,712420	0,5602400
60	7,88E-01	0,647000877	5,54E-01	0,475796
70	0,684740004	5,55E-01	0,456951327	0,409654563

Table A7 Experimental viscosity data of AMP solutions loaded with CO₂ at temperatures 20-80°C

Temperature	Viscosity (m Pa. s) AMP loaded			
	a=0.1	a=0.2	a=0.3	a=0.4
20	4,975587	5,567900	5,71121463	5,61874725
20	4,977292	5,56790022	5,71121463	5,62305972
30	3,35E+00	3,695586	3,80E+00	3,84772614
40	2,39E+00	2,62E+00	2,70E+00	2,7427309
50	1,80E+00	1,93E+00	2,03E+00	2,037191
60	1,400450	1,51E+00	1,5875907	1,6361311
70	1,13E+00	1,20739131	1,219827	1,269571

Table A8 Parameters for viscosity model of AMP and PZ

Solvent	K ₁	K ₂	K ₃	K ₄	K ₅
AMP	1334.83	-1.17944e6	-2486.95	734721	3.73478e8

Kinetics study of CO₂ absorption in AMP and PZ solutions

AMP loaded	174.665	-268159	-2454.96	835364	4.1894e+007
PZ	6571.07	-6.48114e+07	-2071.88	606943	2.10687e+010

Table A9 Henry's constants for AMP solutions at temperatures (25-80°C)

Concentration (mol/liter)	Weight Fraction	Henry's Constant (KPa m ³ mol ⁻¹)						
		25 °C	30 °C	40 °C	50 °C	60 °C	70 °C	80 °C
4	0.11485	5.46829	5.884716	6.583502	7.369889	8.17111	8.98979	10.1531
3	0.269012	5.01856	5.504154	6.41634	7.406092	8.26169	9.22722	10.4183
2	0.179342	4.267829	4.694284	5.593961	6.598371	7.50918	8.66778	10.2287
1	0.008968	4.180086	4.738295	5.860062	7.07235	8.35899	9.85029	11.4247
0.5	0.044795	4.202887	4.787195	5.943822	7.31786	8.75558	10.5632	12.9158
0.1	0.008968	3.797126	4.282685	5.287929	6.35983	7.45828	8.77076	10.4560

Table A10 Henry's constants for Piperazine solutions at temperatures (25-100°C)

Concentration (mol/liter)	Weight Fraction	Henry's Constant (KPa m ³ mol ⁻¹)				
		25	40	60	80	100
1.5	0.11485	4.473241	6.332500	9.034605	11.60172	13.60648
0.5	0.04198	4.067915	5.899495	8.581460	11.28418	13.54295

Table A11 Henry's Constants of 3M AMP with different CO₂ loadings (0.15/0.35/0.93)

Loading (mol CO ₂ /mol AMP)	Henry's Constant (KPa m ³ mol ⁻¹)					
	25°C	40°C	60°C	80°C	100°C	120 °C
0.15	6.026772	7.683699	9.496451655	10.5956651	10.61630782	10.23831704
0.35	7.15167	9.076022	11.29787183	12.74166441	13.57482078	
0.93	6.506544	7.893069	9.403438191			

Table A12 Parameters for solubility model fitting of AMP and PZ

Solvent	K ₁	K ₂	K ₃	K ₄	K ₅
AMP	-624.032	-40718	3065.73	-784212	3.72409e+008
AMP loaded	57.7288	-573263	2559.03	-617724	3.48088e+008
PZ	-825.623	-2.45551e+06	3308.39	-861487	2.48428e+009

Appendix B

Kinetics data of AMP

4M AMP

T	LMa	10 ⁵ . kl	10 ² . kg	10 ² . kg	10 ⁻³ . H _{CO2}	LMP _{CO2}	LMP* _{CO2}	10 ³ .N _{CO2}	10 ³ . kg'	10 ³ . KG	KG/kg	E	k2	kobs	10 ³ .N _{CO2}
(C)	(mol CO ₂ /mol Amine)	(m/s)	(m/s)	(mol/m ² kpa s)	(kpa m ³ /mol)	(kpa)	(kpa)	(mol/m ² s)	(mol/m ² kpa s)	(mol/m ² kpa s)	(%)		m ³ /mol s	(1/s)	(mol/ m ² s)
31,16	0,00	2,17	4,11	1,62	4,13	0,91	0,000	0,61	0,71	0,68	4,18	134,7	3,58	1,4297E+04	1,38
39,26	0,00	2,92	4,26	1,64	4,67	0,90	0,000	0,71	0,82	0,78	4,77	131,4	4,70	1,8638E+04	1,66
47,44	0,00	3,83	4,35	1,63	5,18	0,86	0,000	0,76	0,94	0,88	5,43	126,6	5,85	2,3041E+04	1,91
55,53	0,00	4,84	4,13	1,51	5,65	0,82	0,000	0,79	1,03	0,96	6,39	120,3	6,61	2,6123E+04	2,16
63,60	0,00	5,98	3,67	1,31	6,10	0,76	0,000	0,81	1,15	1,06	8,07	117,2	7,70	3,0338E+04	2,31

3M AMP

T	LMa	10 ⁵ . kl	10 ² . kg	10 ² . kg	10 ⁻³ . HCO ₂	LMPC O ₂	LMP*C O ₂	10 ³ .NCO ₂	10 ³ . kg'	10 ³ . KG	KG/kg	E	k2	kobs	10 ³ .N _{CO2}
(C)	(mol CO ₂ /mol Amine)	(m/s)	(m/s)	(mol/m ² kpa s)	(kpa m ³ /mol)	(kpa)	(kpa)	(mol/ m ² s)	(mol/m ² kpa s)	(mol/m ² kpa s)	(%)		m ³ /mol s	(1/s)	(mol/ m ² s)
31,21	0,00	3,25	4,07	1,60	3,92	0,90	0,000	0,55	0,63	0,61	3,80	76,5	2,42	7,2010E+03	1,48
39,26	0,00	4,22	4,23	1,62	4,40	0,90	0,000	0,63	0,73	0,70	4,32	76,7	3,19	9,4498E+03	1,78
47,36	0,00	5,40	4,28	1,60	4,88	0,88	0,000	0,70	0,85	0,80	5,01	76,4	4,11	1,2103E+04	2,07
55,17	0,00	6,56	4,08	1,49	5,31	0,86	0,000	0,73	0,90	0,85	5,69	72,9	4,45	1,3110E+04	2,35
63,51	0,00	8,14	3,73	1,33	5,76	0,88	0,000	0,74	0,90	0,85	6,37	64,0	4,29	1,2608E+04	2,76

2M AMP

T	LMa	10 ⁵ . kl	10 ² . kg	10 ² . kg	10 ⁻³ . HCO ₂	LMPCO ₂	LMP* CO ₂	10 ³ .N _{CO₂}	10 ³ . kg'	10 ³ . KG	KG/kg	E	k ₂	kobs	10 ³ .N _{CO₂}
(C)	(mol CO ₂ / mol Amine)	(m/s)	(m/s)	(mol/m ² kpa s)	(kpa m ³ /mol)	(kpa)	(kpa)	(mol/ m ² s)	(mol/m ² kpa s)	(mol/m ² kpa s)	(%)		(m ³ / mol.s)	(1/s)	(mol/ m ² s)
31,34	0,00	4,84	4,10	1,61	3,41	0,91	0,000	0,51	0,58	0,56	3,48	41,0	1,61	3,2107E+03	1,67
39,00	0,00	6,12	4,12	1,58	3,89	0,93	0,000	0,56	0,62	0,60	3,78	39,4	1,92	3,8068E+03	1,97
47,58	0,00	7,61	4,18	1,57	4,42	0,90	0,000	0,61	0,71	0,68	4,33	41,2	2,58	5,0918E+03	2,23
55,33	0,00	9,24	4,00	1,46	4,89	0,85	0,000	0,62	0,77	0,73	5,00	40,8	3,06	6,0497E+03	2,40
63,62	0,01	10,93	3,62	1,29	5,38	0,83	0,001	0,63	0,81	0,76	5,89	39,7	3,45	6,6183E+03	2,60

1M AMP

T	LMa	10 ⁵ . kl	10 ² . kg	10 ² . kg	10 ⁻³ . HCO ₂	LMP _{CO₂}	LMP* _{CO₂}	10 ³ .N _{CO₂}	10 ³ . kg'	10 ³ . KG	KG/k g	E	k ₂	kobs	10 ³ .N _{CO₂}
(C)	(mol CO ₂ / mol Amine)	(m/s)	(m/s)	(mol/m ² kpa s)	(kpa m ³ /mol)	(kpa)	(kpa)	(mol/ m ² s)	(mol/m ² kpa s)	(mol/m ² kpa s)	(%)		(m ³ /mol sec)	(1/s)	(mol/ m ² s)
30,81	0,00	7,26	4,13	1,63	3,23	0,94	0,000	0,44	0,48	0,46	2,86	21,3	1,45	1,4482E+03	1,50
39,42	0,00	9,07	4,21	1,61	3,79	0,99	0,000	0,46	0,48	0,47	2,91	20,3	1,64	1,6235E+03	1,83
47,76	0,00	10,93	4,20	1,57	4,34	0,98	0,000	0,49	0,52	0,50	3,18	20,5	1,99	1,9639E+03	2,08
55,41	0,00	13,01	4,00	1,46	4,85	0,95	0,000	0,51	0,56	0,54	3,68	20,8	2,42	2,3905E+03	2,27
63,93	0,02	15,08	3,65	1,30	5,39	1,00	0,001	0,51	0,53	0,51	3,94	19,1	2,34	2,2401E+03	2,65

0.5M AMP

T	L _{Ma}	10 ⁵ . kl	10 ² . kg	10 ² . kg	10 ⁻³ . H _{CO2}	LMP _{CO₂}	LMP* _{CO₂}	10 ³ .N _{CO2}	10 ³ . kg'	10 ³ . KG	KG/kg	E	k ₂	k _{obs} (1/s)	10 ³ .N _{CO2}
(C)	(mol CO ₂ / mol Amine)	(m/s)	(m/s)	(mol/m ² kpa s)	(kpa m ³ /mol)	(kpa)	(kpa)	(mol/ m ² s)	(mol/m ² kpa s)	(mol/m ² kpa s)	(%)				(mol/ m ² s)
30,55	0,00	8,06	4,09	1,61	3,31	0,90	0,000	0,30	0,34	0,33	2,07	14,0	1,35	6,7160E+0 ₂	1,08
38,69	0,00	9,88	4,18	1,61	3,86	1,02	0,000	0,32	0,33	0,32	1,98	12,7	1,36	6,7392E+0 ₂	1,40
47,26	0,00	11,69	4,21	1,57	4,46	1,04	0,000	0,35	0,34	0,34	2,14	13,2	1,65	8,1594E+0 ₂	1,65
55,26	0,00	14,03	3,94	1,44	5,02	1,06	0,000	0,36	0,35	0,34	2,36	12,5	1,78	8,7746E+0 ₂	1,92
63,05	0,02	16,36	3,66	1,31	5,54	1,06	0,002	0,37	0,36	0,35	2,67	12,2	2,02	9,6107E+0 ₂	2,11

0.1M AMP

T	L _{Ma}	10 ⁵ . kl	10 ² . kg	10 ² . kg	10 ⁻³ . H _{CO2}	LMP _{CO₂}	LMP* _{CO₂}	10 ³ .N _{CO2}	10 ³ . kg'	10 ³ . KG	KG/kg	E	k ₂	k _{obs} (1/s)	10 ³ .N _{CO2}
(C)	(mol CO ₂ / mol Amine)	(m/s)	(m/s)	(mol/m ² kpa s)	(kpa m ³ /mol)	(kpa)	(kpa)	(mol/ m ² s)	(mol/m ² kpa s)	(mol/m ² kpa s)	(%)			(1/s)	(mol/ m ² s)
30,55	0,00	8,06	4,09	1,61	3,31	0,90	0,000	0,30	0,34	0,33	2,07	14,0	1,35	6,7160E+0 ₂	1,08
38,69	0,00	9,88	4,18	1,61	3,86	1,02	0,000	0,32	0,33	0,32	1,98	12,7	1,36	6,7392E+0 ₂	1,40
47,26	0,00	11,69	4,21	1,57	4,46	1,04	0,000	0,35	0,34	0,34	2,14	13,2	1,65	8,1594E+0 ₂	1,65
55,26	0,00	14,03	3,94	1,44	5,02	1,06	0,000	0,36	0,35	0,34	2,36	12,5	1,78	8,7746E+0 ₂	1,92
63,05	0,02	16,36	3,66	1,31	5,54	1,06	0,002	0,37	0,36	0,35	2,67	12,2	2,02	9,6107E+0 ₂	2,11

Appendix C

Kinetics of Loaded 3M AMP

CO₂ Loading 0.29 and 25°C

T	LMa	10 ⁵ . kl	10 ² . kg	10 ² . kg	10 ⁻³ . H _{CO2}	LMP _{CO2}	10 ³ .N _{CO2}	10 ³ . kg'	10 ³ . KG	KG/kg	E	k2	kobs	10 ³ .N _{CO2}
(C)	(mol CO ₂ / mol Amine)	(m/s)	(m/s)	(mol/m ² kpa s)	(kpa m ³ /mol)	(kpa)	(mol/ m ² s)	(mol/m ² kpa s)	(mol/m ² kpa s)	(%)		M ³ /m ^{ol} s)	(1/s)	(mol/ m ² s)
32.20	0.30	3.23	3.91	1.54	6.12	0.16	0.10	0.70	0.67	4.35	132.8	17.45	2.1703E+0 ₄	0.11
32.34	0.30	3.25	3.94	1.55	6.12	0.54	0.26	0.50	0.49	3.13	94.5	8.94	1.1080E+0 ₄	0.40
32.56	0.30	3.28	3.98	1.56	6.13	1.54	0.59	0.39	0.38	2.43	72.7	5.39	6.6294E+0 ₃	1.15
32.22	0.30	3.30	3.96	1.55	6.11	2.43	0.82	0.34	0.34	2.16	63.6	4.25	5.2037E+0 ₃	1.78

CO₂ Loading 0.29 and 40°C

T	LMa	10 ⁵ . kl	10 ² . kg	10 ² . kg	10 ⁻³ . H _{CO2}	LMP _{CO2}	10 ³ .N _{CO2}	10 ³ . kg'	10 ³ . KG	KG/kg	E	k2	kobs	10 ³ .N _{CO2}
(C)	(mol CO ₂ / mol Amine)	(m/s)	(m/s)	(mol/m ² kpa s)	(kpa m ³ /mol)	(kpa)	(mol/ m ² s)	(mol/m ² kpa s)	(mol/m ² kpa s)	(%)		M ³ /mol s)	(1/s)	(mol/ m ² s)
38.70	0.30	4.09	4.08	1.57	6.47	-0.12	-0.01	0.04	0.04	0.27	6.8	0.06	7.1661E+0 ₁	-0.11
38.76	0.30	4.08	4.10	1.57	6.47	0.41	0.25	0.64	0.62	3.93	102.2	13.5 ₃	1.6696E+0 ₄	0.36
38.75	0.30	4.08	4.12	1.58	6.47	1.18	0.53	0.46	0.45	2.82	72.9	6.93	8.5092E+0 ₃	1.06
38.91	0.30	4.02	4.16	1.60	6.48	2.06	0.80	0.40	0.39	2.45	64.6	5.27	6.4306E+0 ₃	1.85

CO₂ Loading 0.29 and 50°C

T	L _{Ma}	10 ⁵ . kl	10 ² . kg	10 ² . kg	10 ⁻³ . H _{CO2}	LMP _{CO2}	10 ³ .N _{CO2}	10 ³ . kg'	10 ³ . KG	KG/kg	E	k ₂	k _{obs}	10 ³ .N _{CO2}
(C)	(mol CO ₂ / mol Amine)	(m/s)	(m/s)	(mol/m ² kpa s)	(kpa m ³ /mol)	(kpa)	(mol/ m ² s)	(mol/m ² kpa s)	(mol/m ² kpa s)	(%)		M ³ /m ^{ol} .s)	(1/s)	(mol/ m ² s)
47.60	0.30	5.01	4.18	1.56	6.92	-0.12	0.14	-1.15	-1.25	-7.96	-158.0	37.67	4.629E+04	-0.13
47.60	0.30	5.16	4.13	1.55	6.92	0.43	0.32	0.79	0.75	4.85	106.0	18.04	2.208E+04	0.49
47.87	0.30	5.05	4.08	1.53	6.93	0.81	0.45	0.57	0.55	3.61	78.7	9.49	1.157E+04	0.94
47.84	0.30	5.11	4.07	1.52	6.93	1.19	0.60	0.52	0.50	3.29	70.3	7.78	9.461E+03	1.38

CO₂ Loading 0.22 and 25°C

T	L _{Ma}	10 ⁵ . Kl	10 ² . kg	10 ² . kg	10 ⁻³ . H _{CO2}	LMP _{CO2}	10 ³ .N _{CO2}	10 ³ . kg'	10 ³ . KG	KG/kg	E	k ₂	k _{obs}	10 ³ .N _{CO2}
(C)	(mol CO ₂ / mol Amine)	(m/s)	(m/s)	(mol/m ² kpa s)	(kpa m ³ /mol)	(kpa)	(mol/ m ² s)	(mol/m ² kpa s)	(mol/m ² kpa s)	(%)		M ³ /mol. s)	(1/s)	(mol/ m ² s)
31.46	0.20	3.21	3.98	1.57	6.08	0.34	0.13	0.39	0.38	2.44	74.2	3.67	6.868E+03	0.30
31.54	0.20	3.22	3.99	1.57	6.08	0.73	0.30	0.43	0.42	2.66	81.2	4.41	8.229E+03	0.64
31.55	0.20	3.21	4.01	1.58	6.07	1.72	0.67	0.40	0.39	2.46	75.2	3.79	7.022E+03	1.50
31.79	0.20	3.19	4.04	1.58	6.09	2.58	0.96	0.38	0.37	2.34	72.5	3.47	6.404E+03	2.27

CO₂ Loading 0.22 and 40°C

T	L _{Ma}	10 ⁵ . kl	10 ² . kg	10 ² . kg	10 ⁻³ . H _{CO2}	LMP _{CO2}	10 ³ .N _{CO2}	10 ³ . kg'	10 ³ . KG	KG/kg	E	k ₂	k _{obs}	10 ³ .N _{CO2}
(C)	(mol CO ₂ / mol Amine)	(m/s)	(m/s)	(mol/m ² kpa s)	(kpa m ³ /mol)	(kpa)	(mol/ m ² s)	(mol/m ² kpa s)	(mol/m ² kpa s)	(%)		M ³ /mol.s)	(1/s)	(mol/ m ² s)
38.44	0.20	4.08	4.12	1.58	6.45	0.25	0.10	0.41	0.40	2.52	64.9	3.64	6.776E+03	0.27
38.71	0.20	4.07	4.15	1.59	6.47	0.69	0.32	0.48	0.46	2.91	76.0	4.95	9.171E+03	0.75
38.70	0.20	4.06	4.16	1.60	6.46	1.57	0.69	0.45	0.44	2.74	71.9	4.42	8.163E+03	1.70
38.70	0.20	4.05	4.16	1.60	6.46	2.38	1.03	0.44	0.43	2.71	71.1	4.33	7.947E+03	2.57

CO₂ Loading 0.22 and 50°C

T	LMa	10 ⁵ . kl	10 ² . kg	10 ² . kg	10 ⁻³ . H _{CO2}	LMP _{CO2}	10 ³ .N _{CO2}	10 ³ . kg'	10 ³ . KG	KG/kg	E	k2	kobs (1/s)	10 ³ .N _{CO2}
(C)	(mol CO ₂ / mol Amine)	(m/s)	(m/s)	(mol/m ² kpa s)	(kpa m ³ /mol)	(kpa)	(mol/ m ² s)	(mol/m ² kpa s)	(mol/m ² kpa s)	(%)		(M ³ /mo l.s)		(mol/ m ² s)
46.80	0.20	5.38	4.26	1.59	6.87	0.18	0.07	0.40	0.39	2.44	51.2	3.09	5.7160E+0 ₃	0.24
47.84	0.20	5.21	4.15	1.55	6.93	0.76	0.34	0.47	0.45	2.92	62.2	4.18	7.6960E+0 ₃	1.06
47.85	0.20	5.24	4.16	1.56	6.93	1.17	0.54	0.47	0.46	2.95	62.6	4.29	7.8841E+0 ₃	1.63
48.07	0.20	5.19	4.14	1.55	6.94	2.11	0.94	0.46	0.45	2.89	61.8	4.10	7.4744E+0 ₃	2.95

CO₂ Loading 0.22 and 60°C

T	LMa	10 ⁵ . Kl	10 ² . kg	10 ² . kg	10 ⁻³ . H _{CO2}	LMP _{CO2}	10 ³ .N _{CO2}	10 ³ . kg'	10 ³ . KG	KG/kg	E	k2	kobs	10 ³ .N _{CO2}
(C)	(mol CO ₂ / mol Amine)	(m/s)	(m/s)	(mol/m ² kpa s)	(kpa m ³ /mol)	(kpa)	(mol/ m ² s)	(mol/m ² kpa s)	(mol/m ² kpa s)	(%)		(M ³ /mo l.s)	(1/s)	(mol/ m ² s)
56.86	0.20	6.20	3.34	1.22	7.33	-0.02	0.09	-3.58	-5.07	-41.64	-393.5	186.32	3.4162E+0 ₅	-0.03
56.76	0.20	6.24	3.37	1.23	7.33	0.46	0.31	0.72	0.68	5.54	84.8	8.81	1.6100E+0 ₄	0.79
56.87	0.20	6.28	3.41	1.24	7.33	0.86	0.46	0.55	0.53	4.27	64.8	5.21	9.5077E+0 ₃	1.48
56.83	0.20	6.16	3.38	1.23	7.33	1.26	0.61	0.51	0.49	3.95	60.5	4.37	7.9487E+0 ₃	2.15

CO₂ Loading 0.15 and 25°C

T	LMa	10 ⁵ . Kl	10 ² . kg	10 ² . kg	10 ⁻³ . H _{CO2}	LMP _{CO2}	10 ³ .N _{CO2}	10 ³ . kg'	10 ³ . KG	KG/kg	E	k2	kobs	10 ³ .N _{CO2}
(C)	(mol CO ₂ / mol Amine)	(m/s)	(m/s)	(mol/m ² kpa s)	(kpa m ³ /mol)	(kpa)	(mol/ m ² s)	(mol/m ² kpa s)	(mol/m ² kpa s)	(%)		(M ³ /mo l.s)	(1/s)	(mol/ m ² s)
30.87	0.10	3.15	4.13	1.63	6.03	0.45	0.22	0.50	0.48	2.96	95.1	4.42	1.102E+0 ₄	0.45
30.87	0.10	3.15	4.18	1.64	6.03	0.94	0.47	0.52	0.51	3.07	100.0	4.90	1.219E+0 ₄	0.92
30.96	0.10	3.15	4.20	1.65	6.03	1.91	0.90	0.49	0.47	2.86	93.3	4.28	1.059E+0 ₄	1.89
31.06	0.11	3.14	4.23	1.66	6.04	2.72	1.24	0.47	0.46	2.75	90.1	3.99	9.834E+0 ₃	2.70

CO₂ Loading 0.15 and 40°C

T	LMa	10 ⁵ . Kl	10 ² . kg	10 ² . kg	10 ⁻³ . H _{CO2}	LMP _{CO2}	10 ³ .N _{CO2}	10 ³ . kg'	10 ³ . KG	KG/kg	E	k2	kobs	10 ³ .N _{CO2}
(C)	(mol CO ₂ / mol Amine)	(m/s)	(m/s)	(mol/m ² kpa s)	(kpa m ³ /mol)	(kpa)	(mol/ m ² s)	(mol/m ² kpa s)	(mol/m ² kpa s)	(%)		(m ³ /m ol.s)	(1/s)	(mol/ m ² s)
38.52	0.11	4.03	4.22	1.62	6.45	0.39	0.20	0.53	0.52	3.19	85.6	4.76	1.1510E+04	0.48
38.50	0.11	4.04	4.23	1.63	6.45	0.78	0.46	0.61	0.59	3.60	97.1	6.19	1.4859E+04	0.95
38.81	0.15	4.00	4.23	1.62	6.47	1.67	0.94	0.58	0.56	3.47	94.7	6.30	1.3731E+04	1.96
38.78	0.16	4.02	4.24	1.63	6.47	2.56	1.39	0.56	0.54	3.33	90.5	5.97	1.2658E+04	2.97

CO₂ Loading 0.15 and 50°C

T	LMa	10 ⁵ . kl	10 ² . kg	10 ² . kg	10 ⁻³ . H _{CO2}	LMP _{CO2}	10 ³ .N _{CO2}	10 ³ . kg'	10 ³ . KG	KG/kg	E	k2	kobs	10 ³ .N _{CO2}
(C)	(mol CO ₂ / mol Amine)	(m/s)	(m/s)	(mol/m ² kpa s)	(kpa m ³ /mol)	(kpa)	(mol/ m ² s)	(mol/m ² kpa s)	(mol/m ² kpa s)	(%)		(m ³ /m ol.s)	(1/s)	(mol/ m ² s)
46.69	0.12	5.26	4.24	1.59	6.86	0.26	0.16	0.63	0.61	3.84	82.8	6.14	1.4372E+04	0.40
47.64	0.12	5.17	4.27	1.60	6.92	0.67	0.45	0.70	0.67	4.22	94.1	7.51	1.7448E+04	1.03
47.75	0.12	5.20	4.17	1.56	6.92	1.55	1.01	0.68	0.65	4.20	91.0	7.11	1.6485E+04	2.40
47.48	0.13	5.24	4.30	1.61	6.91	2.31	1.46	0.66	0.63	3.95	87.0	6.83	1.5408E+04	3.51

CO₂ Loading 0.15 and 60°C

T	LMa	10 ⁵ . kl	10 ² . kg	10 ² . kg	10 ⁻³ . H _{CO2}	LMP _{CO2}	10 ³ .N _{CO2}	10 ³ . kg'	10 ³ . KG	KG/kg	E	k2	kobs	10 ³ .N _{CO2}
(C)	(mol CO ₂ / mol Amine)	(m/s)	(m/s)	(mol/m ² kpa s)	(kpa m ³ /mol)	(kpa)	(mol/ m ² s)	(mol/m ² kpa s)	(mol/m ² kpa s)	(%)		(m ³ /m ol.s)	(1/s)	(mol/ m ² s)
56.07	0.14	6.49	3.83	1.40	7.30	-0.09	0.09	-0.95	-1.02	-7.27	-106.1	12.58	2.7739E+04	-0.16
56.02	0.14	6.47	3.83	1.40	7.30	0.27	0.34	1.39	1.27	9.05	157.5	27.72	6.0812E+04	0.50
57.57	0.15	6.65	3.85	1.41	7.38	0.98	0.81	0.88	0.83	5.88	97.9	11.02	2.3827E+04	1.87
56.15	0.17	6.45	3.79	1.39	7.31	1.71	1.30	0.80	0.76	5.49	91.3	9.87	2.0234E+04	3.08

CO₂ Loading 0.15 and 70°C

T	L _{Ma}	10 ⁵ . K _l	10 ² . kg	10 ² . kg	10 ⁻³ . H _{CO2}	LMP _{CO2}	10 ³ .N _{CO2}	10 ³ . kg'	10 ³ . KG	KG/kg	E	k ₂	k _{obs}	10 ³ .N _{CO2}
(C)	(mol CO ₂ / mol Amine)	(m/s)	(m/s)	(mol/m ² kpa s)	(kpa m ³ /mol)	(kpa)	(mol/ m ² s)	(mol/m ² kpa s)	(mol/m ² kpa s)	(%)		(m ³ / mol.s)	(1/s)	(mol/ m ² s)
64.04	0.14	7.81	3.43	1.22	7.60	-0.41	0.22	-0.52	-0.54	-4.41	-50.1	3.35	7.3255E+0 3	-0.91
64.79	0.14	7.71	3.35	1.19	7.63	-0.19	0.38	-1.68	-1.96	-16.41	-165.5	35.20	7.6369E+0 4	-0.43
65.04	0.15	7.70	3.32	1.18	7.64	0.05	0.54	183.76	11.10	93.96	13769. 1	24444 3.11	5.2427E+0 8	0.11
65.14	0.15	7.70	3.37	1.20	7.65	0.77	0.99	1.43	1.28	10.65	142.5	26.63	5.6022E+0 4	1.71

Appendix D

Kinetics data of Piperazine

1.5M PZ at 70°C

T	LMa	10 ⁵ . kl	10 ² . kg	10 ² . kg	10 ⁻³ . H _{CO2}	LMP _{CO2}	10 ³ .N _{CO2}	10 ³ . kg'	10 ³ . KG	KG/kg	E	k2	kobs	10 ³ .N _{CO2}	CO ₂ , bulk	10 ³ .N _{CO2} mod
(C)	(mol CO ₂ /mol Amine)	(m/s)	(m/s)	(mol/m ² kpa s)	(kpa m ³ /mol)	(kpa)	(mol/m ² s)	(mol/m ² kpa s)	(mol/m ² kpa s)	(%)		(m ³ /mol.s)	(1/s)	(mol/m ² s)	(mol/L)	(mol/m ² s)
64.30	0.00	15.83	1.97	0.70	6.19	0.66	3.17	15.30	4.81	68.57	599.8	1560.16	2.3381E+06	1.52	0.00023	1.52
66.94	0.00	16.31	1.89	0.67	6.44	3.08	9.79	6.04	3.18	47.40	239.0	251.05	3.7555E+05	7.13	0.00109	7.13
65.70	0.00	16.01	1.87	0.66	6.32	5.38	18.93	7.49	3.52	52.98	296.4	381.57	5.6952E+05	12.28	0.00191	12.28
65.84	0.00	16.13	1.87	0.66	6.34	7.24	23.81	6.53	3.29	49.62	256.9	290.50	4.3309E+05	16.53	0.00257	16.53

1.5M PZ at 60°C

T	LMa	10 ⁵ . kl	10 ² . kg	10 ² . kg	10 ⁻³ . HCO ₂	LMPCO ₂	10 ³ .NCO ₂	10 ³ . kg'	10 ³ . KG	KG/kg	E	k2	kobs	10 ³ .N _{CO2}	CO ₂ , bulk	10 ³ .N _{CO2} mod
(C)	(mol CO ₂ /mol Amine)	(m/s)	(m/s)	(mol/m ² kpa s)	(kpa m ³ /mol)	(kpa)	(mol/m ² s)	(mol/m ² kpa s)	(mol/m ² kpa s)	(%)		(m ³ /mol.s)	(1/s)	(mol/m ² s)	(mol/L)	(mol/m ² s)
55.95	0.00	13.69	1.90	0.69	5.43	0.73	2.83	8.71	3.87	55.64	346.4	455.97	6.8339E+05	1.57	0.00027	1.57
56.83	0.00	13.68	1.95	0.71	5.51	3.40	8.67	3.98	2.55	35.91	160.5	96.31	1.4410E+05	7.40	0.00124	7.40
57.13	0.00	13.92	1.93	0.70	5.54	5.90	15.52	4.20	2.63	37.34	167.2	107.73	1.6090E+05	12.84	0.00215	12.84
57.31	0.00	13.87	1.98	0.72	5.55	7.51	18.18	3.64	2.42	33.52	146.1	81.42	1.2151E+05	16.47	0.00273	16.47

1.5M PZ at 50°C

T	LMa	10 ⁵ . kl	10 ² . kg	10 ² . kg	10 ⁻³ . H _{CO2}	LMP _{CO2}	10 ³ .N _{CO2}	10 ³ . kg'	10 ³ . KG	KG/kg	E	k2	kobs	10 ³ .N _{CO2}	CO ₂ , bulk	10 ³ .N _{CO2} mod
(C)	(mol CO ₂ /mol Amine)	(m/s)	(m/s)	(mol/m ² kpa s)	(kpa m ³ /mol)	(kpa)	(mol/m ² s)	(mol/m ² kpa s)	(mol/m ² kpa s)	(%)		(m ³ /mol.s)	(1/s)	(mol/m ² s)	mol/L	(mol/m ² s)
47.86	0.00	11.72	1.90	0.71	4.76	0.87	3.61	10.09	4.17	58.67	410.3	553.28	8.2905E+05	1.73	0.00032	1.73
47.97	0.00	11.70	1.93	0.72	4.77	3.57	9.61	4.28	2.69	37.18	174.7	99.80	1.4928E+05	7.19	0.00134	7.19
48.19	0.00	11.69	1.97	0.74	4.79	6.34	16.79	4.13	2.65	35.95	169.4	93.45	1.3951E+05	12.84	0.00237	12.84
48.33	0.00	11.70	1.96	0.73	4.80	8.24	19.80	3.58	2.40	32.76	146.9	70.17	1.0466E+05	16.68	0.00308	16.68

1.5M PZ at 40°C

T	LMa	10 ⁵ . kl	10 ² . kg	10 ² . kg	10 ⁻³ . H _{CO2}	LMP _{CO2}	10 ³ .N _{CO2}	10 ³ . kg'	10 ³ . KG	KG/kg	E	k2	kobs	10 ³ .N _{CO2}	CO ₂ , bulk	10 ³ .N _{CO2} mod
(C)	(mol CO ₂ /mol Amine)	(m/s)	(m/s)	(mol/m ² kpa s)	(kpa m ³ /mol)	(kpa)	(mol/m ² s)	(mol/m ² kpa s)	(mol/m ² kpa s)	(%)		(m ³ /mol.s)	(1/s)	(mol/m ² s)	(mol/L)	(mol/m ² s)
38.44	0.00	9.61	1.93	0.74	4.04	0.83	3.67	11.09	4.45	59.87	467.1	591.92	8.869E+05	1.51	0.00032	1.51
38.77	0.00	9.64	1.91	0.74	4.07	3.76	10.24	4.33	2.73	37.06	182.9	90.73	1.35E+05	6.86	0.00145	6.86
39.03	0.00	9.74	1.89	0.73	4.09	6.70	18.86	4.59	2.81	38.63	192.7	102.45	1.52E+05	12.23	0.00258	12.23
39.07	0.00	9.70	1.93	0.74	4.09	8.44	23.81	4.55	2.82	37.97	192.0	100.99	1.50E+05	15.48	0.00325	15.48

1.5M PZ at 25°C

T	LMa	10 ⁵ . kl	10 ² . kg	10 ² . kg	10 ⁻³ . H _{CO2}	LMP _{CO2}	10 ³ .N _{CO2}	10 ³ . kg'	10 ³ . KG	KG/kg	E	k2	kobs	10 ³ .N _{CO2}	CO ₂ , bulk	10 ³ .N _{CO2} mod
(C)	(mol CO ₂ /mol Am)	(m/s)	(m/s)	(mol/m ² kpa s)	(kpa m ³ /mol)	(kpa)	(mol/m ² s)	(mol/m ² kpa s)	(mol/m ² kpa s)	(%)		(m ³ /mol.s)	(1/s)	(mol/m ² s)	(mol/L)	(mol/m ² s)
26.06	0.00	7.25	1.95	0.78	3.21	0.81	3.69	10.92	4.56	58.23	483.9	485.33	7.27E+5	1.27	0.0003	1.27
26.72	0.00	7.34	1.93	0.78	3.25	3.49	9.88	4.46	2.83	36.51	197.8	81.78	1.22E+5	5.53	0.0014	5.53
27.05	0.00	7.43	1.92	0.77	3.27	6.54	18.58	4.51	2.84	36.98	198.8	84.29	1.25E+5	10.37	0.0026	10.37
26.03	0.00	7.16	1.90	0.76	3.21	8.41	23.44	4.39	2.79	36.51	197.1	79.03	1.17E+5	13.11	0.0033	13.11

1.0M PZ at 70°C

T	10 ⁵ . kl	10 ² . kg	10 ² . kg	10 ⁻³ . H _{CO2}	LMP _{CO2}	10 ³ .N _{CO2}	10 ³ . kg'	10 ³ . KG	KG/kg	E	k2	kobs	10 ³ .N _{CO2}	CO ₂ , bulk	10 ³ .N _{CO2} _{mod}
(C)	(m/s)	(m/s)	(mol/m ² kpa s)	(kpa m ³ /mol)	(kpa)	(mol/m ² s)	(mol/m ² kpa s)	(mol/m ² kpa s)	(%)		(m ³ /mole.s)	(1/s)	(mol/m ² s)	mol/L	(mol/m ² s)
64.67	16.10	1.75	0.62	6.22	0.62	2.77	15.96	4.48	71.94	618.8	2561.14	2.5582E+06	1.20	0.00022	1.20
65.66	16.19	1.87	0.66	6.32	2.95	8.35	4.94	2.83	42.62	193.0	247.90	2.4707E+05	5.87	0.00104	5.87
65.73	16.24	1.72	0.61	6.33	5.41	15.42	5.34	2.85	46.63	208.2	290.88	2.8916E+05	10.50	0.00192	10.50
66.10	16.34	1.80	0.64	6.37	7.01	19.77	5.05	2.82	44.16	197.0	262.23	2.6027E+05	13.81	0.00249	13.81

1.0M PZ at 60°C

T	10 ⁵ . kl	10 ² . kg	10 ² . kg	10 ⁻³ . H _{CO2}	LMP _{CO2}	10 ³ .N _{CO2}	10 ³ . kg'	10 ³ . KG	KG/kg	E	k2	kobs	10 ³ .N _{CO2}	CO ₂ , bulk	10 ³ .N _{CO2} _{mod}
(C)	(m/s)	(m/s)	(mol/m ² kpa s)	(kpa m ³ /mol)	(kpa)	(mol/m ² s)	(mol/m ² kpa s)	(mol/m ² kpa s)	(%)			(1/s)	(mol/m ² s)	mol/L	(mol/m ² s)
57.31	13.83	1.78	0.65	5.55	0.67	2.80	11.94	4.20	64.80	480.5	1308.01	1.3064E+06	1.23	0.00024	1.23
57.27	13.82	1.84	0.67	5.55	3.25	7.48	3.50	2.30	34.34	140.8	112.44	1.1207E+05	6.05	0.00118	6.05
57.16	13.86	1.82	0.66	5.54	5.64	13.45	3.73	2.39	35.97	149.1	127.51	1.2679E+05	10.44	0.00205	10.44
57.05	13.99	1.87	0.68	5.53	7.64	19.00	3.91	2.49	36.44	155.0	140.95	1.3989E+05	14.22	0.00278	14.22

1.0M PZ at 50°C

T	10 ⁵ . kl	10 ² . kg	10 ² . kg	10 ⁻³ . H _{CO2}	LMP _{CO2}	10 ³ .N _{CO2}	10 ³ . kg'	10 ³ . KG	KG/kg	E	k2	kobs	10 ³ .N _{CO2}	CO ₂ , bulk	10 ³ .N _{CO2} _{mod}
(C)	(m/s)	(m/s)	(mol/m ² kpa s)	(kpa m ³ /mol)	(kpa)	(mol/m ² s)	(mol/m ² kpa s)	(mol/m ² kpa s)	(%)		(m ³ /mole.s)	(1/s)	(mol/m ² s)	mol/L	(mol/m ² s)
47.34	11.57	1.96	0.73	4.72	0.61	2.83	12.48	4.62	62.95	509.8	1261.79	1.260E+06	1.06	0.00023	1.06
47.97	11.77	1.89	0.71	4.77	3.38	8.95	4.23	2.65	37.44	171.7	146.60	1.460E+05	5.81	0.00126	5.81
48.22	11.83	1.82	0.68	4.79	6.16	18.36	5.30	2.98	43.82	215.1	231.86	2.301E+05	10.51	0.00231	10.51
48.19	11.77	1.75	0.66	4.79	7.85	23.34	5.42	2.97	45.21	221.0	242.84	2.406E+05	13.26	0.00294	13.26

1.0M PZ at 40°C

T	10 ⁵ . kl	10 ² . kg	10 ² . kg	10 ⁻³ . H _{CO2}	LMP _{CO2}	10 ³ .N _{CO2}	10 ³ . kg'	10 ³ . KG	KG/kg	E	k2	kobs	10 ³ .N _{CO2}	CO ₂ , bulk	10 ³ .N _{CO2} _{mod}
(C)	(m/s)	(m/s)	(mol/m ² kpa s)	(kpa m ³ /mol)	(kpa)	(mol/ m ² s)	(mol/m ² kpa s)	(mol/m ² kpa s)	(%)		(m ³ /mo l.s)	(1/s)	(mol/ m ² s)	mol/L	(mol/ m ² s)
38.55	9.63	1.89	0.73	4.05	0.53	2.87	21.90	5.46	75.06	923.7	3476.99	3.4727E+06	0.82	0.00020	0.82
38.88	9.72	1.92	0.74	4.07	3.52	9.20	4.05	2.62	35.44	170.0	119.54	1.1906E+05	5.50	0.00135	5.50
39.03	9.71	1.90	0.73	4.09	6.42	15.97	3.77	2.49	33.99	158.8	103.96	1.0324E+05	10.03	0.00247	10.03
39.03	9.73	1.94	0.75	4.09	8.33	19.99	3.54	2.40	32.15	148.7	91.67	9.0891E+04	13.07	0.00321	13.07

1.0M PZ at 25°C

T	10 ⁵ . kl	10 ² . kg	10 ² . kg	10 ⁻³ . H _{CO2}	LMP _{CO2}	10 ³ .N _{CO2}	10 ³ . kg'	10 ³ . KG	KG/kg	E	k2	kobs	10 ³ .N _{CO2}	CO ₂ , bulk	10 ³ .N _{CO2} _{mod}
(C)	(m/s)	(m/s)	(mol/m ² kpa s)	(kpa m ³ /mol)	(kpa)	(mol/ m ² s)	(mol/m ² kpa s)	(mol/m ² kpa s)	(%)		(m ³ /mo l.s)	(1/s)	(mol/ m ² s)	mol/L	(mol/ m ² s)
26.10	7.17	1.95	0.78	3.21	0.86	3.21	7.06	3.72	47.41	316.9	304.97	3.0451E+05	1.15	0.00035	1.15
26.32	7.21	1.97	0.79	3.23	3.62	8.21	3.17	2.27	28.64	142.2	61.90	6.1653E+04	4.85	0.00145	4.85
26.06	7.20	1.92	0.77	3.21	6.46	14.45	3.15	2.24	29.05	140.7	61.01	6.0595E+04	8.57	0.00259	8.57
26.79	7.24	1.95	0.78	3.26	8.48	18.25	2.97	2.15	27.52	133.7	54.81	5.4328E+04	11.38	0.00340	11.38

0.5M PZ at 70°C

T	10 ⁵ . kl	10 ² . kg	10 ² . kg	10 ⁻³ . H _{CO2}	LMP _{CO2}	10 ³ .N _{CO2}	10 ³ . kg'	10 ³ . KG	KG/kg	E	k2	kobs	10 ³ .N _{CO2}	CO ₂ , bulk	10 ³ .N _{CO2} _{mod}
(C)	(m/s)	(m/s)	(mol/m ² kpa s)	(kpa m ³ /mol)	(kpa)	(mol/ m ² s)	(mol/m ² kpa s)	(mol/m ² kpa s)	(%)		(m ³ /mo l.s)	(1/s)	(mol/ m ² s)	mol/L	(mol/ m ² s)
63.32	16.60	1.90	0.68	6.10	0.68	2.27	6.57	3.33	49.29	241.5	851.00	4.248E+05	1.03	0.00024	1.03
65.66	16.69	1.97	0.70	6.32	3.12	5.90	2.59	1.89	27.12	98.4	137.01	6.818E+04	4.86	0.00111	4.86
65.73	16.71	1.88	0.67	6.33	5.49	9.86	2.45	1.79	26.86	93.0	123.10	6.107E+04	8.48	0.00195	8.48
65.70	16.63	1.95	0.69	6.33	7.12	11.83	2.19	1.66	24.06	83.3	97.95	4.851E+04	11.06	0.00253	11.06

0.5M PZ at 60°C

T	10 ⁵ . kl	10 ² . kg	10 ² . kg	10 ⁻³ . H _{CO2}	LMP _{CO2}	10 ³ .N _{CO2}	10 ³ . kg'	10 ³ . KG	KG/kg	E	k2	kobs	10 ³ .N _{CO2}	CO ₂ , bulk	10 ³ .N _{CO2} _{mod}
(C)	(m/s)	(m/s)	(mol/m ² kpa s)	(kpa m ³ /mol)	(kpa)	(mol/ m ² s)	(mol/m ² kpa s)	(mol/m ² kpa s)	(%)		(m ³ /m ^{ol} l.s)	(1/s)	(mol/ m ² s)	mol/L	(mol/ m ² s)
56.06	13.61	2.02	0.74	5.44	0.62	2.34	7.84	3.80	51.49	314.1	1109.67	5.5375E+05	0.89	0.00022	0.89
56.61	14.13	2.01	0.73	5.49	3.22	6.32	2.69	1.97	26.81	104.6	131.55	6.5436E+04	4.66	0.00117	4.66
56.91	14.36	2.00	0.73	5.52	5.93	11.12	2.52	1.87	25.76	97.2	117.11	5.8049E+04	8.59	0.00216	8.59
57.02	14.32	1.99	0.72	5.53	7.65	13.49	2.33	1.76	24.32	90.0	100.02	4.9479E+04	11.07	0.00279	11.07

0.5M PZ at 50°C

T	10 ⁵ . kl	10 ² . kg	10 ² . kg	10 ⁻³ . H _{CO2}	LMP _{CO2}	10 ³ .N _{CO2}	10 ³ . kg'	10 ³ . KG	KG/kg	E	k2	kobs	10 ³ .N _{CO2}	CO ₂ , bulk	10 ³ .N _{CO2} _{mod}
(C)	(m/s)	(m/s)	(mol/m ² kpa s)	(kpa m ³ /mol)	(kpa)	(mol/ m ² s)	(mol/m ² kpa s)	(mol/m ² kpa s)	(%)			(1/s)	(mol/ m ² s)	mol/L	(mol/ m ² s)
49.80	12.99	1.96	0.73	4.91	0.73	2.83	8.27	3.89	52.99	313.5	1143.56	5.7064E+05	0.98	0.00027	0.98
49.80	12.94	1.95	0.73	4.92	3.59	6.05	2.19	1.68	23.09	83.2	80.15	3.9879E+04	4.83	0.00134	4.83
49.80	12.94	1.93	0.72	4.92	6.40	10.14	2.03	1.59	21.89	77.2	69.26	3.4351E+04	8.58	0.00239	8.58
49.80	12.89	1.93	0.72	4.92	8.04	12.82	2.05	1.60	22.10	78.2	70.63	3.4956E+04	10.76	0.00301	10.76

0.5M PZ at 40°C

T	10 ⁵ . kl	10 ² . kg	10 ² . kg	10 ⁻³ . H _{CO2}	LMP _{CO2}	10 ³ .N _{CO2}	10 ³ . kg'	10 ³ . KG	KG/kg	E	k2	kobs	10 ³ .N _{CO2}	CO ₂ , bulk	10 ³ .N _{CO2} _{mod}
(C)	(m/s)	(m/s)	(mol/m ² kpa s)	(kpa m ³ /mol)	(kpa)	(mol/ m ² s)	(mol/m ² kpa s)	(mol/m ² kpa s)	(%)		(m ³ /m ^{ol} l.s)	(1/s)	(mol/ m ² s)	mol/L	(mol/ m ² s)
38.81	9.59	1.89	0.73	4.07	0.82	1.87	3.33	2.28	31.37	141.3	160.41	8.0057E+04	0.96	0.00032	0.96
39.03	9.66	1.87	0.72	4.09	3.83	5.98	1.99	1.56	21.63	84.3	57.92	2.8787E+04	4.51	0.00148	4.51
39.21	9.60	1.95	0.75	4.10	6.70	11.14	2.14	1.66	22.14	91.4	67.28	3.3275E+04	7.93	0.00258	7.93
39.21	9.58	1.95	0.75	4.10	8.29	13.11	2.00	1.58	21.11	85.9	59.36	2.9296E+04	9.80	0.00319	9.80

0.5M PZ at 25°C

T	10 ⁵ . kl	10 ² . kg	10 ² . kg	10 ⁻³ . H _{CO2}	LMP _{CO2}	10 ³ .N _{CO2}	10 ³ . kg'	10 ³ . KG	KG/kg	E	k2	kobs	10 ³ .N _{CO2}	CO ₂ , bulk	10 ³ .N _{CO2 mod}
(C)	(m/s)	(m/s)	(mol/m ² kpa s)	(kpa m ³ /mol)	(kpa)	(mol/m ² s)	(mol/m ² kpa s)	(mol/m ² kpa s)	(%)		(m ³ /mol.s)	(1/s)	(mol/m ² s)	mol/L	(mol/ m ² s)
25.62	7.02	1.91	0.77	3.18	0.87	2.75	5.33	3.15	40.96	242.0	345.36	1.7222E+05	0.86	0.00035	0.86
26.83	7.28	1.90	0.76	3.26	3.64	7.04	2.60	1.94	25.40	116.3	83.65	4.1527E+04	3.63	0.00145	3.63
26.72	7.31	1.93	0.77	3.25	6.49	9.69	1.85	1.49	19.31	82.5	42.68	2.1117E+04	6.46	0.00260	6.46
26.65	7.21	1.92	0.77	3.25	8.24	11.66	1.73	1.42	18.36	78.2	37.50	1.8509E+04	8.18	0.00330	8.18

0.1M PZ at 70°C

T	10 ⁵ . kl	10 ² . kg	10 ² . kg	10 ⁻³ . H _{CO2}	LMP _{CO2}	10 ³ .N _{CO2}	10 ³ . kg'	10 ³ . KG	KG/kg	E	k2	kobs	10 ³ .N _{CO2}	CO ₂ , bulk	10 ³ .N _{CO2 mod}
(C)	(m/s)	(m/s)	(mol/m ² kpa s)	(kpa m ³ /mol)	(kpa)	(mol/m ² s)	(mol/m ² kpa s)	(mol/m ² kpa s)	(%)		(m ³ /mol.s)	(1/s)	(mol/m ² s)	mol/L	(mol/ m ² s)
64.78	16.19	1.94	0.69	6.24	1.95	0.93	0.51	0.48	6.92	19.7	26.26	2.6100E+03	1.54	0.00069	1.54
65.66	16.46	1.91	0.68	6.32	3.42	1.62	0.51	0.47	7.01	19.6	26.54	2.6258E+03	2.71	0.00121	2.71
65.73	16.30	1.83	0.65	6.33	5.63	1.62	0.30	0.29	4.43	11.7	9.27	9.1348E+02	4.43	0.00200	4.43
65.70	16.29	1.83	0.65	6.33	7.28	2.21	0.32	0.30	4.68	12.4	10.39	1.0194E+03	5.70	0.00258	5.70

0.1M PZ at 60°C

T	10 ⁵ . kl	10 ² . kg	10 ² . kg	10 ⁻³ . H _{CO2}	LMP _{CO2}	10 ³ .N _{CO2}	10 ³ . kg'	10 ³ . KG	KG/kg	E	k2	kobs	10 ³ .N _{CO2}	CO ₂ , bulk	10 ³ .N _{CO2 mod}
(C)	(m/s)	(m/s)	(mol/m ² kpa s)	(kpa m ³ /mol)	(kpa)	(mol/m ² s)	(mol/m ² kpa s)	(mol/m ² kpa s)	(%)		(m ³ /mol.s)	(1/s)	(mol/m ² s)	(mol/L)	(mol/ m ² s)
56.21	13.34	2.02	0.74	5.46	1.69	1.20	0.78	0.71	9.63	32.1	55.95	5.5531E+03	1.23	0.00062	1.23
56.50	13.87	1.96	0.71	5.49	3.53	2.41	0.75	0.68	9.55	29.8	52.00	5.1275E+03	2.55	0.00129	2.55
57.09	13.92	2.01	0.73	5.54	6.08	3.46	0.62	0.57	7.78	24.6	35.49	3.4717E+03	4.40	0.00221	4.40
57.05	14.01	2.00	0.73	5.54	7.67	6.63	0.98	0.86	11.86	38.9	91.09	8.8067E+03	5.51	0.00280	5.51

0.1M PZ at 50°C

T	10 ⁵ . kl	10 ² . kg	10 ² . kg	10 ⁻³ . H _{CO2}	LMP _{CO2}	10 ³ .N _{CO2}	10 ³ . kg'	10 ³ . KG	KG/kg	E	k2	kobs	10 ³ .N _{CO2}	CO ₂ , bulk	10 ³ .N _{CO2} mod
(C)	(m/s)	(m/s)	(mol/m ² kpa s)	(kpa m ³ /mol)	(kpa)	(mol/ m ² s)	(mol/m ² kpa s)	(mol/m ² kpa s)	(%)		(m ³ /m ol.s)	(1/s)	(mol/ m ² s)	(mol/L)	(mol/ m ² s)
47.42	11.33	1.96	0.73	4.73	1.36	1.54	1.34	1.14	15.49	56.1	147.28	1.4606E +04	0.88	0.00051	0.88
47.93	11.47	1.95	0.73	4.77	3.16	3.77	1.42	1.19	16.32	59.3	168.47	1.6528E +04	2.05	0.00118	2.05
47.97	11.76	1.99	0.74	4.78	6.11	5.22	0.96	0.85	11.47	39.2	78.20	7.5984E +03	3.95	0.00229	3.95
48.11	11.65	1.97	0.74	4.80	8.20	11.42	1.72	1.39	18.87	70.9	255.96	2.4305E +04	5.22	0.00307	5.22

0.1M PZ at 40°C

T	10 ⁵ . kl	10 ² . kg	10 ² . kg	10 ⁻³ . H _{CO2}	LMP _{CO2}	10 ³ .N _{CO2}	10 ³ . kg'	10 ³ . KG	KG/kg	E	k2	kobs	10 ³ .N _{CO2}	CO ₂ , bulk	10 ³ .N _{CO2} mod
(C)	(m/s)	(m/s)	(mol/m ² kpa s)	(kpa m ³ /mol)	(kpa)	(mol/ m ² s)	(mol/m ² kpa s)	(mol/m ² kpa s)	(%)		(m ³ /m ol.s)	(1/s)	(mol/ m ² s)	(mol/L)	(mol/ m ² s)
38.55	9.36	1.94	0.75	4.05	1.48	1.55	1.22	1.05	14.05	52.8	108.30	1.0731E +04	0.85	0.00057	0.85
39.07	9.59	1.97	0.76	4.09	3.94	3.46	0.99	0.88	11.55	42.4	73.28	7.1745E +03	2.27	0.00152	2.27
39.03	9.39	1.92	0.74	4.09	6.47	4.82	0.83	0.75	10.08	36.2	51.74	5.0086E +03	3.69	0.00249	3.69
39.03	9.21	1.92	0.74	4.15	7.47	33.35	11.26	4.47	60.32	508. 6	10888.6 2	9.5812E +05	3.98	0.00327	3.98

0.1M PZ at 25°C

T	10 ⁵ . kl	10 ² . kg	10 ² . kg	10 ⁻³ . H _{CO2}	LMP _{CO2}	10 ³ .N _{CO2}	10 ³ . kg'	10 ³ . KG	KG/kg	E	k2	kobs	10 ³ .N _{CO2}	CO ₂ , bulk	10 ³ .N _{CO2} mod
(C)	(m/s)	(m/s)	(mol/m ² kpa s)	(kpa m ³ /mol)	(kpa)	(mol/ m ² s)	(mol/m ² kpa s)	(mol/m ² kpa s)	(%)		(m ³ /m ol.s)	(1/s)	(mol/ m ² s)	(mol/L)	(mol/ m ² s)
26.94	1.11	1.96	0.79	3.26	1.30	0.09	0.07	0.07	0.90	21.1	1.75	1.7472E +02	0.28	0.00052	0.28
27.53	1.12	1.95	0.78	3.31	4.76	3.11	0.71	0.65	8.37	210. 7	180.07	1.7555E +04	1.01	0.00190	1.01
27.93	1.13	1.95	0.78	3.33	6.66	3.72	0.60	0.56	7.19	178. 6	130.96	1.2669E +04	1.42	0.00265	1.42
27.97	1.12	1.95	0.78	3.34	8.87	3.83	0.46	0.43	5.56	136. 4	75.88	7.2853E +03	1.88	0.00354	1.88

Appendix E

Results of CO₂ Analyses for PZ

No	Name	Remarks		Sample		Blank				pH	Total CO2	[Amine]	diff	loading	loading*	Concentration
		a	t/C	weight (g)	HCL(g)	NaoH(ml)	HCL(g)	NaoH(ml)	(mol/kg)		(mol/kg)	(mol alkalinity)		(mol amine)	(mol/liter)	
1	Kinetics	0	WWC	1.008	40.388	37.961	40.296	39.573	5.25	5.25	0.0845	0.31		0.2728	0.55	0.1
			70C	1.009	40.392	37.956	40.296	39.573	5.25	0.723	0.0849	0.31	0.2			
												0.0847	0.31	0.2		
2	Kinetics	0	WWC	1.007	40.365	38.212	40.296	39.573	5.25	5.25	0.0710	0.21		0.3237	0.65	0.1
			60C	1.011	40.359	38.323	40.296	39.573	5.25	0.723	0.0649	0.21	-4.5			
												0.0680	0.21	0.0		
3	Kinetics	0	WWC	0.970	40.374	35.062	40.296	39.573	5.25	5.25	0.2365	3.02		0.0787	0.16	1.5
			50C	0.959	40.472	35.176	40.296	39.573	5.25	0.723	0.2384	3.01	0.4			
												0.2375	3.02	0.4		
4	Kinetics	0	WWC	1.025	40.300	32.447	40.296	39.573	5.25	5.25	0.3478	2.94		0.1175	0.24	1.5
			60C	1.030	40.453	32.674	40.296	39.573	5.25	0.723	0.3425	2.94	-0.8			
												0.3452	2.94	0.0		
5	Kinetics	0	WWC	1.014	40.316	36.147	40.296	39.573	5.25	5.25	0.1699	1.98		0.0851	0.17	1.0
			60C	1.016	40.309	36.198	40.296	39.573	5.25	0.723	0.1667	1.98	-0.9			
												0.1683	1.98	0.0		

